Mathematical Issues in Blood Flow Problems

A Dissertation

Presented to

the Faculty of the Department of Mathematics

University of Houston

In Partial Fulfillment

of the Requirements for the Degree

Doctor of Philosophy

By

Taebeom Kim

December 2009

Mathematical Issues in Blood Flow Problems

Taebeom Kim

APPROVED:

Dr. Sučica Čanić, Chairman

Dr. Giovanna Guidoboni,

Dr. David Wagner

Dr. Ralph Metcalfe,
Department of Mechanical Engineering

Dean, College of Natural Sciences
and Mathematics

ACKNOWLEDGEMENTS

First, I would like to deeply thank my advisor, Dr. Sučica Čanić, for her amazing support since I started a study under her guidance. She has patiently explained the problem again and again and corrected my mistakes despite her very busy schedule. Without her supervision, I would not have reached the end of this long journey. I would also like to thank my other advisor, Dr. Giovanna Guidoboni, for her effort and advice on the joint work together with Dr. Čanić and me. She also gave me the opportunity to work with her concerning a numerical study. My special thanks goes to Dr. Josip Tambača and Dr. Andro Mikelic for spending their time and providing various ideas for my work, even though they reside far away from Houston.

I would like to thank my dissertation committee members, Dr. David Wagner and Dr. Ralph Metcalfe, for taking the time to read the dissertation and giving me helpful suggestions. I am also thankful to all faculty and staff, especially Dr. Jeff Morgan, Dr. Roland Glowinski, and Dr. Shanju Ji for their support.

The friends I made in Houston, Mate, Dekang, Kawin, Pap, Sunrye, and Justin, also deserve to hear my thanks. They helped me a lot while studying in Universtiy of Houston. In addition, I am grateful to my Korean friends, specially Dr. Jeong in Baylor Collage of Medicine and his family, who are always delighted to see and treat my wife and me as their family.

Finally, I would like to thank my family for their endless support. My mother and farther have always encouraged and supported me to do what I pursued. My brother and sister have not only helped me study abroad but also have always been good friends and supporters. I also thank my aunts and their husbands, who have always guided me since I was very young, for their constant concern. My thanks also goes to my best friend and the biggest supporter in my life, my lovely wife, Eunji Jo.

Mathematical Issues in Blood Flow Problems

An Abstract of a Dissertation

Presented to

the Faculty of the Department of Mathematics

University of Houston

In Partial Fulfillment

of the Requirements for the Degree

Doctor of Philosophy

By

Taebeom Kim

December 2009

ABSTRACT

The present work is motivated by the study of blood flow in arteries.

This dissertation is divided into two parts. The first part is devoted to the proof of existence of a mild solution to a nonlinear moving boundary problem which approximates the flow of a viscous, incompressible, Newtonian fluid in a long and slender viscoelastic tube with small aspect ratio. The resulting problem is of Biot type and it has been used to model blood flow in large-to-medium arteries. The second part of the dissertation presents a numerical study of the qualitative properties of the solution of Bingham fluid flows in cylinders. The Bingham model has been used to describe the blood flow in small vessels, such as arterioles and capillaries, where the size of the vessel diameter is comparable to the size of blood cells.

The problem considered in the first part of the dissertation consists of a hyperbolic-parabolic system of partial differential equations with degenerate diffusion. The degenerate diffusion is a consequence of the fact that the effects of the fluid viscosity in the axial direction of a long and slender tube are small in comparison with the effects of the fluid viscosity in the radial direction. Degenerate fluid diffusion and hyperbolicity induce lower regularity of a weak solution and are a source of the main difficulties associated with the existence proof.

The viscoelasticity of vessel wall plays a crucial role in the proof of existence of solutions for both the linearized and the nonlinear problems. Wall viscoelasticity provides the main smoothing mechanisms in the energy estimates which, via the compactness arguments, leads to the proof of the existence of a solution. This has interesting consequences for the understanding of the underlying hemodynamics application. Our analysis shows that the viscoelasticity of the vessel walls is crucial in smoothing sharp wave fronts that might be generated by the steep pressure pulses emanating from the heart, which are known to occur in, for example, patients with aortic insufficiency.

In the second part of the dissertation we present some numerical results related to Bingham flow in a cylinder, which is modeled by a nonlinear parabolic equation. Our results showed that the solution has a finite extinction time, which means that the fluid axial velocity drops to zero in a finite time if there are no external forces, e.g. pressure drop acting on the system. We also found that the extinction time increases as the fluid viscosity decreases.

Contents

List of Tables

List of Figures

Chapter I

An Effective Model for Fluid-Structure Interaction in Blood Flow

1 Introduction

This work was motivated by the study of blood flow in pulsatile arteries. In medium-to-large arteries, blood can be modeled as an incompressible, viscous fluid utilizing the incompressible Navier-Stokes equations. To model the mechanical properties of arterial walls, we follow the bioengineering literature indicating that vessel walls are viscoelastic. In particular, experimental measurements of the viscoelastic properties of the human femoral artery and of the canine abdominal aorta presented in [6, 7, 8], indicate that the viscoelasticity of the vessel walls is of the Kelvin-Voight type. In [12] Canic et al. derived two models for the vessel wall behavior assuming Kelvin-Voight viscoelasticity: the cylindrical linearly viscoelastic membrane and the cylindrical linearly viscoelastic Koiter shell. Both models were coupled to the fluid equations describing fluid flow driven by the time-dependent pressure drop between

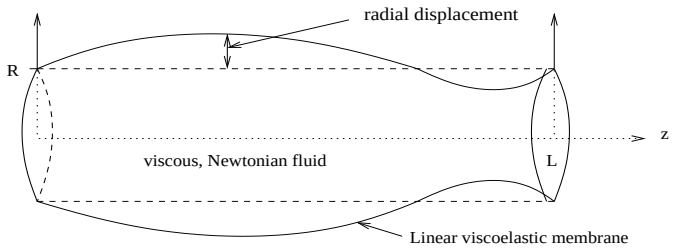

Figure I.1: Domain $\Omega(t)$

the inlet and the outlet of a cylindrical domain of length L and reference radius R. Assuming axially symmetric flow and small aspect ratio $\epsilon = R/L$, a set of closed, reduced, effective equations in two-space dimensions was obtained in [12]. It was proved in [12] that this reduced, effective problem approximates the original problem to the ϵ^2 accuracy. The leading-order effective equations are in the form of a nonlinear, moving-boundary problem for a system of partial differential equations of mixed hyperbolic-parabolic type in two-space dimensions. They are given in terms of the unknown functions v_z and η where v_z is the axial component of the fluid velocity, and η is the radial displacement of the tube wall.

The leading-order nonlinear moving-boundary problem holds in the cylindrical domain $\Omega(t)$, shown in Figure I-1.1:

$$\Omega(t) = \Big\{ x \in I\!R^3; x = (r\cos\vartheta, r\sin\vartheta, z),\ 0 < r < R + \eta(z,t),\ \vartheta \in [0, 2\pi),\ 0 < z < L \Big\}, \tag{I-1.1}$$

for $0 < t < T$, with $T > 0$. The lateral boundary of $\Omega(t)$ is denoted by $\Sigma(t)$:

$$\Sigma(t) = \left\{ (R(z) + \eta(t,z))\cos\vartheta, (R(z) + \eta(t,z))\sin\vartheta, z) \in \mathbb{R}^3 : \vartheta \in [0, 2\pi), z \in (0, L) \right\}.$$

The reference configuration corresponds to that of a straight cylinder with radius R and length L. The effective reduced problem reads

$$\frac{\partial (R+\eta)^2}{\partial t} + \frac{\partial}{\partial z}\int_0^{R+\eta} 2 r v_z dr = 0, \qquad 0 < z < L,\ 0 < t < T, \tag{I-1.2}$$

$$\varrho_F \frac{\partial v_z}{\partial t} - \mu_F \frac{1}{r}\frac{\partial}{\partial r}\left(r \frac{\partial v_z}{\partial r} \right) = -\frac{\partial p}{\partial z}, \qquad (z, r, t) \in \Omega(t),\ 0 < t < T, \tag{I-1.3}$$

with

$$p - p_{\text{ref}} = \left(\frac{hE}{R(1-\sigma^2)} K + p_{\text{ref}} \right) \frac{\eta}{R} + \frac{hC_v}{R^2} \frac{\partial \eta}{\partial t}, \quad 0 < z < L,\ 0 < t < T, \tag{I-1.4}$$

where

$$K = \begin{cases} 1 + \frac{h^2}{12R^2} & \text{for Koiter shell} \\ 1 & \text{for membrane.} \end{cases} \tag{I-1.5}$$

As we shall see later, equation (I-1.4) is the leading-order approximation of a cylindrical viscoelastic membrane/Koiter shell model. Problem (I-1.2)-(I-1.4) is supplemented by the following initial and boundary conditions

$$v_z(0, z, t) - \text{ bounded},\ v_z(R + \eta(z,t), z, t) = 0,\ v_z(r, z, 0) = v_z^0(r, z), \tag{I-1.6}$$

$$\eta(z, 0) = \eta^0(z),\ p(0, t) = P_0(t),\ p(L, t) = P_L(t). \tag{I-1.7}$$

Here ϱ_F is the fluid density, μ_F is the fluid dynamic viscosity coefficient, and p is the fluid pressure with p_{ref} denoting the pressure at which the reference configuration is assumed. The constants describing the structure properties are the Young's modulus of elasticity E, the Poisson ratio σ, the wall thickness h, and the structure viscoelasticity constant C_v. The first equation (I-1.2), derived from the conservation of mass, describes the transport of $(R + \eta)^2$ with the averaged fluid velocity $U := \dfrac{1}{(R+\eta)^2} \displaystyle\int_0^{R+\eta} v_z r dr$, while the second equation (I-1.3), describing the balance of momentum, incorporates diffusion due to the fluid viscosity which is dominant in the radial direction. The diffusion in the axial direction z is of order ϵ^2 and thus drops out from the leading-order effective equations. Furthermore, the nonlinear fluid advection term turns out to be of order ϵ, thereby appearing only in the ϵ-correction of the leading-order equations, which are easy to calculate. Thus, this models shows that the nonlinearity due to the fluid-structure coupling is dominant over the nonlinearity due to fluid advection. Equation (I-1.4) is the ϵ^2 approximation of the viscoelastic membrane equation and the viscoelastic shell equation (with different constant K), presented below in equations (I-2.5) and (I-2.4), respectively.

The hyperbolic waves described by the first equation might develop shock wave solutions since there is no smoothing in the second equation by the fluid viscosity in the axial direction. Nevertheless, the viscoelasticity of the structure given by the time-differentiated term in equation (I-1.4), which appears under the z-derivative in equation (I-1.3), will suffice to prevent shock formation in the vessel walls. As we shall see in this paper, we prove the existence of a weak solution to this moving-boundary problem near a configuration that corresponds to a straight vessel with radius R and fluid velocity $v_z = 0$. The spaces definding a weak solution reflect the parabolic degeneracy in the second equation and the mixed, hyperbolic-parabolic nature of the coupled problem.

This reduced problem has many interesting features. It captures the main properties of the fluid-structure interaction in blood flow with physiologically reasonable equations and data, while at the same time the problem is simple enough to allow fast computations and analysis related to its well-posedness. The design of a numerical method for this reduced problem is much simpler than for the full three-dimensional problem. The numerical algorithm, constructucted in [13], has the complexity of one-dimensional solvers, enabling fast and stable computation of a numerical solution to this fluid-structure interaction problem. Additionally, a comparison between the numerical results and the experimental measurements showed excellent agreement between the two [14].

We focus in this work on the proof of the existence of a solution to this effective fluid-structure interaction problem.

Within the past ten years there has been considerable progress in the analysis of fluid-structure interaction problems between an incompressible, viscous fluid and an elastic or viscoelastic structure. All the results that are related to an elastic structure interacting with a viscous fluid have been obtained under the assumption that the structure is entirely immersed in the fluid, see e.g., [17, 18, 21]. To our

knowledge, there have been no results showing existence of a solution to a fluid-structure interaction problem where an elastic structure is a part of the fluid boundary, which is the case, for example, in modeling blood flow through elastic arteries. Often times additional ad hoc terms of viscoelastic nature are added to the vessel wall model to provide stability and convergence of the underlying numerical algorithm [32, 34], or to provide enough regularity in the proof of the existence of a solution as in [16, 18, 28, 37]. Similarly, in [16, 17] terms describing bending (flexion) rigidity were added to provide smoothing mechanisms for the evolution of the structure displacement.

From the literature in which interaction between a viscoelastic structure and a viscous fluid is studied, the following two are the most closely related to our present work: the local in time existence of a strong, two-dimensional solution by da Vega in [37] and the existence of a weak solution for a viscoelastic plate interacting with a three-dimensional viscous incompressible fluid by Chambolle et al. in [16].

In [37] a two-dimensional problem was considered. The viscoelastic structure was a one-dimensional curve, satisfying the so called generalized string model, used by Quarteroni et al. in [34] to model the mechanical properties of vessel walls. This model involves the fourth-order derivative of the displacement with respect to the axial variable $\partial^4\eta/\partial z^4$ and the viscoelastic term of the form $\partial^3\eta/\partial t\partial z^2$. It was crucial for the existence proof that the coefficient in front of the viscoelastic term be strictly positive. Additional restriction in the existence proof was the requirement that the ratio of the density of the fluid over the density of the structure be sufficiently small, which is not the case in the blood flow application. (In the blood flow application the ratio is around 1.) Periodic boundary conditions in the axial direction were considered and the main forcing came from the initial displacement from the reference configuration.

In [16] the three-dimensional incompressible, viscous Navier-Stokes equations were coupled to the motion of a two-dimensional viscoelastic plate. The viscoelastic term

was in the form of the fifth-order derivative $\partial^5\eta/\partial t\partial z^4$. Again, it was crucial for the existence proof that the coefficient in front of the viscoelastic term be strictly positive. Additional assumption was used in this work requiring that the displacement from the structure never touches the bottom (fixed) surface of the domain. The main contribution from this work was in providing the existence of a weak solution with less regularity than those obtained in previous studies.

Both of these studies make use, in a crucial way, of the higher-order derivative terms describing the viscoelastic smoothing to prove the existence of a solution. These kinds of terms typically appear when modeling bending rigidity in "thin" structures. They provide better control in the energy estimates and give rise to higher regularity of solutions, provided that the data are smooth enough.

In the present work, we consider the structure equation (I-1.4) containing only the lowest-order derivative with respect to time of the displacement η. A model of this form was also considered by Pontrelli [33] and Armetano et al. [6, 7, 8] to discribe the viscoelasticity of vessel walls. In particular, the work of Armetano et al. provides the measurement data for the value of the viscoelastic coefficient appearing in this model. Thus, the viscoelastic model we consider here has additional importance related to the applicability of the model to the blood flow simulations. In [12] we showed that in cylindrical geometry, with axially symmetric flows, equation (I-1.4) is the model that arises in the limit, as $\epsilon \to 0$, of the coupling between the fluid and structure in the case of the viscoelastic membrane and the viscoelastic Koiter shell, when the fluid and the structure density are of the same order of magnitude (the physiologically relevant regime). More precisely, we showed that the bending rigidity terms of the (Koiter) shell and the acceleration of the shell and membrane are of order ϵ^2 or smaller, giving rise to (I-1.4) in both the membrane and the shell problem with a different coefficient K, corresponding to the two different cases. From the analysis point of view, dealing with only the lowest-order derivative terms in the structure model is more involving.

Nontrivial energy estimates are required to obtain enough control over the solution in order to prove its existence. Additional difficulty exists in this reduced model due to the lack of the fluid viscous regularization in the axial direction. Although this presents some problems in the analysis, it was this property that allowed us to use essentially one-dimensional arguments in the derivation of the energy estimates, substantially simplifying our arguments. Our main result states, in a nut shell, that if the initial displacement from the reference cylinder of radius R is small enough, and if the initial fluid velocity is small, and, furthermore, if the inlet and outlet pressure data are close to the reference pressure, then there exists a unique (mild) solution to the nonlinear moving boundary problem describing the leading-order fluid-structure interaction between an incompressible, viscous fluid and a viscoelastic structure of Kelvin-Voight type.

The main novelty of this work is in considering a problem with the viscoelastic smoothing in the structure equation described by the lowest possible time derivative appearing in the physiologically relevant equations allowing the use of measurements data to describe the viscoelastic arterial wall properties.

In the next section we show how the reduced, effective problem is related to the full three-dimensional axially symmetric problem, and present the details of the model(s) describing the viscoelastic structure.

2 Derivation of the Model Problem

We consider the Navier-Stokes equations for a viscous, incompressible fluid. Assuming cylindrical geometry and axially symmetric flow, the fluid velocity $\boldsymbol{v}(r,z,t) = (v_r(r,z,t), v_z(r,z,t))$ and pressure $p(r,z,t)$ satisfy

$$\rho_F\Big\{\frac{\partial v_r}{\partial t} + v_r\frac{\partial v_r}{\partial r} + v_z\frac{\partial v_r}{\partial z}\Big\} - \mu_F\left(\frac{\partial^2 v_r}{\partial r^2} + \frac{\partial^2 v_r}{\partial z^2} + \frac{1}{r}\frac{\partial v_r}{\partial r} - \frac{v_r}{r^2}\right) + \frac{\partial p}{\partial r} = 0, \quad \text{(I-2.1)}$$

$$\rho_F\Big\{\frac{\partial v_z}{\partial t} + v_r\frac{\partial v_z}{\partial r} + v_z\frac{\partial v_z}{\partial z}\Big\} - \mu_F\left(\frac{\partial^2 v_z}{\partial r^2} + \frac{\partial^2 v_z}{\partial z^2} + \frac{1}{r}\frac{\partial v_z}{\partial r}\right) + \frac{\partial p}{\partial z} = 0, \quad \text{(I-2.2)}$$

$$\frac{\partial v_r}{\partial r} + \frac{\partial v_z}{\partial z} + \frac{v_r}{r} = 0. \quad \text{(I-2.3)}$$

The Navier-Stokes equations hold in the cylindrical domain $\Omega(t)$.

To model the behavior of vessel walls we consider the cylindrical, linearly viscoelastic Koiter shell, and the cylindrical linearly viscoelastic membrane model under the assumption that the longitudinal displacement of the shell/membrane is negligible. A discussion showing why this is a reasonable assumption for the underlying application can be found in [31]. Denoting by η the radial displacement of the wall with respect to the reference configuration assumed for $r = R$, the equations for a linearly viscoelastic cylindrical Koiter shell read, [12]:

$$-f_r = \rho_w h\frac{\partial^2\eta}{\partial t^2} + E_0\eta - E_1\frac{\partial^2\eta}{\partial z^2} + E_2\frac{\partial^4\eta}{\partial z^4} + V_0\frac{\partial\eta}{\partial t} - V_1\frac{\partial^3\eta}{\partial t\partial z^2} + V_2\frac{\partial^5\eta}{\partial t\partial z^4} \quad \text{(I-2.4)}$$

where f_r is the radial component of the loading force, ρ_w denotes the shell (wall) density, h is the shell thickness, and

$$E_0 = \frac{h}{R^2}\frac{E}{1-\sigma^2}\left(1 + \frac{h^2}{12R^2}\right) + \frac{p_{\text{ref}}}{R}, \quad E_1 = 2\frac{h^3}{12R^2}\frac{E\sigma}{1-\sigma^2}, \quad E_2 = \frac{h^3}{12}\frac{E}{1-\sigma^2},$$
$$V_0 = \frac{h}{R^2}C_v\left(1 + \frac{h^2}{12R^2}\right), \qquad V_1 = 2\frac{h^3}{12R^2}D_v, \qquad V_2 = \frac{h^3}{12}C_v.$$

The constants C_v and D_v (the subscript v stands for "viscoelastic") correspond to the viscous counterparts of the Lamé constants of elasticity, see [12].

The equation for the dynamics of the pre-stressed, linearly viscoelastic cylindrical

membrane is given by:

$$-f_r = \rho_w h \frac{\partial^2 \eta}{\partial t^2} + \left(\frac{hE}{R^2(1-\sigma^2)} + p_{\text{ref}} \right) \eta + \frac{hC_v}{R^2} \frac{\partial \eta}{\partial t}. \tag{I-2.5}$$

Notice that the difference between the two models is in the terms involving h^3/R^2 accounting for the bending rigidity of the Koiter shell. See [12] for details.

We consider the time-dependent flow driven by the pressure drop between the inlet (z = 0) and the outlet boundary (z = L) and with the flow entering the tube parallel with the axis of symmetry. Equivalently, at the inlet and outlet of the tube we can prescribe the inlet and outlet dynamic pressure, with the radial component of the velocity equal to zero.

Inlet and Outlet Boundary Conditions (Fluid):

$$p + \rho(v_z)^2/2 = P_{0,L}(t) + p_{\text{ref}} \text{ and } v_r = 0 \text{at } z = 0, L. \tag{I-2.6}$$

At the inlet and outlet, we consider the structure diplacement fixed and equal to zero. In addition, for the Koiter shell model we need to prescribe one more condition. We consider the Koiter shell to be clamped.

Inlet and Outlet Boundary Conditions (Structure):

$$\eta(0,t) = \eta_0(t), \text{and } \eta(L,t) = \eta_L(t), \tag{I-2.7}$$

$$\frac{\partial \eta}{\partial z} = 0, \text{ at } z = 0, L \text{ (Koiter shell only)}. \tag{I-2.8}$$

Initially, we will be assuming "small" displacement from the reference configuration and the fluid and structure velocity "close" to zero.

Initial Conditions:

$$\boldsymbol{v}(r,z,0) = \boldsymbol{v}^0(r,z), \eta(z,0) = \eta^0(z), \frac{\partial \eta}{\partial t}(z,0) = \eta_t^0(z). \tag{I-2.9}$$

The coupling between the fluid and the structure is described by the lateral boundary conditions. We will be assuming the no-slip boundary condition requiring the

velocity of the fluid to be equal to the velocity of the structure, and the dynamic boundary condition requiring balance of the contact force at $\Sigma(t)$.

Lateral Boundary Conditions (Fluid-Structure Coupling):

$$v_r(R+\eta(z,t),z,t) = \frac{\partial \eta(z,t)}{\partial t}, \quad v_z(R+\eta(z,t),z,t) = 0. \tag{I-2.10}$$

$$f_r = \left[(p-p_{\text{ref}})\mathbf{I} - 2\mu_F D(\boldsymbol{v})\right]\boldsymbol{n}\cdot\boldsymbol{e}_r\left(1+\frac{\eta}{R}\right)\sqrt{1+(\partial_z\eta)^2}, \tag{I-2.11}$$

where f_r is given either by the viscoelastic shell model (I-2.4) or by the viscoelastic membrane model (I-2.5). The right-hand side of (I-2.11) describes the contact force of the fluid, $\boldsymbol{n}$ is the vector normal to the deformed boundary $\Sigma(t)$, and $\boldsymbol{e}_r$ is the radial unit vector. Tensor $D(\boldsymbol{v})$ is the symmetrized gradient of velocity, defined for an axially symmetric vector valued function $\boldsymbol{\varphi} = \varphi_r\boldsymbol{e}_r + \varphi_z\boldsymbol{e}_z$ as follows

$$D(\boldsymbol{\varphi}) = \begin{pmatrix} \dfrac{\partial\varphi_r}{\partial r} & 0 & \dfrac{1}{2}\Big(\dfrac{\partial\varphi_r}{\partial z}+\dfrac{\partial\varphi_z}{\partial r}\Big) \\ 0 & \dfrac{\varphi_r}{r} & 0 \\ \dfrac{1}{2}\Big(\dfrac{\partial\varphi_r}{\partial z}+\dfrac{\partial\varphi_z}{\partial r}\Big) & 0 & \dfrac{\partial\varphi_z}{\partial z} \end{pmatrix}. \tag{I-2.12}$$

See [13] for more details.

Assuming that the aspect ratio ϵ is small, using asymptotic analysis and homogenization theory for porous media flows, this three-dimensional, axially symmetric problem was reduced in [12] to an effective, closed problem with the leading-order approximation that is a nonlinear, moving-boundary problem of mixed, hyperbolic-parabolic type in two-space dimensions. The unknown functions are the leading-order approximations of the axial component of the velocity v_z, the pressure p and the radial displacement η. It was shown in [12] that the leading-order radial component of the velocity equals zero. Additionally, the pressure is hydrostatic to ϵ^2-order, and so p is independent of the radial variable.

Thus, we are looking for $v_z = v_z(r,z,t)$ defined on $\Omega(t)$, and $\eta = \eta(z,t)$ and $p = p(z,t)$, defined for $z \in (0,L), 0 < t < T$, such that

$$\frac{\partial(R+\eta)^2}{\partial t} + \frac{\partial}{\partial z}\int_0^{R+\eta} 2rv_z dr \;=\; 0, \tag{I-2.13}$$

$$\varrho_F \frac{\partial v_z}{\partial t} - \mu_F \frac{1}{r}\frac{\partial}{\partial r}\left(r\frac{\partial v_z}{\partial r}\right) = -\frac{\partial p}{\partial z}, \tag{I-2.14}$$

with

$$p - p_{\text{ref}} = \left(\frac{hE}{R(1-\sigma^2)}K + p_{\text{ref}}\right)\frac{\eta}{R} + \frac{hC_v}{R^2}K\frac{\partial \eta}{\partial t}, \tag{I-2.15}$$

where

$$K = \begin{cases} 1 + \frac{h^2}{12R^2} & \text{for Koiter shell} \\ 1 & \text{for membrane} \end{cases}$$

and the following initial and boundary conditions

$$v_z(0,z,t) - \text{ bounded},\ v_z(R+\eta(z,t),z,t) = 0,\ v_z(r,z,0) = v_z^0(r,z), \tag{I-2.16}$$

$$\eta(z,0) = \eta^0(z),\ p(0,t) = P_0(t),\ p(L,t) = P_L(t). \tag{I-2.17}$$

Equation (I-2.13) is the averaged conservation of mass equation, with the kinematic boundary condition (I-2.10) taken into account. Equation (I-2.14) is the leading-order balance of axial momentum. The dynamic lateral boundary condition (I-2.11) to the leading order is given by equation (I-2.15). Notice that the only difference between the leading-order fluid-structure interaction problem for the Koiter shell and the leading-order fluid-structure interaction problem for the membrane is in the coefficient K appearing in equation (I-2.15). This was proved in [12, 13]. The value of the viscoelastic constant C_v can be obtained from the measurements presented in [6, 7, 8], see [12].

Problem (I-2.13)-(I-2.17) is nonlinear in the first equation, and in the lateral boundary condition for v_z which is evaluated at the moving-boundary $r = R+\eta(z,t)$. Although this problem is still a problem in two spatial variables z and r plus time, with a singularity at $r = 0$ associated with the three-dimensional axially symmetric flows, system (I-2.13), (I-2.14) is still simpler than the original three-dimensional problem. In particular, the nonlinear term due to fluid advection does not appear in these equations, since, it was shown in [12] that it is of ϵ-order. The ϵ correction

of the reduced problem can be easily calculated once the zero-th order problem is solved, see [12].

This reduced problem reveals the main features of this fluid-structure interaction problem. It shows that the primary difficulties associated with the nonlinearities in the problem are due to the fluid-structure coupling, and not due to the nonlinear advection by the fluid.

In the next several section we will prove the existence of a unique (mild) solution to the reduced problem (I-2.13)-(I-2.17), denoted in the Introduction as (I-1.2)-(I-1.7).

3 Formulation of the Nonlinear Problem

We begin studying the existence of a weak solution to the nonliear moving-boundary problem (I-1.2)-(I-1.7) by first transforing the problem into a problem defined on a fixed domain. At the same time we will be introducing the non-dimensional variables to derive the corresponding nonlinear problem defined on a fixed domain in non-dimensional form.

To simplify notation we introduce

$$\gamma(z,t) := R + \eta(z,t).$$

Introduce the mapping

$$r \mapsto \frac{r}{\gamma} =: \tilde{r}$$

which maps $\Omega(t)$ onto the fixed domain $(\tilde{r}, z, t) \in (0,1) \times (0,L) \times (0,T)$. In addition, let us introduce the following scaling of the independent and dependent variables that will transform the problem to its non-dimensional form:

$$z = L\tilde{z},\ t = \tau\tilde{t},\ v_z = V\tilde{v_z},\ \eta = N\tilde{\eta},\ V = \frac{L}{\tau}.$$

Also, denote

$$\tilde{\gamma} = 1 + \frac{N}{R}\tilde{\eta},\ \text{so that } \gamma = R\tilde{\gamma},$$

and $\tilde{T} = T/\tau$. With these transformations, the problem is now defined on the scaled fixed domain

$$\tilde{\Omega} = \{(\tilde{r}\cos\vartheta, \tilde{r}\sin\vartheta, \tilde{z}) | \tilde{r} \in (0,1), \tilde{z} \in (0,1), \vartheta \in [0, 2\pi))\} \tag{I-3.1}$$

for the functions

$$\tilde{v}_z = \tilde{v}_z(\tilde{r}, \tilde{z}, \tilde{t}), \tilde{\gamma} = \tilde{\gamma}(\tilde{z}, \tilde{t}),$$

that satisfy the following **nonlinear, fixed-boundary problem** (in non-dimensional form) for $0 < \tilde{t} < \tilde{T}$:

$$\tilde{\gamma}\frac{\partial\tilde{\gamma}}{\partial\tilde{t}} + \frac{\partial}{\partial\tilde{z}}\int_0^1 \tilde{\gamma}^2\tilde{v}_z\tilde{r}\ d\tilde{r} = 0, \quad 0 < \tilde{z} < 1, \tag{I-3.2}$$

$$\frac{\partial \tilde{v}_z}{\partial \tilde{t}} - C_1 \frac{1}{\tilde{\gamma}^2} \frac{1}{\tilde{r}} \frac{\partial}{\partial \tilde{r}} \left(\tilde{r} \frac{\partial \tilde{v}_z}{\partial \tilde{r}} \right) - \frac{\tilde{r}}{\tilde{\gamma}} \frac{\partial \tilde{\gamma}}{\partial \tilde{t}} \frac{\partial \tilde{v}_z}{\partial \tilde{r}} = -C_2 \frac{\partial \tilde{\gamma}}{\partial \tilde{z}} - C_3 \frac{\partial^2 \tilde{\gamma}}{\partial \tilde{z} \partial \tilde{t}}, \quad (\tilde{z}, \tilde{r}) \in \tilde{\Omega}, \tag{I-3.3}$$

with

$$\begin{cases} \tilde{\gamma}(0, \tilde{t}) = \tilde{\gamma}_0(\tilde{t}), \ \tilde{\gamma}(1, \tilde{t}) = \tilde{\gamma_L}(\tilde{t}), \ \tilde{\gamma}(\tilde{z}, 0) = \tilde{\gamma}^0(\tilde{z}) \\ \tilde{v}_z(1, \tilde{z}, \tilde{t}) = 0, \tilde{v}_z(\tilde{r}, \tilde{z}, \tilde{t} = 0) = \tilde{v}_z^0(\tilde{r}, \tilde{z}), \ \left| \tilde{v}_z(0, \tilde{z}, \tilde{t}) \right| < +\infty. \end{cases} \tag{I-3.4}$$

where

$$C_1 = \frac{\mu_{_F} \tau}{\rho_{_F} R^2}, \ C_2 = \left(\frac{Eh}{(1-\sigma^2)R} K + p_{ref} \right) \frac{1}{V^2 \rho_{_F}}, \ C_3 = \frac{hC_v K}{RLV \rho_{_F}}. \tag{I-3.5}$$

The inlet and outlet data $\tilde{\gamma}_0$ and $\tilde{\gamma}_L$ are obtained from the pressure data $P_0(t)$ and $P_L(t)$ given in (I-1.7), by integrating the pressure-displacement relationship (I-1.4) with respect to t, and then transforming the result into the non-dimensional form. Thus, $\tilde{\gamma}_0$ and $\tilde{\gamma}_L$ are scaled by R. They describe the inlet and outlet deformation around the reference domain with radius $\tilde{r} = 1$. It is easy to see that one solution of this problem is given by the following:

Proposition I-3.1 *Functions $\tilde{\gamma} = R = 1$, $v_z = 0$ satisfy problem* (I-3.2)-(I-3.5) *with the initial data $\tilde{\gamma}^0 = R = 1$, $v_z^0 = 0$, and with boundary data $\tilde{\gamma}_0 = \tilde{\gamma_L} = R = 1$.*

We will show below, by using the Implicit Function Theorem, that problem (I-3.2)-(I-3.5) has a unique "mild" solution whenever the initial and boundary data are "close" to those listed in Proposition I-3.1, namely, whenever the inital and boundary displacement from the reference radius $r = R = 1$ is small and wheven the inital velocity v_z^0 is close to zero.

In the rest of this work (Chapters I and II), we will be working with the non-dimensional form of the problem. To simplify notation, the superscript "wiggle" that denotes the non-dimensional variables, will now be dropped, and this nomenclature will continue throughout the rest of the manuscript. Also, whenever R is used in the remainder of the paper, it refers to $R = 1$.

Mild Solution of the Nonlinear Problem

We will consider solutions of problem (I-3.2)-(I-3.5) with the initial and boundary data corresponding to the following spaces:

$$\gamma^0 \in H^1(0,1),\ v_z^0 \in H^1_{0,0}(\Omega, r),\ \gamma_0, \gamma_L \in H^2(0,T), \tag{I-3.6}$$

where

$$H^1_{0,0}(\Omega, r) = \Big\{ w \in L^2(\Omega, r) : \frac{\partial w}{\partial r} \in L^2(\Omega, r),\ \int_0^1 w\ r dr \in H^1(0,1), \\ w|_{r=1} = 0,\ |\ w|_{r=0}\ | < +\infty \Big\}.$$

The norm on $H^1_{0,0}(\Omega, r)$ is given by:

$$\|w\|^2_{H^1_{0,0}(\Omega,r)} = \int_\Omega \left(|w|^2 + \left| \frac{\partial w}{\partial r} \right|^2 \right)\ r dr dz + \int_0^1 \left| \frac{\partial}{\partial z} \int_0^1 w\ r dr \right|^2 dz.$$

Thus, we define the space of data Λ to be

$$\Lambda = H^1(0,1) \times H^1_{0,0}(\Omega, r) \times (H^2(0,T))^2. \tag{I-3.7}$$

In order to define a mild solution of problem (I-3.2)-(I-3.5) we introduce the solution space

$$X = X_1 \times X_2, \tag{I-3.8}$$

where X_1 is the space of the displacements

$$X_1 := \left\{ \gamma \in H^1(0,T; H^1(0,1)) \mid \partial_t \gamma \in L^\infty(0,T; L^2(0,1)) \right\},$$

and X_2 is the space of velocities

$$X_2 := \Big\{ v \in L^2(0,T; H^1_{0,0}(\Omega, r)) \cap L^\infty(0,T; L^2(\Omega, r)) \mid \partial_t v \in L^2(0,T; L^2(\Omega, r)), \\ \Delta_r v \in L^2(0,T; L^2(\Omega, r)), \partial^2_{z,z} < v > \in L^2(0,T; L^2(0,1)) \Big\}.$$

Here

$$< v >:= \int_0^1 v r dr.$$

Definition I-3.2 *Suppose that the initial data* $\gamma^0 \in H^1(0,1)$, $v_z^0 \in H^1_{0,0}(\Omega, r)$ *and that boundary data* $(\gamma_0, \gamma_L) \in (H^2(0,T))^2$. *Function* $(\gamma, v_z) \in X_1 \times X_2$ *is called a mild solution of problem* (I-3.2)-(I-3.5) *if* (I-3.2)-(I-3.5) *holds for a.a* $z \in (0,1), r \in [0,1)$ *and* $t \in (0,T)$, *namely, if*

$$\frac{1}{2}\frac{\partial(\gamma^2)}{\partial t} + \frac{\partial}{\partial z}\int_0^1 \gamma^2 v_z r dr = 0, \ a.e.\ z \in (0,1), t \in (0,T), \tag{I-3.9}$$

$$\frac{\partial v_z}{\partial t} - C_1\frac{1}{\gamma^2}\Delta_r v_z - \frac{r}{\gamma}\frac{\partial \gamma}{\partial t}\frac{\partial v_z}{\partial r} + C_2\frac{\partial \gamma}{\partial z} + C_3\frac{\partial^2 \gamma}{\partial z \partial t} = 0, \ a.e.\ (r,z) \in \Omega, t \in (0,T) \tag{I-3.10}$$

with

$$\begin{cases} \gamma(0,t) = \gamma_0(t), \ \gamma(1,t) = \gamma_L(t), \ \gamma(z,0) = \gamma^0(z) \\ v_z(1,z,t) = 0, v_z(r,z,0) = v_z^0(r,z), \ v_z(0,z,t) - bounded. \end{cases} \tag{I-3.11}$$

Chapter II

Existence of a Unique Solution to the Nonlinear Problem

1 The Framework

We aim at using the the Implicit Function Theorem of Hildebrandt and Graves [40] to prove the (local) existence of a mild solution in a neighborhood of the solution stated in Proposition I-3.1.

Theorem II-1.1 (Implicit Function Theorem [40]) *Suppose that:*

- $F : U(\lambda_0, x_0) \subset \Lambda \times X \to Z$ *is defined on an open neighborhood* $U(\lambda_0, x_0)$ *and* $F(\lambda_0, x_0) = 0$*, where* Λ, X, Z *are Banach spaces.*
- F_x *exists as a Frechét partial derivative on* $U(\lambda_0, x_0)$ *and*

$$F_x(\lambda_0, x_0) : X \to Z$$

  is bijective,

- F *and* F_x *are continuous at* (λ_0, x_0)*.*

Then the following are true:

- *Existence and uniqueness: There exist positive numbers* δ_0 *and* δ *such that for every* $\lambda \in \Lambda$ *satisfying* $\|\lambda - \lambda_0\| \leq \delta_0$ *there is exactly one* $x \in X$ *for which* $\|x - x_0\| \leq \delta$ *and* $F(\lambda, x(\lambda)) = 0$.

- *Continuity: If* F *is continuous in a neighborghood of* (λ_0, x_0)*, than* x *is continuous in a neighborhood of* λ_0.

2 The Mapping F

In order to use this theorem to prove the existence of a mild solution we first need to define the mapping F. To define F we first remark that we will consider the conservation of mass equation (I-3.9) as a condition which will be satisfied for all possible candidates for a solution (γ, v_z). More precisely, when considering the continuity of F and F_x and when showing the bijective property of F_x we will be "perturbing" our function F by a small source term f only in the balance of momentum equation, and not in the conservation of mass equation, preserving the conservation of mass property identically for all possible solutions, which is physically reasonable.

To define the mapping F we first notice that the conservation of mass equation (I-3.9) can be rewritten, by dividing equation (I-3.9) by γ, as a linear operator in γ $\mathcal{L}_{<v_z>}(\gamma^0, \gamma_0, \gamma_L)$, which to each given $< v_z >$ and initial and boundary data γ^0, γ_0 and γ_L associates the (unique) solution γ of the following linear transport problem:

$$\frac{\partial \gamma}{\partial t} + 2 < v_z > \frac{\partial \gamma}{\partial z} + \gamma \frac{\partial < v_z >}{\partial z} = 0, \tag{II-2.1}$$

with $\gamma(0,t) = \gamma_0(t)$ whenever $< v_z >$ is positive, $\gamma(1,t) = \gamma_L(t)$ whenever $< v_z >$ is negative, and $\gamma(z,0) = \gamma^0(z)$.

We will then define mapping F via the momentum equation (I-3.10) where γ in equation (I-3.10) is obtained from the conservation of mass "condition" (II-2.1).

Definition II-2.1 (Mapping F) *Let*

$$Z := L^2(0,T;L^2(\Omega,r)).$$

Define mapping

$$F : U((R,0,R,R),((R,0)) \subset \Lambda \times X \to Z,$$

which to each $((\gamma^0, v_z^0, \gamma_0, \gamma_L),(\gamma, v_z)) \in U((R,0,R,R),(R,0))$ *associates an* $f \in Z$

$$F : ((\gamma^0, v_z^0, \gamma_0, \gamma_L),(\gamma, v_z)) \mapsto f \tag{II-2.2}$$

where

$$F : ((\gamma^0, v_z^0, \gamma_0, \gamma_L),(\gamma, v_z)) := \frac{\partial v_z}{\partial t} - C_1 \frac{1}{\gamma^2}\Delta_r v_z - \frac{r}{\gamma}\frac{\partial \gamma}{\partial t}\frac{\partial v_z}{\partial r} + C_2 \frac{\partial \gamma}{\partial z} + C_3 \frac{\partial^2 \gamma}{\partial z \partial t}, \tag{II-2.3}$$

with γ *in* (II-2.3) *satisfying*

$$\frac{\partial \gamma}{\partial t} + 2 < v_z > \frac{\partial \gamma}{\partial z} + \gamma \frac{\partial < v_z >}{\partial z} = 0, \tag{II-2.4}$$

and with the initial and boundary conditions for γ *and* v_z *given by* (I-3.11).

Denote by $(\lambda_0, x_0) = ((R,0,R,R),(R,0))$. Then we see, by Proposition I-3.1, that

$$F(\lambda_0, x_0) = 0.$$

We will be using the Implicit Function Theorem to show the existence of a unique mild solution $(\gamma, v_z) \in X$ for each set of data $\lambda = (\gamma^0, v_z^0, \gamma_0, \gamma_L)$ in a neighborhood of $\lambda_0 = (R,0,R,R)$, by considering the small perturbations of our solution (λ_0, x_0) in the class of all the functions $(\gamma, v_z) \in X$ for which the incompressibility condition (I-3.2) is satisfied.

Proposition II-2.2 *Mapping* F *is continuous at* $(\lambda_0, x_0) = ((R,0,R,R),(R,0))$.

The proof is a direct consequence of the form of the left-hand side of (I-3.10) and of the continuous dependence of the solution γ of (I-3.9) on the coefficients depending

on $< v_z >$ and on the initial and boundary data. This implies that $\forall \varepsilon > 0$ there exists a $\delta > 0$ such that

$$\|((\gamma^0, v_z^0, \gamma_0, \gamma_L), (\gamma, v_z)) - ((R, 0, R, R), (R, 0))\|_{\Lambda \times X} < \delta \Rightarrow$$
$$\|(F((\gamma^0, v_z^0, \gamma_0, \gamma_L), (\gamma, v_z)) - (F((R, 0, R, R), (R, 0))\|_Z < \varepsilon.$$

3 The Frechét Derivative of F

With a slight obuse of notation, let us introduce the perturbations of γ and v_z around $\hat{\gamma}$ and $\hat{v}_z$, respectively, as follows:

$$\gamma = \hat{\gamma} + \delta\eta, \quad v_z = \hat{v}_z + \delta w_z, \quad \delta > 0.$$

Then the Frechét derivative of F with respect to $x = (\gamma, v_z)$ is a mapping

$$F_x((\hat{\gamma}^0, \hat{v}_z^0, \hat{\gamma}_0, \hat{\gamma}_L), (\hat{\gamma}, \hat{v}_z)) : X \to Z$$

defined by

$$F_x((\hat{\gamma}^0, \hat{v}_z^0, \hat{\gamma}_0, \hat{\gamma}_L), (\hat{\gamma}, \hat{v}_z))(\eta, w_z) := \frac{\partial w_z}{\partial t} - C_1 \frac{1}{\hat{\gamma}^2} \Delta_r w_z + C_1 \frac{2}{\hat{\gamma}^3} \eta \Delta_r \hat{v}_z \qquad \text{(II-3.1)}$$
$$- \frac{r}{\hat{\gamma}} \frac{\partial \eta}{\partial t} \frac{\partial \hat{v}_z}{\partial r} - \frac{r}{\hat{\gamma}} \frac{\partial \hat{\gamma}}{\partial t} \frac{\partial w_z}{\partial r} + \frac{r}{\hat{\gamma}^2} \eta \frac{\partial \hat{\gamma}}{\partial t} \frac{\partial \hat{v}_z}{\partial r} + C_2 \frac{\partial \eta}{\partial z} + C_3 \frac{\partial^2 \eta}{\partial z \partial t},$$

where η satisfies the linearized conservation of mass equation

$$\frac{\partial \eta}{\partial t} + 2 < \hat{v}_z > \frac{\partial \eta}{\partial z} + 2 < w_z > \frac{\partial \hat{\gamma}}{\partial z} + \hat{\gamma} \frac{\partial < w_z >}{\partial z} + \eta \frac{\partial < \hat{v}_z >}{\partial z} = 0, \qquad \text{(II-3.2)}$$

with

$$\begin{cases} \eta(0, t) = 0, \ \eta(1, t) = 0, \ \eta(z, 0) = 0, \\ w_z(1, z, t) = 0, w_z(r, z, 0) = 0, \ w_z(0, z, t) - \textit{bounded}. \end{cases} \qquad \text{(II-3.3)}$$

By similar arguments as those used for continuity of the mapping F one can see that the following is true.

Theorem II-3.1 *The Frechét derivative F_x is a continuous mapping from X to Z.*

4 Bijection of the Frechét Derivative

Next we show that the Frechét derivative, evaluated at (λ_0, x_0), is a bijection. From (II-3.2)-(II-3.3) we see that the Frechét derivative evaluated at $(\lambda_0, x_0) = ((R, 0, R, R), (R, 0))$ is given by the following

$$F_x((R,0,R,R),(R,0))(\eta, w_z) := \frac{\partial w_z}{\partial t} - C_1 \frac{1}{R^2} \Delta_r w_z + C_2 \frac{\partial \eta}{\partial z} + C_3 \frac{\partial^2 \eta}{\partial z \partial t}, \qquad \text{(II-4.1)}$$

where η satisfies

$$2\frac{\partial \eta}{\partial t} + R\frac{\partial}{\partial z} < w_z >= 0, \qquad \text{(II-4.2)}$$

with

$$\begin{cases} \eta(0,t) = 0,\ \eta(1,t) = 0,\ \eta(z,0) = 0, \\ w_z(1,z,t) = 0, w_z(r,z,0) = 0,\ w_z(0,z,t) - \textit{bounded}. \end{cases} \qquad \text{(II-4.3)}$$

Theorem II-4.1 *The Frechét derivative defined by* (II-4.2)-(II-4.3) *is a bijection from X to Z.*

To prove Theorem II-4.1 we will show that for every $f \in L^2(0,T; L^2(\Omega, r))$ and $(\eta, w_z^0, \eta_0, \eta_L) \in \Lambda$ there exists a unique solution $(\eta, w_z) \in X_1 \times X_2$ satisfying for a.e. $0 < z < 1, 0 \le r < 1, 0 \le t \le T$

$$\frac{\partial \eta}{\partial t} + R\frac{\partial}{\partial z} < w_z >= 0, \qquad \text{(II-4.4)}$$

$$\frac{\partial w_z}{\partial t} - \frac{C_1}{R^2} \triangle_r\, w_z + C_2 \frac{\partial \eta}{\partial z} + C_3 \frac{\partial^2 \eta}{\partial z \partial t} = f(r,z,t), \qquad \text{(II-4.5)}$$

with

$$\begin{cases} \eta(0,t) = 0,\ \eta(1,t) = 0,\ \eta(z,0) = 0 \\ w_z(1,z,t) = 0,\ w_z(0,z,t) - \text{bounded},\ w_z(r,z,0) = 0, \end{cases} \qquad \text{(II-4.6)}$$

This implies that the Frechét derivative defined by (II-3.1)-(II-4.3) is a bijection on X.

We will, in fact, show an even more general result:

Theorem II-4.2 *Let* $f \in L^2(0,T;L^2(\Omega,r))$ *and* $\eta_0, \eta_L \in H^2(0,T)$, $\eta^0 \in H^1(0,1)$ *and* $w_z^0 \in H^1_{0,0}(\Omega,r)$. *Then, there exists a unique (mild) solution* $(\eta, w_z) \in X_1 \times X_2$ *satisfying for a.e.* $0 < z < 1, 0 \le r < 1, 0 < t \le T$

$$\frac{\partial \eta}{\partial t} + R\frac{\partial}{\partial z} < w_z >= 0, \tag{II-4.7}$$

$$\frac{\partial w_z}{\partial t} - \frac{C_1}{R^2} \triangle_r \, w_z + C_2\frac{\partial \eta}{\partial z} + C_3\frac{\partial^2 \eta}{\partial z \partial t} = f(r,z,t), \tag{II-4.8}$$

with

$$\begin{cases} \eta(0,t) = \eta_0(t), \ \eta(1,t) = \eta_L(t), \ \eta(z,0) = \eta^0(z) \\ w_z(1,z,t) = 0, \ w_z(0,z,t) - \text{bounded}, \ w_z(r,z,0) = w_z^0(r,z). \end{cases} \tag{II-4.9}$$

This result motivated the choice of the parameter space Λ, given in (I-3.7).

To prove this result we proceed in two steps:

1. Show the existence of a unique *weak solution* to (II-4.7), (II-4.8) and (II-4.9).

2. Obtain energy estimates which provide higher regularily of the weak solution, giving rise to the *mild solution* $(\eta, w_z) \in X_1 \times X_2$ satisfying (II-4.7), (II-4.8) and (II-4.9) for almost all $0 < z < 1, 0 \le r < 1, 0 < t \le T$.

4.1 Existence of a Unique Weak Solution to the Linearized Problem.

Introduce the function $\bar{\eta}$ which satisfies the homogeneous boundary data at $z = 0$ and $z = 1$:

$$\bar{\eta} = \eta(z,t) - ((\eta_L(t) - \eta_0(t))z + \eta_0(t)). \tag{II-4.10}$$

Problem (II-4.4)-(II-4.9) can then be rewritten in terms of $\bar{\eta}$ as follows

$$\frac{\partial \bar{\eta}}{\partial t} + R\frac{\partial}{\partial z} < w_z >= -g_1, \tag{II-4.11}$$

$$\frac{\partial w_z}{\partial t} - \frac{C_1}{R^2} \triangle_r w_z + C_2 \frac{\partial \bar{\eta}}{\partial z} + C_3 \frac{\partial^2 \bar{\eta}}{\partial z \partial t} = f - g_2. \tag{II-4.12}$$

with

$$\begin{cases} \bar{\eta}(0,t) = 0, \ \bar{\eta}(1,t) = 0, \ \bar{\eta}(z,0) = (\eta_L(0) - \eta_0(0))z + \eta_0(0) = \bar{\eta}^0(z), \\ w_z(1,z,t) = 0, \ w_z(0,z,t) - \text{bounded}, \ w_z(r,z,0) = w^0(r,z), \end{cases} \tag{II-4.13}$$

where

$$\begin{cases} g_1(z,t) = ((\eta_L'(t) - \eta_0'(t))z + \eta_0'(t)), \\ g_2(r,z,t) = C_2(\eta_L(t) - \eta_0(t)) + C_3(\eta_L'(t) - \eta_0'(t)). \end{cases} \tag{II-4.14}$$

To define a weak solution introduce the following function spaces

$$\Gamma = H^1(0,T : L^2(0,1)), \tag{II-4.15}$$

$$V = \{w \in L^2(0,T : H^1_{0,0}(\Omega, r)) : \frac{\partial w}{\partial t} \in L^2(0,T : H^{-1}_{0,0}(\Omega, r))\}. \tag{II-4.16}$$

Definition II-4.3 *We say that* $(\bar{\eta}, w_z) \in \Gamma \times V$ *is a weak solution of* (II-4.11)-(II-4.14) *provided that for all* $\varphi \in H^1_0(0,1)$ *and* $\xi \in H^1_{0,0}(\Omega, r)$ *the following holds*

$$\int_0^1 \frac{\partial \bar{\eta}}{\partial t} \varphi \ dz - R \int_0^1 < w_z > \frac{\partial \varphi}{\partial z} \ dz = - \int_0^1 g_1 \varphi \ dz \tag{II-4.17}$$

$$\begin{aligned} &\int_\Omega \frac{\partial w_z}{\partial t} \xi \ r dr dz + \frac{C_1}{R^2} \int_\Omega \frac{\partial w_z}{\partial r} \frac{\partial \xi}{\partial r} \ r dr dz - C_2 \int_0^1 \bar{\eta} \ \frac{\partial}{\partial z} < \xi > \ dz, \\ &- C_3 \int_0^1 \frac{\partial \bar{\eta}}{\partial t} \ \frac{\partial}{\partial z} < \xi > \ dz = \int_0^1 f \varphi \ dz - \int_0^1 g_2 \varphi \ dz, \ a.e. \ 0 \le t \le T, \end{aligned} \tag{II-4.18}$$

with

$$\bar{\eta}(z,0) = \bar{\eta}^0(z), \quad w_z(r,z,0) = w_z^0(r,z). \tag{II-4.19}$$

We first show that for the boundary data η_0 and η_L in $H^1(0,T)$ and for the initial data $\eta^0 \in L^2(0,1)$, $w_z^0 \in L^2(\Omega, r)$, there exists a unique weak solution of (II-4.11)-(II-4.14).

Notice that the weak formulation of the problem reflects lack of regularity in the z-direction due to the parabolic degeneracy in the z-direction in the momentum equation (II-4.18) and due to the hyperbolic nature of the averaged conservation of mass equation (II-4.17). This will introduce various difficulties in the proof of the existence of a unique weak solution which we state next.

Theorem II-4.4 *Assume that the initial data* $\bar{\eta}^0$ *and* w_z^0 *satisfy* $\bar{\eta}^0 \in L^2(0,1)$ *and* $w_z^0 \in L^2(\Omega, r)$ *and that the boundary data* $\eta_0(t)$ *and* $\eta_L(t)$ *satisfy* $\eta_0, \eta_1 \in H^1(0,T)$. *Then there exists a unique weak solution* $(\bar{\eta}, w_z) \in \Gamma \times V$ *of* (II-4.11)-(II-4.14).

Proof. The proof is an application of the Galerkin method combined with the non-trivial energy estimates to deal with the lack of regularity in the z-direction. We present the proof in the following four steps:

1. Construction of the Galerking approximations.

2. Uniform energy estimates.

3. Weak convergence of a sub-sequence of Galerking approximations to a solution using compactness arguments.

4. Uniqueness of the weak solution.

Construction of the Galerkin Approximations: Let $\{\phi_k\}_{k=1}^{\infty}$ be the smooth functions which are orthogonal in $H_0^1(0,1)$, orthonormal in $L^2(0,1)$ and span the solution space for $\bar{\eta}$. Furthermore, let $\{w_k\}_{k=1}^{\infty}$ be the smooth functions which satisfy $w_k|_{r=1} = 0$, and are orthonormal in $L^2(\Omega, r)$ and span the solution space for the velocity w_z. Introduce the function space

$$C_{0,0}^k(\Omega) = \left\{ v \in C^k(\Omega) : v|_{r=1} = 0 \right\},$$

for any $k = 0, 1, ..., \infty$.

Fix positive integers m and n. We look for the functions $\bar{\eta}_m : [0,T] \to C_0^\infty(0,1)$ and $w_{z_n} : [0,T] \to C_{0,0}^\infty(\Omega)$ of the form

$$\bar{\eta}_m(t) = \sum_{i=1}^{m} d_i^m(t)\,\phi_i, \tag{II-4.20}$$

$$w_{z_n}(t) = \sum_{j=1}^{n} l_j^n(t)\,w_j, \tag{II-4.21}$$

where the coefficient functions d_h^m and l_k^n are chosen so that the functions $\bar{\eta}_m$ and w_{z_n} satisfy the weak formulation (II-4.17)-(II-4.19) of the linear problem (II-4.11)-(II-4.14), projected onto the finite dimensional subspaces spanned by $\{\phi_i\}$ and $\{w_j\}$ respectively:

$$\int_0^1 \frac{\partial \bar{\eta}_m}{\partial t}\phi_h\,dz - R\int_0^1 < w_{z_n} > \frac{\partial \phi_h}{\partial z}\,dz = -\int_0^1 g_1\phi_h\,dz \tag{II-4.22}$$

$$\begin{aligned}&\int_\Omega \frac{\partial w_{z_n}}{\partial t}w_k\,rdrdz + \frac{C_1}{R^2}\int_\Omega \frac{\partial w_{z_n}}{\partial r}\frac{\partial w_k}{\partial r}\,rdrdz - C_2\int_0^1 \bar{\eta}_m\,\frac{\partial}{\partial z} < w_k > \,dz \\ &- C_3\int_0^1 \frac{\partial \bar{\eta}_m}{\partial t}\,\frac{\partial}{\partial z} < w_k > \,dz = \int_\Omega f\xi_k\,dz - \int_\Omega g_2 w_k\,rdrdz\end{aligned} \tag{II-4.23}$$

for a.e $0 \le t \le T$, $h = 1, \cdots, m$ and $k = 1, \cdots, n$, and

$$\begin{cases} d_h^m(0) = \int_0^1 \bar{\eta}^0(z)\phi_h(z)dz, \\ l_k^n(0) = \int_\Omega w_z^0 w_k rdrdz. \end{cases} \tag{II-4.24}$$

The existence of the coefficient functions satisfying these requirements is guaranteed by the following Lemma.

Lemma II-4.5 *Assume that $f \in L^2(0,T;L^2(\Omega,r))$. For each $m = 1,2,...$ and $n = 1,2,...$ there exist unique functions $\bar{\eta}_m$ and w_{z_n} of the form (II-4.20) and (II-4.21), respectively, satisfying* (II-4.22)-(II-4.24). *Moreover*

$$(\bar{\eta}_m, v_{w_n}) \in C^1(0,T : C_0^\infty(0,1)) \times C^1(0,T : C_{0,0}^\infty(\Omega)).$$

Proof. To simplify notation, let us first introduce the following vector functions:

$$d^m(t) = \begin{pmatrix} d_1^m(t) \\ \vdots \\ d_m^m(t) \end{pmatrix}, \quad l^n(t) = \begin{pmatrix} l_1^n(t) \\ \vdots \\ l_n^n(t) \end{pmatrix}, \quad Y(t) = \begin{pmatrix} d^m(t) \\ l^n(t)) \end{pmatrix}. \tag{II-4.25}$$

Then, equation (II-4.22) written in matrix form reads:

$$A_1 d^{m'}(t) + A_2 l^n(t) = S_1(t), \tag{II-4.26}$$

where A_1 is an $m \times m$ matrix, A_2 an $m \times n$ matrix and S_1 an $m \times 1$ matrix defined by the following:

$$[A_1]_{h,i} = (\phi_i, \phi_h)_{L^2(0,1)} = \delta_{h,i}, \ [A_2]_{h,i} = -R\left(< w_j >, \frac{\partial \phi_h}{\partial z} \right)_{L^2(0,1)}$$

$$[S_1(t)]_{h,1} = (g_1, \phi_h)_{L^2(0,1)}$$

where $h, i = 1, ..., m$ and $j = 1, ..., n$. Similarly, equation (II-4.23) written in matrix form reads:

$$B_1 l^{n'}(t) + B_2 l^n(t) - B_3 d^m(t) - B_4 d^{m'}(t) = S_2(t), \tag{II-4.27}$$

where B_1 and B_2 are $n \times n$ matrices, B_3 and B_4 are $n \times m$ matrices, and $S_2(t)$ is an $n \times 1$ matrix defined by the following:

$$[B_1]_{k,j} = (w_j, w_k)_{L^2(\Omega,r)} = \delta_{k,j}, \ [B_2]_{k,j} = \frac{C_1}{R^2} \left(\frac{\partial w_j}{\partial r}, \frac{\partial w_k}{\partial r} \right)_{L^2(\Omega,r)},$$

$$[B_3]_{k,i} = C_2 \left(\frac{\partial}{\partial z} < w_k >, \phi_i \right)_{L^2(0,1)}, [B_4]_{k,i} = C_3 \left(\frac{\partial}{\partial z} < w_k >, \phi_i \right)_{L^2(0,1)},$$

$$[S_2(t)]_{k,1} = (f_2 - g_2, w_k)_{L^2(\Omega,r)},$$

where $k, j = 1, ..., n$ and $i = 1, ..., m$.

Equations (II-4.26) and (II-4.27) can be written together as the following system

$$\begin{cases} AY'(t) + BY(t) = S(t), \\ Y(0) = \begin{pmatrix} d^m(0) \\ \\ l_k^n(0) \end{pmatrix}, \end{cases} \tag{II-4.28}$$

where Y is defined in (II-4.25) and

$$A = \begin{pmatrix} A_1^{m\times m} & 0^{m\times n} \\ -B_4^{n\times m} & B_1^{n\times n} \end{pmatrix}_{(m+n)\times(m+n)},$$

$$B = \begin{pmatrix} 0^{m\times m} & A_2^{m\times n} \\ -B_3^{n\times m} & B_2^{n\times n} \end{pmatrix}_{(m+n)\times(m+n)},$$

$$S(t) = \begin{pmatrix} -S_1(t) \\ -S_2(t) \end{pmatrix}_{(m+n)\times 1}.$$

Function S incorporates the initial and boundary data obtained from the right hand-sides of equations (II-4.26) and (II-4.27).

To guarantee the existence of a solution $Y(t)$ of appropriate regularity first notice that linear independence of the sets $\{\phi_1, \cdots, \phi_m\}$ and $\{w_1, \cdots, w_n\}$ guarantees that the matrix $A(t)$ is nonsingular for all $t \in [0, T]$. Additionally, since the coefficient matrices are constant, there exists a unique C^1 function $Y(t) = (d^m(t), l^n(t))$ satisfying (II-4.28). Moreover $(\bar{\eta}_m, w_{z_n})$, defined via $d^m(t)$ and $l^n(t)$ in (II-4.20) and (II-4.21) respectively, solves (II-4.22)-(II-4.24) for all $0 \le t \le T$, thus

$$(\bar{\eta}_m, w_{z_n}) \in C^1(0, T : C_0^\infty(0, 1)) \times C^1(0, T : C_{0,0}^\infty(\Omega)).$$

This completes the proof of Lemma II-4.5.

Energy Estimate: We continue our proof of the existence of a weak solution to (II-4.11)-(II-4.14) by obtaining an energy estimate for $\bar{\eta}_m$ and w_{z_n} which is uniform in m and n. The estimate will bound the L^2-norms of $\bar{\eta}_m$ and w_{z_n}, the L^2-norms of $\frac{\partial w_{z_n}}{\partial r}$ and $\frac{\partial \bar{\eta}_m}{\partial t}$, and the $L^2(0, T; H_{0,0}^{-1}(\Omega, r))$-norm of $\frac{\partial w_{z_n}}{\partial t}$, in terms of the initial and boundary data and the coefficients of (II-4.11)-(II-4.13). Notice again the lack of information about the smoothness in z of the functions $\bar{\eta}$ and w_z.

Theorem II-4.6 *There exists a constant C depending on $1/R, T, C_2$, and C_3, such that*

$$\sup_{0\le t\le T}\left[\|w_{z_n}\|^2_{L^2(\Omega,r)}+\frac{C_2}{R}\|\bar\eta_m\|^2_{L^2(0,1)}\right]+\frac{2C_1}{R^2}\left\|\frac{\partial w_{z_n}}{\partial r}\right\|^2_{L^2(0,T;L^2(\Omega,r))} \tag{II-4.29}$$
$$+\frac{C_3}{R}\left\|\frac{\partial\bar\eta_m}{\partial t}\right\|^2_{L^2(0,T;L^2(0,1))}+\left\|\frac{\partial w_{z_n}}{\partial t}\right\|^2_{L^2(0,T;H^{-1}_{0,0}(\Omega,r))}\le C\left[\|\bar\eta^0\|^2_{L^2(0,1)}\right.$$
$$\left.+\left\|w^0_z\right\|^2_{L^2(0,T;L^2(\Omega,r))}+\|f\|^2_{L^2(0,T;L^2(\Omega,r))}+\|\eta_L-\eta_0\|^2_{H^1(0,T)}+\|\eta_0\|^2_{H^1(0,T)}\right].$$

Furthermore,

$$\frac{\partial}{\partial z}\int_0^1 w_{z_n}r dr\in L^2(0,T;L^2(0,1)), \tag{II-4.30}$$

and its $L^2(0,T;L^2(0,1))$-norm is bounded by the right-hand side of the energy estimate (II-4.29).

Proof. We aim at using the Gronwall's inequality. However, due to the lack of smoothness in z, it is impossible to control the terms with the z-derivative of $\bar\eta_m$. To deal with this problem, we manipulate the conservation of mass and balance of momentum equations in order to cancel the unwanted terms. The remaining terms, which we will estimate in terms of the data, will be those appearing in the estimate above.

We begin by first multiplying (II-4.23) by l^n_k and summing $k=1,\cdots,n$ to find

$$\frac{1}{2}\frac{d}{dt}\int_\Omega |w_{z_n}|^2\ r dr dz+\frac{C_1}{R^2}\int_\Omega\left|\frac{\partial w_{z_n}}{\partial r}\right|^2\ r dr dz-\underbrace{C_2\int_0^1\bar\eta_m\frac{\partial}{\partial z}<w_{z_n}>\ dz}_{(i)} \tag{II-4.31}$$
$$\underbrace{-C_3\int_0^1\frac{\partial\bar\eta_m}{\partial t}\frac{\partial}{\partial z}<w_{z_n}>\ dz}_{(ii)}=\int_\Omega f w_{z_n}\ r dr dz-\int_\Omega g_2 w_{z_n}\ r dr dz.$$

Multiply (II-4.22) by d^m_h and sum $h=1,\cdots,m$ to find

$$\frac{1}{2}\frac{d}{dt}\int_0^1|\bar\eta_m|^2\ dz-\underbrace{R\int_0^1<w_{z_n}>\frac{\partial\bar\eta_m}{\partial z}\ dz}_{(i)}=-\int_0^1 g_1\bar\eta_m\ dz. \tag{II-4.32}$$

Multiply (II-4.22) by $\dot{d}_h^m$ and sum $h = 1, \cdots, m$ to find

$$\int_0^1 \left|\frac{\partial \bar{\eta}_m}{\partial t}\right|^2 \, dz - \underbrace{R\int_0^1 < w_{z_n} > \frac{\partial^2 \bar{\eta}_m}{\partial t \partial z} \, dz}_{(ii)} = -\int_0^1 g_1 \frac{\partial \bar{\eta}_m}{\partial t} \, dz. \tag{II-4.33}$$

Multiply equation (II-4.32) by $\frac{C_2}{R}$ and (II-4.33) by $\frac{C_3}{R}$ and add those two resulting equations to equation (II-4.31) to obtain

$$\begin{aligned} &\frac{1}{2}\frac{d}{dt}\left[\int_\Omega |w_{z_n}|^2 \, rdrdz + \frac{C_2}{R}\int_0^1 |\bar{\eta}_m|^2 \, dz\right] + \frac{C_1}{R^2}\int_\Omega \left|\frac{\partial w_{z_n}}{\partial r}\right|^2 \, rdrdz \\ &+ \frac{C_3}{R}\int_0^1 \left|\frac{\partial \bar{\eta}_m}{\partial t}\right|^2 \, dz = \int_\Omega f w_{z_n} \, rdrdz - \int_\Omega g_2 w_{z_n} \, rdrdz \\ &- \frac{C_2}{R}\int_0^1 g_1 \bar{\eta}_m \, dz - \frac{C_3}{R}\int_0^1 g_1 \frac{\partial \bar{\eta}_m}{\partial t} \, dz. \end{aligned} \tag{II-4.34}$$

We can see that the terms denoted by (i) and (ii), which we cannot control, cancelled out. By using the Cauchy inequality to estimate the right-hand side of (II-4.34) we obtain

$$\begin{aligned} &\frac{1}{2}\frac{d}{dt}\left[\|w_{z_n}\|^2_{L^2(\Omega,r)} + \frac{C_2}{R}\|\bar{\eta}_m\|^2_{L^2(0,1)}\right] + \frac{C_1}{R^2}\left\|\frac{\partial w_{z_n}}{\partial r}\right\|^2_{L^2(\Omega,r)} + \frac{C_3}{2R}\left\|\frac{\partial \bar{\eta}_m}{\partial t}\right\|^2_{L^2(0,1)} \\ &\leq \|f_2\|^2_{L^2(\Omega,r)} + \frac{1}{4}\|g_2\|^2_{L^2(0,1)} + \frac{C_2+C_3}{2R}\|g_1\|^2_{L^2(0,1)} + \frac{1}{2}\|w_{z_n}\|^2_{L^2(\Omega,r)} + \frac{C_2}{2R}\|\bar{\eta}_m\|^2_{L^2(0,1)}. \end{aligned}$$

We are now in a position to apply the differential form of the Gronwall's inequality to obtain

$$\begin{aligned} &\sup_{0\leq t\leq T}\left[\|w_{z_n}\|^2_{L^2(\Omega,r)} + \frac{C_2}{R}\|\bar{\eta}_m\|^2_{L^2(0,1)}\right] + \frac{2C_1}{R^2}\int_0^T \left\|\frac{\partial w_{z_n}}{\partial r}\right\|^2_{L^2(\Omega,r)} \, dt \\ &+ \frac{C_3}{2R}\int_0^T \left\|\frac{\partial \bar{\eta}_m}{\partial t}\right\|^2_{L^2(0,1)} \, dt \leq \left[\frac{C_2}{R}\|\bar{\eta}^0\|^2_{L^2(0,1)} + \left\|w_z^0\right\|^2_{L^2(\Omega,r)} + 2\|f\|^2_{L^2(0,T:L^2(\Omega,r))}\right. \\ &\left.+\frac{1}{2}\|g_2\|^2_{L^2(0,T:L^2(0,1))} + \frac{C_2+C_3}{R}\|g_1\|^2_{L^2(0,T:L^2(0,1))}\right] e^{(1+\frac{C_2}{R})T}. \end{aligned}$$

Thus there exists a constant $C > 0$ depending on T, C_2, C_3 and $1/R$ such that

$$\sup_{0\leq t\leq T}\left[\|w_{z_n}\|^2_{L^2(\Omega,r)} + \frac{C_2}{R}\|\bar{\eta}_m\|^2_{L^2(0,1)}\right] + \frac{2C_1}{R^2}\int_0^T \left\|\frac{\partial w_{z_n}}{\partial r}\right\|^2_{L^2(\Omega,r)} \, dt$$

$$+\frac{C_3}{2R}\int_0^T \left\|\frac{\partial\bar{\eta}_m}{\partial t}\right\|^2_{L^2(0,1)} dt \le C\left[\|\bar{\eta}^0\|^2_{L^2(0,1)} + \left\|w_z^0\right\|^2_{L^2(\Omega,r)}\right.$$
$$\left. + \|f\|^2_{L^2(0,T:L^2(\Omega,r))} + \|\eta_1-\eta_0\|^2_{H^1(0,T)} + \|\eta_0\|_{H_0^1(0,T)}\right]. \tag{II-4.35}$$

We conclude the proof of the theorem stating the energy estimate by showing that

$$\frac{\partial w_{z_n}}{\partial t} \in L^2(0,T;H^{-1}_{0,0}(\Omega,r)),$$

and that $\partial v_{z_n}/\partial t$ satisfies the estimate (II-4.29).

Fix $\nu \in H^1_{0,0}(\Omega,r)$ such that $\|\nu\|_{H^1_{0,0}(\Omega,r)} \le 1$. Since $C^\infty_{0,0}(\Omega)$ is dense in $H^1_{0,0}(\Omega,r)$, we can write $\nu = \nu_1 + \nu_2$, where $\nu_1 \in$ span $\{w_j\}_{j=1}^n$ and $(\nu_2, w_j)_{L^2(\Omega,r)} = 0$ for $j = 1,\cdots,n$. Then (II-4.21) and (II-4.23) imply that for a.e. $0 \le t \le T$

$$\left|\int_\Omega \frac{\partial w_{z_n}}{\partial t}\nu\, rdrdz\right| \le \left[\frac{C_1}{R}\left\|\frac{\partial w_n}{\partial r}\right\|_{L^2(\Omega,r)} + C_2\left\|\bar{\eta}_m\right\|_{L^2}\right.$$
$$\left. + C_3\left\|\frac{\partial\bar{\eta}_m}{\partial t}\right\|_{L^2} + \|f\|_{L^2} + \|g_2\|_{L^2}\right]\|\nu\|_{H^1_{0,0}(\Omega,r)}.$$

Thus, since $\|\nu_1\|_{H^1_{0,0}(\Omega,r)} \le 1$, by using the energy estimate (II-4.35), we obtain that there exists a constant $\tilde{C}$ depending on $T, 1/R, C_2, C_3$ such that

$$\int_0^T \left\|\frac{\partial w_{z_n}}{\partial t}\right\|^2_{H^{-1}_{0,0}(\Omega,r)} dt \le \tilde{C}\left[\|\bar{\eta}^0\|^2_{L^2(0,1)} + \left\|w_z^0\right\|^2_{L^2(\Omega,r)}\right. \tag{II-4.36}$$
$$\left. + \|f\|^2_{L^2(0,T;L^2(\Omega,r))} + \|\eta_1-\eta_0\|^2_{H^1(0,T)} + \|\eta_0\|^2_{H_0^1(0,T)}\right].$$

This concludes the proof of Theorem II-4.6.

It is interesting to notice that the coefficient of the vessel wall viscosity, C_3, governs the estimate for the time-derivative of the structure displacement, which is to be expected. Thus, our estimate shows how the structure viscoelasticity regularizes the time evolution of the structure.

Also, notice that the right-hand side of the energy estimate incorporates the initial data for both the structure displacement and the structure velocity, but the boundary data for only the structure displacement. This is a consequence of the parabolic

denegeracy in the balance of momentum equation and is an interesting feature of this reduced, effective model.

To obtain the third step the proof of Theorem II-4.4 we use compactness arguments to pass to the weak limit of Galerkin approximations and show that the limiting functions satisfy (II-4.11)-(II-4.14) in the weak sense.

Weak convergence to a solution: We use the uniform energy estimate, presented in Theorem II-4.6, to conclude that there exist convergent subsequences that converge weakly to the functions which satisfy (II-4.11)-(II-4.14) in the weak sense. This is a standard approach except for the fact that we need to deal with the weighted L^2-norms in Ω, with the weight r that is present due to the axial symmetry of the problem. We deal with this technical obstacle by using the following Lemma, [1], with $p = 2$ and $\nu = 1$.

Lemma II-4.7 *[1] If* $\nu > 0,\ p \geq 1,$ *and* $u \in C^1(0, R)$ *then*

$$\int_0^R |u(r)|^p \, r^{\nu-1} dr \leq \frac{\nu+1}{\nu T} \int_0^R |u(r)|^p \, r^{\nu} dr + \frac{p}{\nu} \int_0^R |u(r)|^{p-1} \, |u'(r)| \, r^{\nu} dr.$$

By the energy estimate (II-4.29) we see that the sequence $\{\bar{\eta}_m\}_{m=1}^{\infty}$ is bounded in $H^1(0, T; L^2(0, 1))$. Similarly, $\{w_{z_n}\}_{n=1}^{\infty}$ is bounded in $L^2(0, T; H^1_{0,0}(\Omega, r))$ and that $\partial w_{z_n}/\partial t$ is bounded in $L^2(0, T; H^{-1}_{0,0}(\Omega, r)$.

Therefore, there exist convergent subsequences $\left\{\bar{\eta}_{m_j}\right\}_{m_j=1}^{\infty}$ and $\left\{w_{z_{n_j}}\right\}_{n_j=1}^{\infty}$ such that

$$\begin{cases} \eta_{m_j} \rightharpoonup \eta & \text{weakly in } H^1(0, T; L^2(0, 1)), \\ w_{z_{n_j}} \rightharpoonup w_z & \text{weakly in } L^2(0, T; L^2(\Omega, r)), \\ \dfrac{\partial w_{z_{n_j}}}{\partial r} \rightharpoonup \dfrac{\partial w_z}{\partial r} & \text{weakly in } L^2(0, T; L^2(\Omega, r)), \\ \dfrac{\partial w_{z_{n_j}}}{\partial t} \rightharpoonup \dfrac{\partial w_z}{\partial t} & \text{weakly in } L^2(0, T; H^{-1}_{0,0}(\Omega, r)). \end{cases} \tag{II-4.37}$$

We need to show that the limiting functions satisfy (II-4.11)-(II-4.14) in the weak sense. To show this, fix two integers M and N and consider the functions $\Phi \in$

$C^1([0,T]:H_0^1(0,1))$ and $\mathbf{w}\in C^1([0,T]:H_{0,0}^1(\Omega,r))$ of the form

$$\Phi(t)=\sum_{k=1}^{M}d_k(t)\phi_k,\quad \mathbf{w}(t)=\sum_{p=1}^{N}l_p(t)w_p,$$

where $\{d_k\}_{k=1}^M$ and $\{l_p\}_{p=1}^N$ are smooth functions. Let $n\geq N$ and $m\geq M$. Multiply (II-4.22) and (II-4.23), written in terms of the subsequences of $\bar{\eta}_m$ and w_{z_n}, by $d_k(t)$, $l_p(t)$, sum over k and p for $k=1,\cdots,N$ and $p=1,\cdots,M$ and then integrate over $(0,T)$ with respect to t to obtain

$$\int_0^T\int_0^1\frac{\partial\bar{\eta}_{m_j}}{\partial t}\Phi\ dzdt-R\int_0^T\int_0^1<w_{z_{n_i}}>\frac{\partial\Phi}{\partial z}\ dzdt=-\int_0^T\int_0^1 g_1\Phi\ dzdt,\quad\text{(II-4.38)}$$

and

$$\begin{aligned}&\int_0^T\int_\Omega\frac{\partial w_{z_{n_i}}}{\partial t}\mathbf{w}\ rdrdzdt+\frac{C_1}{R^2}\int_0^T\int_\Omega\frac{\partial w_{z_{n_i}}}{\partial r}\frac{\partial\mathbf{w}}{\partial r}\ rdrdzdt\qquad\text{(II-4.39)}\\&-C_2\int_0^T\int_0^1\bar{\eta}_{m_j}\frac{\partial}{\partial z}<\mathbf{w}>\ dzdt-C_3\int_0^T\int_0^1\frac{\partial\bar{\eta}_{m_j}}{\partial t}\frac{\partial}{\partial z}<\mathbf{w}>\ dzdt\\&=\int_0^T\int_\Omega f\mathbf{w}\ rdrdzdt-\int_0^T\int_\Omega g_2\mathbf{w}\ rdrdzdt.\end{aligned}$$

Take the weak limit as $i,j\to\infty$ to find that, in the limit, the following hold:

$$\int_0^T\int_0^1\frac{\partial\bar{\eta}}{\partial t}\Phi\ dzdt-R\int_0^T\int_0^1<w_z>\frac{\partial\Phi}{\partial z}\ dzdt=-\int_0^T\int_0^1 g_1\Phi\ dzdt,\quad\text{(II-4.40)}$$

and

$$\begin{aligned}&\int_0^T\int_\Omega\frac{\partial w_z}{\partial t}\mathbf{w}\ rdrdzdt+\frac{C_1}{R^2}\int_0^T\int_\Omega\frac{\partial w_z}{\partial r}\frac{\partial\mathbf{w}}{\partial r}\ rdrdzdt\qquad\text{(II-4.41)}\\&-C_2\int_0^T\int_0^1\bar{\eta}\frac{\partial}{\partial z}<\mathbf{w}>\ dzdt-C_3\int_0^T\int_0^1\frac{\partial\bar{\eta}}{\partial t}\frac{\partial}{\partial z}<\mathbf{w}>\ dzdt\\&=\int_0^T\int_\Omega f\mathbf{w}\ rdrdzdt-\int_0^T\int_\Omega g_2\mathbf{w}\ rdrdzdt.\end{aligned}$$

These equations hold for all the functions $\mathbf{w}\in L^2(0,T:H_{0,0}^1(\Omega,r))$ and $\Phi\in L^2(0,T:H_0^1(0,1))$. This implies that for all $\phi\in H_0^1(0,1)$ and $w\in H_{0,0}^1(\Omega,r)$ and $0\leq t\leq T$ the weak form of (II-4.22) and (II-4.23) is satisfied

$$\int_0^1\frac{\partial\bar{\eta}}{\partial t}\phi\ dz-R\int_0^1<w_z>\frac{\partial\phi}{\partial z}\ dz=-\int_0^1 g_1\phi\ dz,\qquad\text{(II-4.42)}$$

and

$$\int_\Omega \frac{\partial w_z}{\partial t} w \; r dr dz + \frac{C_1}{R^2}\int_\Omega \frac{\partial w_z}{\partial r}\frac{\partial w}{\partial r}\; r dr dz - C_2 \int_0^1 \bar{\eta}\frac{\partial}{\partial z} < w > \; dz \qquad \text{(II-4.43)}$$
$$- C_3 \int_0^1 \frac{\partial \bar{\eta}}{\partial t}\frac{\partial}{\partial z} < w > \; dz = \int_\Omega f w \; r dr dz - \int_\Omega g_2 w \; r dr dz.$$

Moreover, since $\frac{\partial \bar{\eta}}{\partial t} \in L^2(0,T : L^2(0,1))$, we have $\frac{\partial}{\partial z} < w_z > \in L^2(0,T : L^2(0,1))$.

To check that the limiting functions satisfy the initial data we proceed as follows. Let $\Phi \in C^1([0,T] : H_0^1(0,L))$ with $\Phi(T) = 0$. Integrate (II-4.40) by parts once with respect to t to obtain

$$\int_0^T \int_0^1 \bar{\eta}\frac{\partial \Phi}{\partial t}\; dz dt - R\int_0^T \int_0^1 < w_z > \frac{\partial \Phi}{\partial z}\; dz dt$$
$$- \int_0^1 \bar{\eta}\Phi \; dz|_{t=0} = -\int_0^T \int_0^1 g_1 \Phi \; dz dt.$$

Similarly from (II-4.38) we deduce

$$\int_0^T \int_0^1 \frac{\partial \bar{\eta}_{m_j}}{\partial t}\Phi \; dz dt - R\int_0^T \int_0^1 < w_{z_{n_i}} > \frac{\partial \Phi}{\partial z}\; dz dt$$
$$- \int_0^1 \bar{\eta}_{m_j}\Phi \; dz|_{t=0} = -\int_0^T \int_0^1 g_1 \Phi \; dz dt.$$

Set $m = m_j$ in the above equation, and let $m_j \to \infty$. Since $\Phi(0)$ is arbitrary, and because of the convergence (II-4.37) and the initial data (II-4.13) we conclude that $\bar{\eta}_m$ converges weakly to a function $\bar{\eta}$ which satisfies

$$\bar{\eta}(z,0) = \bar{\eta}^0(z).$$

A similar approach verifies the initial data for the limiting function w_z.

Therefore $(\bar{\eta}, w_z) \in \Gamma \times V$ is a weak solution of (II-4.11)-(II-4.13).

Uniqueness: Uniqueness of the weak solution is a direct consequence of the linearity of the problem.

This completes the proof of Theorem II-4.4.

Corollary II-4.8 *The energy estimate stated in Theorem II-4.6 implies that, in fact,*

$$\bar{\eta} \in L^\infty(0,T;L^2(0,1)) \cap H^1(0,T;L^2(0,1)), \tag{II-4.44}$$

$$w_z \in L^2(0,T;H^1_{0,0}(\Omega,r)) \cap L^\infty(0,T;L^2(\Omega,r)) \text{ with } \frac{\partial w_z}{\partial t} \in L^2(0,T;H^{-1}_{0,0}(\Omega,r)). \tag{II-4.45}$$

This proof completes the first step in the proof of Theorem II-4.1 which states that the Frechét derivative F_X is a bijective mapping from X to Z. What is left to show is that the weak solution has higher regularity and that it, in fact, belongs to the space X.

4.2 Higher Regularity of the Weak Solution of the Linearized Problem

To show that our weak solution $(\bar{\eta}, w_z)$ is actually in $X = X_1 \times X_2$ we proceed in two steps. First we show that the sequence $\{\frac{\partial w_{z_n}}{\partial t}\}_{n=1}^\infty$ is bounded in $L^2(0,T;L^2(\Omega,r))$, and then, using this information, we show that $(\bar{\eta}, w_z) \in X$. To show this improved regularity property of our weak solution we need to assume, as usual, some higher regularity of the initial and boundary data. The precise assumptions are given below.

We begin by first showing that $\{\frac{\partial w_{z_n}}{\partial t}\}_{n=1}^\infty$ is bounded in $L^2(0,T;L^2(\Omega,r))$.

Theorem II-4.9 *(Improved Regularity: Part I) Suppose that the boundary data $\eta_1, \eta_0 \in H^2(0,T)$ and the initial data $\bar{\eta}^0 \in L^2(0,1)$, $w_z^0 \in H^1_{0,0}(\Omega,r)$. Then the weak solution $(\bar{\eta}, w_z) \in \Gamma \times V$ belongs to*

$$\frac{\partial \bar{\eta}}{\partial t} \in L^\infty(0,T:L^2(0,1)),\ \frac{\partial w_z}{\partial r} \in L^\infty(0,T:L^2(\Omega,r)),\ \frac{\partial w_z}{\partial t} \in L^2(0,T:L^2(\Omega,r)).$$

Moreover, the following estimate holds

$$\sup_{0\le t\le T}\left[\frac{C_3}{R}\left\|\frac{\partial \bar{\eta}}{\partial t}\right\|^2_{L^2(0,1)} + \frac{2C_1}{R^2}\left\|\frac{\partial w_z}{\partial r}\right\|^2_{L^2(\Omega,r)}\right] + 2\int_0^T \left\|\frac{\partial w_z}{\partial t}\right\|^2_{L^2(\Omega,r)} ds \tag{II-4.46}$$

$$\le C\left(\|f\|^2_{L^2(0,T:L^2(\Omega,r))} + \|\eta_1-\eta_0\|^2_{H^2(0,T)} + \|\eta_0\|^2_{H^2(0,T)} + \left\|\bar{\eta}^0\right\|^2_{L^2(0,1)} + \left\|w_z^0\right\|^2_{H^1_{0,0}(\Omega,r)}\right).$$

where C depends on $1/R, C_2, C_3, T$.

Proof. Again we need to deal with the lack of regularity in the z direction by cancelling the terms which we cannot control at this point. As before, we need to manipulate the conservation of mass equation and the conservation of momentum equation in such as way that, when they are added up, the unwanted terms cancel out and produce an equation whose terms on the right hand-side can be estimated using the Cauchy's and Young's inequalities. The energy estimate will then follow by an application of the Gronwall's inequality.

Thus, we begin by multiplying (II-4.23) by $\dot{l}_k^n(t)$, and summing $k = 1, \cdots, n$ to find

$$\begin{aligned} &\int_\Omega \frac{\partial w_{z_n}}{\partial t}\frac{\partial w_{z_n}}{\partial t}\, rdrdz + \frac{C_1}{2R^2}\frac{d}{dt}\int_\Omega \frac{\partial w_{z_n}}{\partial r}\frac{\partial w_{z_n}}{\partial r}\, rdrdz \\ &+ \underbrace{C_2\int_\Omega \frac{\partial \bar{\eta}_m}{\partial z}\frac{\partial w_{z_n}}{\partial t}\, rdrdz}_{(a)} + \underbrace{C_3\int_\Omega \frac{\partial^2 \bar{\eta}_m}{\partial t \partial z}\frac{\partial w_{z_n}}{\partial t}\, rdrdz}_{(b)} \\ &= \int_\Omega f\frac{\partial w_{z_n}}{\partial t}\, rdrdz - \int_\Omega g_2 \frac{\partial w_{z_n}}{\partial t}\, rdrdz. \end{aligned} \tag{II-4.47}$$

Next, differentiate (II-4.22) with respect to t, multiply by $\dot{d}_h^m(t)$, and sum $h = 1, \cdots, m$ to get

$$\frac{1}{2}\frac{d}{dt}\int_0^1 \frac{\partial \bar{\eta}_m}{\partial t}\frac{\partial \bar{\eta}_m}{\partial t}\, dz - \underbrace{R\int_\Omega \frac{\partial w_{z_n}}{\partial t}\frac{\partial^2 \bar{\eta}_m}{\partial t \partial z}\, rdrdz}_{(b)} = -\int_0^1 \frac{\partial g_1}{\partial t}\frac{\partial \bar{\eta}_m}{\partial t}\, dz. \tag{II-4.48}$$

Finally, differentiate (II-4.22) with respect to t, multiply by $d_h^m(t)$, and sum $h = 1, \cdots, m$ to find

$$\int_0^1 \frac{\partial^2 \bar{\eta}_m}{\partial t^2}\bar{\eta}_m\, dz - \underbrace{R\int_{\Omega,r} \frac{\partial w_{z_n}}{\partial t}\frac{\partial \bar{\eta}_m}{\partial z}\, rdrdz}_{(a)} = -\int_0^1 \frac{\partial g_1}{\partial t}\bar{\eta}_m\, dz. \tag{II-4.49}$$

Multiply (II-4.48) and (II-4.49) by $\frac{C_3}{R}$ and $\frac{C_2}{R}$, respectively, and add them to (II-4.47). We obtain

$$\frac{1}{2}\frac{d}{dt}\left[\frac{C_3}{R}\left\|\frac{\partial \bar{\eta}_m}{\partial t}\right\|^2_{L^2(0,1)} + \frac{C_1}{R^2}\left\|\frac{\partial w_{z_n}}{\partial r}\right\|^2_{L^2(\Omega,r)}\right] + \left\|\frac{\partial w_{z_n}}{\partial t}\right\|^2_{L^2(\Omega,r)} \tag{II-4.50}$$

$$= \int_\Omega f \frac{\partial w_{z_n}}{\partial t}\, r dr dz - \int_\Omega g_2 \frac{\partial w_{z_n}}{\partial t}\, r dr dz - \frac{C_2}{R}\int_0^1 \frac{\partial g_1}{\partial t}\bar{\eta}_m\, dz$$
$$- \frac{C_3}{R}\int_0^1 \frac{\partial g_1}{\partial t}\frac{\partial \bar{\eta}_m}{\partial t}\, dz + \frac{C_2}{R}\int_0^1 \frac{\partial^2 \bar{\eta}_m}{\partial t^2}\bar{\eta}_m\, dz.$$

Before we estimate the right-hand side of this equation, we will integrate the entire equation with respect to t in order to deal with the term on the right-hand side which contains the second derivative with respect to t of $\bar{\eta}_m$. We obtain

$$\frac{1}{2}\left[\frac{C_3}{R}\left\|\frac{\partial \bar{\eta}_m(t)}{\partial t}\right\|^2_{L^2(0,1)} + \frac{C_1}{R^2}\left\|\frac{\partial w_{z_n}(t)}{\partial r}\right\|^2_{L^2(\Omega,r)}\right] + \int_0^t \left\|\frac{\partial w_{z_n}}{\partial s}\right\|^2_{L^2(\Omega,r)} ds \qquad \text{(II-4.51)}$$
$$= \int_0^t\int_\Omega f\frac{\partial w_{z_n}}{\partial s}\, r dr dz ds - \int_0^t\int_\Omega g_2\frac{\partial w_{z_n}}{\partial s}\, r dr dz ds - \frac{C_2}{R}\int_0^t\int_0^1 \frac{\partial g_1}{\partial s}\bar{\eta}_m\, dz ds$$
$$- \frac{C_3}{R}\int_0^t\int_0^1 \frac{\partial g_1}{\partial s}\frac{\partial \bar{\eta}_m}{\partial s}\, dz ds + \frac{C_2}{R}\int_0^t\int_0^1 \frac{\partial^2 \bar{\eta}_m}{\partial s^2}\bar{\eta}_m\, dz ds$$
$$+ \frac{1}{2}\left[\frac{C_3}{R}\left\|\frac{\partial \bar{\eta}_m(0)}{\partial t}\right\|^2_{L^2(0,1)} + \frac{C_1}{R^2}\left\|\frac{\partial w_{z_n}(0)}{\partial r}\right\|^2_{L^2(\Omega,r)}\right].$$

We estimate first four terms on the right-hand side as follows

$$\left|\int_0^t\int_\Omega f\frac{\partial w_{z_n}}{\partial s}\, r dr dz ds\right| \le \|f\|^2_{L^2(0,t:L^2(\Omega,r))} + \frac{1}{4}\left\|\frac{\partial w_{z_n}}{\partial s}\right\|^2_{L^2(0,t:L^2(\Omega,r))},$$

$$\left|\int_0^t\int_\Omega g_2\frac{\partial w_{z_n}}{\partial s}\, r dr dz ds\right| \le \|g_2\|^2_{L^2(0,t:L^2(\Omega,r))} + \frac{1}{4}\left\|\frac{\partial w_{z_n}}{\partial s}\right\|^2_{L^2(0,t:L^2(\Omega,r))},$$

$$\left|\frac{C_2}{R}\int_0^t\int_0^1 \frac{\partial g_1}{\partial s}\bar{\eta}_m\, dz ds\right| \le \frac{C_2}{2R}\left(\left\|\frac{\partial g_1}{\partial s}\right\|^2_{L^2(0,t:L^2(0,1))} + \|\bar{\eta}_m\|^2_{L^2(0,t:L^2(0,1))}\right),$$

$$\left|\frac{C_3}{R}\int_0^t\int_0^1 \frac{\partial g_1}{\partial s}\frac{\partial \bar{\eta}_m}{\partial s}\, dz ds\right| \le \frac{C_3}{2R}\left(\left\|\frac{\partial g_1}{\partial s}\right\|^2_{L^2(0,t:L^2(0,1))} + \left\|\frac{\partial \bar{\eta}_m}{\partial s}\right\|^2_{L^2(0,t:L^2(0,1))}\right).$$

To estimate the fifth term, we integrate by parts with respect to t to obtain

$$-\frac{C_2}{R}\int_0^t\int_0^1 \frac{\partial^2 \bar{\eta}_m}{\partial s^2}\bar{\eta}_m\, dz ds = \frac{C_2}{R}\int_0^t\int_0^1 \left|\frac{\partial \bar{\eta}_m}{\partial s}\right|^2 dz ds$$
$$-\frac{C_2}{R}\int_0^1 \frac{\partial \bar{\eta}_m(z,t)}{\partial t}\bar{\eta}_m(z,t)\, dz + \frac{C_2}{R}\int_0^1 \frac{\partial \bar{\eta}_m(z,0)}{\partial t}\bar{\eta}_m(z,0)\, dz$$

$$= \frac{C_2}{R}\int_0^t\int_0^1 \left|\frac{\partial\bar\eta_m}{\partial s}\right|^2\,dzds - \frac{C_2}{R}\int_0^1 \frac{\partial\bar\eta_m(z,t)}{\partial t}\bar\eta_m(z,t)\,dz$$
$$-\frac{C_2}{R}\int_0^1 g_1(0)\bar\eta_m(z,0)\,dz - C_2R\int_0^1\frac{\partial}{\partial z} < w_{z_n} > (z,0)\eta_m(z,0)\,dz.$$

This implies

$$\left|\frac{C_2}{R}\int_0^t\int_0^1 \frac{\partial^2\bar\eta_m}{\partial s^2}\bar\eta_m\,dzds\right| \le \tilde K\left(\left\|\frac{\partial\bar\eta_m}{\partial s}\right\|^2_{L^2(0,T:L^2(0,1))} + \|\bar\eta_m(t)\|^2_{L^2(0,1)}\right.$$
$$\left. + \left\|\bar\eta^0\right\|^2_{H^1(0,1)} + \left\|w_z^0\right\|^2_{H^1_{0,0}(\Omega,r)} + \|g_1(0)\|^2_{L^2(0,1)}\right) + \frac{C_3}{4R}\left\|\frac{\partial\bar\eta_m(t)}{\partial t}\right\|^2_{L^2(0,1)}$$

where $\tilde K > 0$ depends on $C_2, C_3, 1/C_3, 1/R, R$.

The last two terms in (II-4.51) can be estimated by first using the conservation of mass equation (II-4.22) to obtain

$$\int_0^1 \frac{\partial\bar\eta_m(0)}{\partial t}\frac{\partial\bar\eta_m(0)}{\partial t}dz = -\int_0^1\frac{\partial}{\partial z} < w_{z_n}(0) > \frac{\partial\bar\eta_m(0)}{\partial t}\,dz - \int_0^1 g_1(0)\frac{\partial\bar\eta_m(0)}{\partial t}\,dz.$$

and then by Cauchy's inequality

$$\int_0^1\left|\frac{\partial\bar\eta_m(0)}{\partial t}\right|^2 dz \le \left\|\frac{\partial}{\partial z} < w_z^0 >\right\|^2_{L^2(0,1)} + \|g_1(0)\|^2_{L^2(0,1)}$$

to obtain

$$\frac{1}{2}\left[\frac{C_3}{R}\left\|\frac{\partial\bar\eta_m(0)}{\partial t}\right\|^2_{L^2(0,1)} + \frac{C_1}{R^2}\left\|\frac{\partial w_{z_n}(0)}{\partial r}\right\|^2_{L^2(\Omega,r)}\right] \le$$
$$\tilde C\left(\left\|w_z^0\right\|^2_{H^1_{0,0}(\Omega,r)} + (\eta_1'(0)-\eta_0'(0))^2 + (\eta_0'(0))^2\right)$$

where $\tilde C > 0$ depends on $C_1, C_3, 1/R$.

By combining these estimates and by using the energy estimate stated in Theorem II-4.6 we see that there exists a constant $C > 0$ depending on $C_1, C_2, C_3, 1/R, R$ such that

$$\frac{C_3}{4R}\left\|\frac{\partial\bar\eta_m(t)}{\partial t}\right\|^2_{L^2(0,1)} + \frac{C_1}{2R^2}\left\|\frac{\partial w_{z_n}(t)}{\partial r}\right\|^2_{L^2(\Omega,r)} + \frac{1}{2}\int_0^t\left\|\frac{\partial w_{z_n}}{\partial s}\right\|^2_{L^2(\Omega,r)}ds$$
$$\le C(\|f\|^2_{L^2(0,T:L^2(\Omega,r))} + \|\eta_1-\eta_0\|^2_{H^2(0,T)} + \|\eta_0\|^2_{H^2(0,T)} + \left\|\bar\eta^0\right\|^2_{H^1(0,1)}$$

$$+ \left\|w_z^0\right\|^2_{L^2_{0,0}(\Omega,r)} + |\eta_1'(0) - \eta_0'(0)|^2 + (\eta_0'(0))^2)$$

for a.e $0 \leq t \leq T$. Passing to the limit as $m \to \infty$ and $n \to \infty$ we recover the estimate (II-4.46). This completes the proof of Theorem II-4.9.

Next we show that the weak solution $(\bar{\eta}, w_z)$ is, in fact a *mild solution*, namely, that $(\bar{\eta}, w_z) \in X$ under some additional assumptions on the smoothness of the initial data. It is in this step that we can finally take control over certain derivatives with respect to z of our solution.

Theorem II-4.10 *(Improved regularity: Part II) Assume, in addition to the assumptions of Theorem II-4.9, that the initial data $\bar{\eta}^0 \in H^1(0,1)$. Then the weak solution $\bar{\eta}$ satisfies $\bar{\eta} \in H^1(0,T;H^1(0,1))$. Furthermore, the following estimate holds:*

$$\sup_{0\leq t\leq T} \frac{C_2C_3}{12}\left\|\frac{\partial\bar{\eta}}{\partial z}\right\|^2_{L^2(0,1)} + \frac{C_3^2}{12}\left\|\frac{\partial^2\bar{\eta}}{\partial t\partial z}\right\|^2_{L^2(0,T:L^2(0,1)} \tag{II-4.52}$$
$$\leq C\left(\|f\|^2_{L^2(0,T:L^2(\Omega,r))} + \|\eta_1 - \eta_0\|^2_{H^2(0,T)} + \|\eta_0\|^2_{H^2(0,T)} + \left\|\bar{\eta}^0\right\|^2_{H^1(0,1)} + \left\|w_z^0\right\|^2_{H^1_{0,0}(\Omega)}\right),$$

where C depends on $1/R, C_2, C_3, T$. This implies that, in fact,

$$\frac{\partial^2 < w_z >}{\partial z^2} \in L^2(0,T:L^2(0,1)), \quad \Delta_r w_z \in L^2(0,T:L^2(\Omega,r)). \tag{II-4.53}$$

Proof. The proof is based on the following idea. We will use the weak form of the momentum equation (II-4.23) to estimate $\partial\bar{\eta}/\partial z$ and $\partial^2\bar{\eta}/\partial z\partial t$. In order to obtain the desired estimate, we will substitute the test function w_k in the weak form of the momentum equation (II-4.23) by $(1-r)\frac{\partial\phi_k(z)}{\partial z} \in C^1_{0,0}(\Omega)$. We will then use the fact that

$$(1-r)\frac{\partial^2\bar{\eta}_m}{\partial z\partial t} = (1-r)\sum_{k=1}^m \dot{d}_k^m(t)\frac{\partial\phi_k(z)}{\partial z} = \sum_{k=1}^m \dot{d}_k^m(t)\underbrace{(1-r)\frac{\partial\phi_k(z)}{\partial z}}_{w_k(r,z)},$$

where

$$w_k(r,z) = (1-r)\frac{\partial\phi_k(z)}{\partial z} \in C^1_{0,0}(\Omega,r). \tag{II-4.54}$$

Notice that, without loss of generality, we could have used the space $C^1_{0,0}$ in the definition of the Galerkin approximation for the velocity, instead of the space $C^\infty_{0,0}$. Thus, everything obtained will hold assuming $w_k \in C^1_{0,0}$. This relaxed choice of the space for w_k is now important to obtain improved regularity.

We now proceed by substituting w_k in (II-4.23) with (II-4.54) and by multiplying equation (II-4.23) by $\dot{d}^m_k(t)$ and summing over $k = 1, ...m$ to obtain

$$\begin{aligned}
&\int_\Omega \frac{\partial w_{z_n}}{\partial t}\frac{\partial^2 \bar{\eta}_m}{\partial z \partial t}\ (1-r)rdrdz - \frac{C_1}{R^2}\int_\Omega \frac{\partial w_{z_n}}{\partial r}\frac{\partial^2 \bar{\eta}_m}{\partial z \partial t}\ rdrdz \qquad \text{(II-4.55)}\\
&+ C_2\int_\Omega \frac{\partial \bar{\eta}_m}{\partial z}\frac{\partial^2 \bar{\eta}_m}{\partial z \partial t}\ (1-r)rdrdz + C_3\int_\Omega \left|\frac{\partial \bar{\eta}_m}{\partial z \partial t}\right|^2\ (1-r)rdrdz\\
&= \int_\Omega f\frac{\partial^2 \bar{\eta}_m}{\partial z \partial t}\ (1-r)rdrdz - \int_\Omega g_2\frac{\partial^2 \bar{\eta}_m}{\partial z \partial t}\ (1-r)rdrdz.
\end{aligned}$$

Multiplying (II-4.55) by C_3, we have

$$\begin{aligned}
&\frac{C_2C_3}{12}\frac{d}{dt}\left\|\frac{\partial \bar{\eta}_m}{\partial z}\right\|^2_{L^2(0,1)} + \frac{C_3^2}{6}\left\|\frac{\partial^2 \bar{\eta}_m}{\partial t \partial z}\right\|^2_{L^2(0,1)} \qquad \text{(II-4.56)}\\
&= -C_3\int_\Omega \frac{\partial w_{z_n}}{\partial t}(1-r)\frac{\partial^2 \bar{\eta}_m}{\partial t \partial z}\ rdrdz + \frac{C_1C_3}{R^2}\int_\Omega \frac{\partial w_{z_n}}{\partial r}\frac{\partial^2 \bar{\eta}_m}{\partial t \partial z}\ rdrdz\\
&+ C_3\int_\Omega f(1-r)\frac{\partial^2 \bar{\eta}_m}{\partial t \partial z}\ rdrdz + C_3\int_\Omega g_2\frac{\partial^2 \bar{\eta}_m}{\partial t \partial z}\ (1-r)rdrdz.
\end{aligned}$$

By Cauchy inequality

$$\left|C_3\int_\Omega \frac{\partial w_{z_n}}{\partial t}(1-r)\frac{\partial^2 \bar{\eta}_m}{\partial t \partial z}\ rdrdz\right| \leq \left\|\frac{\partial w_{z_n}}{\partial t}\right\|^2_{L^2(\Omega,r)} + \frac{C_3^2}{48}\left\|\frac{\partial^2 \bar{\eta}_m}{\partial t \partial z}\right\|^2_{L^2(0,1)},$$

$$\left|\frac{C_1C_3}{R^2}\int_\Omega \frac{\partial w_{z_n}}{\partial r}\frac{\partial^2 \bar{\eta}_m}{\partial t \partial z}\ rdrdz\right| \leq \frac{6C_1^2}{R^4}\left\|\frac{\partial w_{z_n}}{\partial r}\right\|^2_{L^2(\Omega,r)} + \frac{C_3^2}{48}\left\|\frac{\partial^2 \bar{\eta}_m}{\partial t \partial z}\right\|^2_{L^2(0,1)},$$

$$\left|C_3\int_\Omega f(1-r)\frac{\partial^2 \bar{\eta}_m}{\partial t \partial z}\ rdrdz\right| \leq \|f\|^2_{L^2(\Omega,r)} + \frac{C_3^2}{48}\left\|\frac{\partial^2 \bar{\eta}_m}{\partial t \partial z}\right\|^2_{L^2(0,1)},$$

$$\left|C_3\int_\Omega g_2(1-r)\frac{\partial^2 \bar{\eta}_m}{\partial t \partial z}\ rdrdz\right| \leq \frac{1}{2}\|g_2\|^2_{L^2(0,1)} + \frac{C_3^2}{48}\left\|\frac{\partial^2 \bar{\eta}_m}{\partial t \partial z}\right\|^2_{L^2(0,1)}.$$

By combining the above estimates, by using the differential form of Gronwall's inequality, and by employing the improved regularity estimate (II-4.46) we obtain

$$\begin{aligned}
&\frac{C_2C_3}{12}\sup_{0\le t\le T}\left\|\frac{\partial\bar{\eta}_m}{\partial z}\right\|^2_{L^2(0,1)}+\frac{C_3^2}{12}\int_0^T\left\|\frac{\partial^2\bar{\eta}_m}{\partial t\partial z}\right\|^2_{L^2(0,1)}dt\\
&\le C(\|f\|^2_{L^2(0,T:L^2(\Omega,r))}+\|\eta_1-\eta_0\|^2_{H^2(0,T)}+\|\eta_0\|^2_{H^2(0,T)}+\left\|\bar{\eta}^0\right\|^2_{H^1(0,1)}\\
&+\left\|w_z^0\right\|^2_{H^1_{0,0}(\Omega)}+|\eta_1'(0)-\eta_0'(0)|^2+(\eta_0'(0))^2).
\end{aligned}$$

Passing to limit we recover the desired estimate (II-4.52). Moreover since $\bar{\eta}\in H^1(0,T;H^1(0,1))$, from equations (II-4.11) and (II-4.12), we conclude (II-4.53). This concludes the proof of Theorem II-4.10.

With this proof we have completed the second step in showing that problem (II-4.7)-(II-4.9) has a unique mild solution. This result implies, in particular, that the Frechét derivative is a bijection from X to Z and, thus, completes the proof of Theorem II-4.1.

This result now completes the verification of all the properties of the mapping F and its Frechét derivative F_X so that the Implicit Function Theorem II-1.1 can be used to deduce the existence of a unique, mild solution to the nonlinear, moving boundary problem (I-2.13)-(I-2.17).

5 Main Result

In order to state the main result of this chapter in terms of the pressure inlet and outlet boundary data as formulated in (I-2.17) we remark that the condition on the boundary data $\eta_0,\eta_L\in H^2(0,T)$ translates into the following condition in terms of the pressure $P_0,P_L\in H^3(0,T)$. This is due to the pressure-displacement relationship (I-2.15). Thus, we introduce the corresponding parameter space

$$\tilde{\Lambda}:=H^1(0,L)\times H^1_{0,0}(\Omega,r)\times(H^1(0,T))^2, \tag{II-5.1}$$

and recall the solution space

$$X = X_1 \times X_2,$$

where

$$X_1 := \left\{ \gamma \in H^1(0,T;H^1(0,1)) \mid \partial_t \gamma \in L^\infty(0,T;L^2(0,1)) \right\},$$

and X_2 is the space of velocities

$$X_2 := \left\{ v \in L^2(0,T;H^1_{0,0}(\Omega,r)) \cap L^\infty(0,T;L^2(\Omega,r)) \mid \partial_t v \in L^2(0,T;L^2(\Omega,r)), \right.$$
$$\left. \Delta_r v \in L^2(0,T;L^2(\Omega,r)), \partial^2_{z,z} < v > \in L^2(0,T;L^2(0,1)) \right\}.$$

By using the results from Chapters I and II, the Implicit Function Theorem II-1.1 implies:

Theorem II-5.1 (Main Result) *Assume that the initial data for the displacement η from the reference cylinder of radius R, η^0, is in $H^1(0,L)$, and that the initial data for the axial component of the velocity, v_z^0, is in $H^1_{0,0}(\Omega,r)$. Furthermore, suppose that the inlet and outlet pressure data $P_0(t)$ and $P_L(t)$ which correspond to the fluctuations of the pressure around the reference pressure p_{ref}, stated in* (I-2.17)*, are such that $P_0, P_L \in H^1(0,T)$. Then, there exists a neighborhood $S(0,0) \subset X$ around the solution $\eta = 0, v_z = 0$, and a neighborhood $D(0,0,p_{\text{ref}},p_{\text{ref}}) \subset \tilde{\Lambda}$ around the initial and boundary data $\eta^0 = 0, v_z^0 = 0, P_0 = p_{\text{ref}}, P_L = p_{\text{ref}}$ such that there exists exactly one solution $(\eta, v_z) \in S(0,0) \subset X$ for each choice of the initial data $(\eta^0, v_z^0, P_0, P_L) \in D(0,0,p_{\text{ref}},p_{\text{ref}}) \subset \tilde{\Lambda}$.*

This completes the work, presented in this Thesis in Chapters I and II, related to the study of fluid-structure interaction between a viscous, incompressible fluid and a viscoelastic structure, in the flow regimes associated with blood flow in medium-to-large human arteries.

In the remaining two Chapters we will study some mathematical properties of Bingham fluid flows in cylinders. Bingham fluid models have been used to study

blood flow in arterioles and capillaries, and so we continue the presentation of this Ph.D. work by focusing on the fluids with the rheology which can be associated to that of blood flow in small blood vessels.

Chapter III

Some Mathematical Properties of the Solution of Bingham Fluid Flows in Cylinders

1 Introduction

Bingham fluids are materials which behave as rigid bodies at low shear stress but flow as viscous fluids at high shear stress. The name is due to Eugene C. Bingham who, for the first time, proposed a mathematical description for this visco-plastic behavior [10]. Common examples of Bingham fluids are tooth paste and paint. The Bingham model has also been used to describe the blood flow in small vessels, such as arterioles and capillaries, where the size of the vessel diameter is comparable to the size of blood cells, see e.g. [38]. Since the pulsatile motion of the capillaries as well as arterioles is negligible, in this section we focus on a study of Bingham fluid flow in a cylinder with fixed walls.

The *isothermal* and *unsteady flow* of an *incompressible Bingham visco-plastic medium,* during the time interval $(0, T)$, is modeled by the following system of equa-

tions (clearly of the *Navier-Stokes* type):

$$\varrho[\partial_t \mathbf{u} + (\mathbf{u}\cdot\nabla)\mathbf{u}] = \nabla\cdot\boldsymbol{\sigma} + \mathbf{f} \quad \text{in } \Omega\times(0,T), \tag{III-1.1}$$

$$\nabla\cdot\mathbf{u} = 0 \quad \text{in } \Omega\times(0,T), \tag{III-1.2}$$

$$\boldsymbol{\sigma} = -p\mathbf{I} + \sqrt{2}g\mathbf{D}(\mathbf{u})/|\mathbf{D}(\mathbf{u})| + 2\mu\mathbf{D}(\mathbf{u}), \tag{III-1.3}$$

$$\mathbf{u}(0) = \mathbf{u}_0 \quad (\text{with } \nabla\cdot\mathbf{u}_0 = 0). \tag{III-1.4}$$

Here Ω is an open and connected subset of $\mathbb{R}^N$ ($N = 2$ or 3 in applications), and Γ is the boundary of Ω.

For simplicity, we shall consider only *Dirichlet boundary conditions*, namely:

$$\mathbf{u} = \mathbf{u}_B \text{ on } \Gamma\times(0,T), \text{ with } \int_\Gamma \mathbf{u}_B(t)\cdot\mathbf{n}\,d\Gamma = 0, \text{ a.e. on } (0,T). \tag{III-1.5}$$

In system (III-1.1)-(III-1.5):

- ϱ (resp., μ and g) is the *density* (resp., are the *viscosity* and *plasticity yield*) of the Bingham medium; we have $\varrho > 0$, $\mu > 0$ and $g > 0$.
- $\mathbf{f}$ is a density of external forces.
- $\mathbf{D}(\mathbf{v}) = \frac{1}{2}[\nabla\mathbf{v} + (\nabla\mathbf{v})^t] (= D_{ij}(\mathbf{v})_{1\le i,j\le N})$, $\forall \mathbf{v}\in(H^1(\Omega))^N$.
- $|\mathbf{D}(\mathbf{v})|$ is the *Frobenius norm* of tensor $\mathbf{D}(\mathbf{v})$, i.e.,

$$|\mathbf{D}(\mathbf{v})| = \left(\sum_{1\le i,j\le N} |D_{ij}(\mathbf{v})|^2\right)^{\frac{1}{2}}.$$

- $\mathbf{n}$ is the outward unit normal vector at Γ.
- We have denoted (and will denote later on) by $\varphi(t)$ the function $x \to \varphi(x,t)$.

We observe that if $g = 0$, system (III-1.1)-(III-1.5) reduces to the Navier-Stokes equations modeling isothermal incompressible Newtonian viscous fluid flow.

The *isothermal* and *unsteady axial* flow of an *incompressible visco-plastic Bingham fluid* in an infinitely long cylinder of (bounded) *cross section* Ω is a particular case of (III-1.1)-(III-1.5). The problem is (formally) modeled by the following *nonlinear parabolic* equation (where Γ is the boundary of Ω):

$$\begin{cases} \varrho \partial_t u - \mu \nabla^2 u - g \nabla \cdot (\nabla u / |\nabla u|) = C \quad \text{in } \Omega \times (0,T), \\ u = 0 \quad \text{on } \Gamma \times (0,T), \\ u(0) = u_0. \end{cases} \tag{III-1.6}$$

In system (III-1.6):

- u is the *axial flow velocity*, i.e., $\mathbf{u} = \{0, 0, u\}$, assuming that the fluid flows in the Ox_3-direction, Ω being parallel to the (Ox_1, Ox_2)-plane.
- C is the *pressure drop* per unit length (it is a function of t, only, and possibly a constant).

System (III-1.6) can be seen as a generalization of the following system:

$$\begin{cases} \dfrac{\partial u}{\partial t} = \operatorname{div}\left(\dfrac{Du}{|Du|}\right) \quad \text{in } Q = (0,\infty) \times \Omega \\ u(t,x) = 0 \quad \text{on } S = (0,\infty) \times \Gamma \\ u(0,x) = u_0(x) \quad \text{in } x \in \Omega. \end{cases} \tag{III-1.7}$$

System (III-1.7) represents the Dirichlet problem for the *total variation flow*. Problems related to total variation flows arise not only in continuum mechanics, but also in material science [30] and image processing [35].

Existence and uniqueness of solutions to system (III-1.7) have been obtained in [2, 3, 29]. Solutions to system (III-1.7) also enjoy some interesting properties, such as finite extinction time (meaning that $u(t) \to 0$ in a finite time) and no propagation of the support of the initial datum (meaning that the support of the normalized solution $u(t,x)/\|u(t,x)\|_{L^2(\Omega)}$ is equal to the support of the initial datum), see e.g. [2, 3, 29].

In the present work, we are going to use numerical simulations to investigate whether the properties of finite extinction time and no propagation of the support of the initial datum apply also to system (III-1.6) and, if yes, to which extent. We emphasize here that the model for total variation flow, see system (III-1.7), can be obtained from the model for Bingham flow in cylinders, see system (III-1.6), by setting fluid viscosity and pressure drop equal to zero, namely $\mu = 0$ and $C = 0$, and by setting the ratio between fluid density and plasticity yield equal to one, namely $\varrho/g = 1$.

2 Total Variation Flow. Properties of Solutions.

In this section we will summarize some of the main theorems concerning the solutions to total variation flow problems of the form (III-1.7). We start by introducing the definition of some useful functional spaces, ad then we will present the main theorems.

2.1 Total Variation Flow. Functional Spaces.

Let Ω be a bounded set in $\mathbb{R}^N$ with Lipschitz continuous boundary Γ. A function u defined in Ω is said to be a *function of bounded variation* if $u \in L^1(\Omega)$ and its partial derivatives (in the sense of distributions) are measures with finite total variation in Ω. The class of such functions will be denoted by $BV(\Omega)$. Thus $u \in BV(\Omega)$ if and only if there are Radon measures $\mu_1, \cdots, \mu_N$ defined in Ω, with finite total mass in Ω, and

$$\int_\Omega u D_i \varphi dx = -\int_\Omega \varphi d\mu_i$$

for all $\varphi \in C_0^\infty(\Omega)$, $i = 1, \ldots, N$. Thus the gradient of u is a vector-valued measure with finite total variation

$$|Du|(\Omega) = \sup\left\{\int_\Omega u \ \mathrm{div}\varphi dx : \varphi \in C_0^\infty(\Omega, \mathbb{R}^n), |\varphi(x)| \leq 1 \text{ for } x \in \Omega\right\}.$$

Let us now define the set

$$X(\Omega) = \left\{ z \in L^\infty(\Omega, \mathbb{R}^N) : \ \mathrm{div}(z) \in L^1(\Omega) \right\}.$$

If $z \in X(\Omega)$ and $w \in BV(\Omega) \cap L^\infty(\Omega)$ the functional $(z, Dw) : C_0^\infty(\Omega) \to \mathbb{R}$ is defined by the formula

$$< (z, Dw), \varphi >= -\int_\Omega w\varphi \mathrm{div}(z) dx - \int_\Omega wz \cdot \nabla\varphi dx.$$

Then (z, Dw) is a Radon measure in Ω,

$$\int_\Omega (z, Dw) = \int_\Omega z \cdot \nabla w dx$$

for all $w \in W^{1,1}(\Omega) \cap L^\infty(\Omega)$ and

$$\left| \int_B (z, Dw) \right| \leq \int_B |(z, Dw)| \leq \|z\|_\infty \int_B |Dw|$$

for any Borel set $B \subseteq \Omega$. Moreover, (z, Dw) is absolutely continuous with respect to $|Dw|$ with Radon-Nikodym derivative $\theta(z, Dw, x)$ which is a $|Dw|$ measurable function from Ω to $\mathbb{R}$ such that

$$\int_B (z, Dw) = \int_B \theta(z, Dw, x)|Dw|(\Omega)$$

for any Borel set $B \subseteq \Omega$. Moreover

$$\|\theta(z, Dw, \cdot)\|_{L^\infty(\Omega, ||Dw||)} \leq ||z||_{L^\infty(\Omega, \mathbb{R}^N)}.$$

In [5] a weak trace on Γ of the normal component of $z \in X(\Omega)$ is defined. Concretely, it is proved that there exists a linear operator $\gamma : X(\Omega) \to L^\infty(\Gamma)$ such that

$$||\gamma(z)||_\infty \leq ||z||_\infty,$$
$$\gamma(z)(x) = z(x) \cdot n(x) \quad \text{for all } \ x \in \Gamma \ \text{ if } \ z \in C^1(\bar{\Omega}, \mathbb{R}^N).$$

We shall denote $\gamma(z)(x)$ by $[z, n](x)$. Moreover the following Green's formula, relating the function $[z, n]$ and the measure (z, Dw) for $z \in X(\Omega)$ and $w \in BV(\Omega) \cap L^\infty(\Omega)$, is established:

$$\int_\Omega w \ \mathrm{div}(z) dx + \int_\Omega (z, Dw) = \int_\Gamma [z, n] \ w \ dH^{N-1}, \qquad \text{(III-2.1)}$$

where H^{N-1} is the Hausdorff $(N-1)$-dimensional measure in $\mathbb{R}^N$. We denote by $L^1_w(0,T;BV(\Omega))$ the space of functions $w:[0,T]\to BV(\Omega)$ such that $w\in L^1((0,T)\times\Omega)$, the maps $t\in[0,T]\to<Dw(t),\phi>$ are measurable for every $\phi\in C^1_0(\Omega,\mathbb{R}^N)$ and such that $\int_0^T\|Dw(t)\|\,dt<\infty$. See details in [4].

For any compact subset $\mathcal{K}$ of Ω, let $\mathcal{D}_{\mathcal{K}}(\Omega)$ be the set of all functions $f\in C^\infty_0(\Omega)$ such that $\mathrm{supp}(f)\subseteq\mathcal{K}$. We denote by $\mathcal{D}'(\Omega)$ the set of all linear functional $\mathcal{T}$ defined and continuous on $\mathcal{D}(\Omega)$ where

$$\mathcal{D}(\Omega)=\cap_{\mathcal{K}\subseteq\Omega}\mathcal{D}_{\mathcal{K}}(\Omega).$$

The linear functional $\mathcal{T}$ ls called a distribution in Ω. See details in [39].

2.2 Total Variation Flow. Overview of the Related Main Results.

The theorem below concerns existence and uniqueness of solutions [3].

Theorem III-2.1 *Let $u_0\in L^2(\Omega)$. Then for every $T>0$ there exists a unique weak solution to problem* (III-1.7) *in $(0,T)\times\Omega$ such that $u(0)=u_0$. Moreover, the solution to problem* (III-1.7) *is characterized as $u\in C([0,T],L^2(\Omega))\cap W^{1,2}_{loc}(0,T;L^2(\Omega))$, $u\in L^1_w(0,T;BV(\Omega))$, and there exists $z(t)\in X(\Omega)$, such that $\|z(t)\|_\infty\le 1$, $u'(t)=\mathrm{div}(z(t))$ in $\mathcal{D}'(\Omega)$ a.e. $t\in(0,T)$ and*

$$\int_\Omega(z(t),Du(t))=|Du(t)|(\Omega) \tag{III-2.2}$$

$$[z(t),n]\in\mathrm{sign}(-u(t))\quad H^{N-1}\text{-a.e. on }\Gamma. \tag{III-2.3}$$

Finally, we have the following comparison principle: if $u(t)$ and $\hat u(t)$ are solutions corresponding to the initial data u_0 and $\hat u_0$, respectively, then

$$\|(u(t)-\hat u(t))^+\|_1\le\|(u_0-\hat u_0)^+\|_1\quad\textit{and}\quad\|u(t)-\hat u(t)\|_1\le\|u_0-\hat u_0\|_1, \tag{III-2.4}$$

for all $t\in[0,T]$.

More general versions of Theorem III-2.1 can be found in [9] and [19].

The following theorem proves the existence of a finite extinction time for solutions to problem (III-1.7). The theorem also provides upper bounds for the extinction time and the L^∞-norm of the solution [4].

Theorem III-2.2 *Let $u_0 \in L^\infty(\Omega)$ and let $u(t,x)$ be the unique solution to problem* (III-1.7). *Let $d(\Omega)$ be the smallest radius of a ball containing Ω. Then we have*

$$\|u(t)\|_\infty \leq \frac{N}{d(\Omega)} \left(\frac{d(\Omega)\,\|u_0\|_\infty}{N} - t \right)^+ . \tag{III-2.5}$$

Moreover, if $T^*(u_0) = \inf\{t > 0 : u(t) = 0\}$, then

$$T^*(u_0) \leq \frac{d(\Omega)\,\|u_0\|_\infty}{N} . \tag{III-2.6}$$

An explicit solution $u(t,x)$ can be obtained if the support of u_0 is contained in a ball $B(0,r) \subset\subset \Omega$, where $\chi_{B(0,r)}$ is the characteristic function of $B(0,r)$.

The following Lemma was proved in [4].

Lemma III-2.3 *Assume that $B(0,r) \subset\subset \Omega$ and let $u_0 = \kappa\chi_{B(0,r)}$. Then the unique solution $u(t,x)$ to problem* (III-1.7) *is given by*

$$u(t,x) = \operatorname{sign}(k)\frac{N}{r} \left(\frac{|k|r}{N} - t \right)^+ \chi_{B(0,r)}(x) . \tag{III-2.7}$$

We remark that the support of the solution $u(t,x)$ is the same as the support of the initial datum u_0, namely $\chi_{B(0,r)}$. In this sense, there is no propagation of the support of the initial datum. Next, we are going to prove a lemma similar to Lemma III-2.3, but for a slightly more general problem. The result of this lemma will be used for comparison with numerical experiments.

Lemma III-2.4 *Assume that $B(0,r) \subset\subset \Omega$ and let $u_0 = \kappa\chi_{B(0,r)}$, where $\chi_{B(0,r)}$ is*

the characteristic function of $B(0,r)$. *Then the unique solution* $u(t,x)$ *to problem*

$$\begin{cases} \dfrac{\partial u}{\partial t} = \beta \ \mathrm{div}\left(\dfrac{Du}{|Du|}\right) & \text{in } Q = (0,\infty)\times\Omega \\ u(t,x) = 0 \quad \text{on } S = (0,\infty)\times\Gamma \\ u(0,x) = u_0(x) \quad \text{in } x \in \Omega, \end{cases} \tag{III-2.8}$$

with $\beta > 0$, *is given by*

$$u(t,x) = \mathrm{sign}(k)\frac{N}{r}\left(\frac{|k|r}{\beta N} - t\right)^{+}\chi_{B(0,r)}(x). \tag{III-2.9}$$

Proof. The proof of this lemma follows the ideas presented in [4]. Suppose that $k > 0$ (if $k < 0$ the solution can be constructued in a similar way). We look for a solution to (III-2.8) of the form $u(t,x) = \alpha(t)\chi_{B(0,r)}(x)$ on some time interval $(0,T)$. Then, we shall look for some $z(t) \in X(\Omega)$ with $\|z\|_\infty \le 1$ such that

$$u'(t) = \ \beta \ \mathrm{div}(z(t)) \quad \text{in } \mathcal{D}'(\Omega), \tag{III-2.10}$$

$$\int_\Omega (z(t), Du(t)) = |Du(t)|(\Omega), \tag{III-2.11}$$

$$[z(t), n] \in \mathrm{sign}(-u(t)) \quad H^{N-1} - \text{a.e.} \tag{III-2.12}$$

If we take $z(t)(x) = \frac{-x}{r}$ for $x \in \partial B(0,r)$, integrating the equation (III-2.10) we obtain

$$\alpha'(t)|B(0,r)| = \beta \int_{B(0,r)} \mathrm{div}(z(t))dx = \beta \int_{\partial B(0,r)} z(t)\cdot n = -\beta H^{N-1}\partial B(0,r). \tag{III-2.13}$$

Thus

$$\alpha'(t) = -\frac{\beta N}{r}.$$

Therefore,

$$\alpha = k - \frac{\beta N}{r}t, \quad T = \frac{kr}{\beta N}.$$

To construct z $(0,T)\times(\Omega \setminus B(0,r))$ we shall look for z of the form $z = \rho(||x||)x/||x||$ such that $\mathrm{div}(z(t)) = 0$, $\rho(r) = -1$. Since

$$\mathrm{div}(z(t)) = \nabla\rho(||x||)\cdot\frac{x}{||x||} + \rho(||x||)\mathrm{div}\left(\frac{x}{||x||}\right) = \rho'(||x||) + \rho(||x||)\frac{N-1}{||x||}$$

we must have

$$\rho'(s) + \rho(s)\frac{N-1}{s} = 0 \quad \text{for } s > r. \tag{III-2.14}$$

The solution of (III-2.14) such that $\rho(t) = -1$ is $\rho(s) = -r^{N-1}s^{1-N}$. Thus in $\Omega \setminus B(0,r)$,

$$z(t) = -r^{N-1}\frac{x}{||x||^N}.$$

Consequently, the candidate to $z(t)$ is the vector field

$$z(t) := \begin{cases} -\frac{x}{r} & \text{if } x \in B(0,r),\ 0 \le t \le T, \\ -r^{N-1}\frac{x}{||x||^N} & \text{if } x \in \Omega \setminus B(\bar{0},r),\ 0 \le t \le T, \\ 0 & \text{if } x \in \Omega,\ t > T. \end{cases}$$

and $u(t,x)$ is the function

$$u(t,x) = \left(k - \frac{\beta N}{r}t\right)\chi_{B(0,r)}(x)\chi_{[0,T]}(t),$$

where $T = kr/\beta N$. Let us see that $u(t,x)$ satisfies (III-2.10),(III-2.11) and (III-2.12). Since $u(t,x) = 0$ if $x \in \Gamma$, it is easy to check that (III-2.12) holds. On the order hand, if $\varphi \in \mathcal{D}(\Omega)$ and $0 \le t \le T$, we have

$$\begin{aligned} \int_\Omega \frac{\partial z_i(t)}{\partial x_i}\varphi\ dx = &-\frac{1}{r}\int_{B(0,r)}\varphi\ dx + \int_{\partial B(0,r)}\frac{x_i}{r}\frac{x_i}{r}\varphi\ dH^{N-1} \\ &- \int_{\Omega\setminus B(0,r)}\frac{\partial}{\partial x_i}\left(\frac{r^{N-1}x}{||x||^N}\right)\varphi\ dx - \int_{\partial B(0,r)}\frac{r^{N-1}}{r^N}x_i\frac{x_i}{r}\varphi\ dH^{N-1}. \end{aligned}$$

Hence

$$\int_\Omega \text{div } z(t)\varphi\ dx = -\frac{N}{r}\int_{B(0,r)}\varphi\ dx,$$

and consequently (III-2.10) holds. Finally, if $0 \le t \le T$, by Green's formula (III-2.1) we have

$$\begin{aligned} \int_\Omega (z(t), Du(t))dx &= -\int_\Omega \text{div } z(t)u(t)\ dx + \int_\Gamma [z(t),n]u(t)dH^{N-1} \\ &= -\int_{B(0,r)}\text{div } z(t)\left(k - \frac{\beta N}{r}t\right)\ dx = \int_{B(0,r)}\left(k - \frac{\beta N}{r}t\right)\frac{\beta N}{r}\ dx \end{aligned}$$

$$= \left(k - \frac{\beta N}{r}t\right) \frac{\beta N}{r}|B(0,r)| = \left(k - \frac{\beta N}{r}t\right) H^{N-1}(\partial B(0,r))$$
$$= |Du(t)|(\Omega).$$

Therefore $u(t,x)$ is the solution of (III-2.8).

Chapter IV

Numerical Methods for the Solution of Bingham Flows in Cylinders

1 Background

It follows from references [22] and [23] that a mechanically and mathematically correct formulation of problem (III-1.6) is provided by the following *variational inequality* type model:

$$\begin{cases} \text{Find } \; u(t) \in H_0^1(\Omega) \;\; \text{a.e. on } \; (0,T), \\ \varrho \displaystyle\int_\Omega \partial_t u(v-u)\,dx + \mu \int_\Omega \nabla u \cdot \nabla(v-u)\,dx \\ \qquad +g(j(v)-j(u)) \geq C \displaystyle\int_\Omega (v-u)\,dx, \quad \forall v \in H_0^1(\Omega), \\ u(0) = u_0, \end{cases} \tag{VI-1.1}$$

with

$$j(v) = \int_\Omega |\nabla v|\,dx. \tag{VI-1.2}$$

The *backward Euler scheme*, described below, is the only scheme preserving the *asymptotic behavior* of the solution of the continuous problem (namely, problem (VI-1.1)), including the *finite extinction time*, see [20]. This scheme reads as follows (with $\Delta t(>0)$ a *time discretization step* that we suppose constant, for simplicity):

$$u^0 = u_0 \ ; \tag{VI-1.3}$$

then, for $n \geq 1$, *compute* u^n *from* u^{n-1} *via the solution of*

$$\left\{ \begin{array}{l} \text{Find } \ u^n \in H_0^1(\Omega), \\ \varrho \displaystyle\int_\Omega (u^n - u^{n-1})(v - u^n)\, dx + \mu \Delta t \int_\Omega \nabla u^n \cdot \nabla (v - u^n)\, dx \\ \qquad + g\Delta t (j(v) - j(u^n)) \geq \Delta t C^n \displaystyle\int_\Omega (v - u^n)\, dx, \quad \forall v \in H_0^1(\Omega), \end{array} \right. \tag{VI-1.4}$$

with $C^n = C(n\Delta t)$. It follows from, e.g., [[26], Chapter I] that (VI-1.4) is an *elliptic variational inequality* (of the second kind) problem, which has a *unique solution*. Problem (VI-1.4) can be rewritten as

$$\left\{ \begin{array}{l} \text{Find } \ u \in H_0^1(\Omega), \\ \alpha \displaystyle\int_\Omega u(v - u)\, dx + \mu \int_\Omega \nabla u \cdot \nabla (v - u)\, dx \\ \qquad + g(j(v) - j(u)) \geq \displaystyle\int_\Omega f(v - u)\, dx, \ \ \forall v \in H_0^1(\Omega), \end{array} \right. \tag{VI-1.5}$$

with $\alpha \geq 0$ and $f \in L^2(\Omega)$.

A classical method to solve problem (VI-1.5) is the one introduced in reference [15]; it reduces the solution of the above problem to the solution of a sequence of linear Dirichlet problems for the operator $\alpha \mathbf{I} - \mu \nabla^2$ and simple projection operations. The method relies on the equivalence between (VI-1.5) and

$$\left\{ \begin{array}{l} \alpha u - \mu \nabla^2 u - g \nabla \cdot \boldsymbol{\lambda} = f \ \text{ in } \ \Omega, \\ u = 0 \ \text{ on } \ \Gamma, \\ \boldsymbol{\lambda} \cdot \nabla u = |\nabla u|, \ \ \boldsymbol{\lambda} \in \boldsymbol{\Lambda}, \end{array} \right. \tag{VI-1.6}$$

the last two relations implying that

$$\boldsymbol{\lambda} = P_{\boldsymbol{\Lambda}}(\boldsymbol{\lambda} + rg\nabla u), \ \ \forall r \geq 0, \tag{VI-1.7}$$

with the operator $P_{\boldsymbol{\Lambda}}$ defined by

$$P_{\boldsymbol{\Lambda}}(\mathbf{q})(x) = \frac{\mathbf{q}(x)}{\max(1, |\mathbf{q}(x)|)}, \ \ \text{a.e. on } \ \Omega, \ \forall \mathbf{q} \in (L^2(\Omega))^2 \, . \tag{VI-1.8}$$

In order to solve (VI-1.5), via relation (VI-1.6) and (VI-1.7), we advocate (following [15]) the *fixed point* algorithm below:

$$\boldsymbol{\lambda}^0 \ \ \textit{is given in} \ \ \boldsymbol{\Lambda} \tag{VI-1.9}$$

then, for $n \geq 0$*, assuming that* $\boldsymbol{\lambda}^n$ *is known, we compute* u^n *and then* $\boldsymbol{\lambda}^{n+1}$ *as follows:*

solve

$$\alpha u^n - \mu \nabla^2 u^n = f + g\nabla \cdot \boldsymbol{\lambda}^n \ \ \textit{in} \ \ \Omega, \quad u^n = 0 \ \ \textit{on} \ \ \Gamma, \tag{VI-1.10}$$

and

$$\boldsymbol{\lambda}^{n+1} = P_{\boldsymbol{\Lambda}}\big(\boldsymbol{\lambda}^n + rg\nabla u^n\big). \tag{VI-1.11}$$

Suppose that the system (VI-1.6) has a solution $\{u, \boldsymbol{\lambda}\} \in H_0^1(\Omega) \times \boldsymbol{\Lambda}$ (which is indeed the case); it can be shown (see, e.g., refs. [26] and [27]) that the above pair is necessarily a *saddle-point* over $H_0^1(\Omega) \times \boldsymbol{\Lambda}$ of the Lagrangian functional

$$\mathcal{L} : H^1(\Omega) \times (L^2(\Omega))^2 \to \mathbb{R}$$

defined by

$$\mathcal{L}(v, \boldsymbol{\mu}) = \frac{1}{2}\left[\alpha \|v\|^2_{L^2(\Omega)} + \mu \|\nabla v\|^2_{(L^2(\Omega))^2}\right] + g\int_\Omega \boldsymbol{\mu} \cdot \nabla v \, dx - \int_\Omega fv \, dx \tag{VI-1.12}$$

i.e., the pair $\{u, \boldsymbol{\lambda}\}$ verifies (from the definition of a saddle-point; see, e.g., [[25], Chapter 4])

$$\begin{cases} \{u, \boldsymbol{\lambda}\} \in H_0^1(\Omega) \times \boldsymbol{\Lambda}, \\ \mathcal{L}(u, \boldsymbol{\mu}) \leq \mathcal{L}(u, \boldsymbol{\lambda}) \leq \mathcal{L}(v, \boldsymbol{\lambda}), \ \ \forall \{v, \boldsymbol{\mu}\} \in H_0^1(\Omega) \times \boldsymbol{\Lambda}. \end{cases} \tag{VI-1.13}$$

Conversely, any solution of (VI-1.13) is solution of system (VI-1.6). It follows from the above reference that algorithm (VI-1.9)-(VI-1.11) is nothing but an *Uzawa algorithm* applied to the solution of the saddle-point problem (VI-1.13) with $\mathcal{L}(\,\cdot\,,\,\cdot\,)$ defined by (VI-1.12); for a systematic study of Uzawa algorithms, see, e.g., [[25], Chapter 4] and the references therein.

2 Numerical Experiments

In this section we present some numerical results related to problem (III-1.6), with the goal of investigating the qualitative properties (i.e. finite extinction time and propagation of support of initial data) of solutions to the Bingham flow in a cylinder. The results will then be compared with the properties of solutions of total variation flow problems of the form (III-2.8), which can be (formally) viewed as a limit of problem (III-1.6) as viscosity goes to zero.

In all our simulations, the spatial domain is chosen to be the unit square in $\mathbb{R}^2$, namely $\Omega = (0,1) \times (0,1)$ [m×m]. The fluid density and plasticity yield are chosen to be $\rho = 1$ [Kg m^{-3}] and $g = 2$ [Pa]. For what concerns the fluid viscosity, we run simulations with $\mu = 0.25$ and $\mu = 0.0025$ [Pa s], in order to investigate how the fluid viscosity affects the dynamics of the flow. Moreover, we assume the pressure drop to be equal to zero, namely $C = 0$ [Pa m^{-1}], so that the flow is driven only by the initial conditions. These choices are summarized in Table IV.1.

We are going to consider a set of five different initial conditions:

Case I - Characteristic function of a disk. The initial velocity u_0 is given by:

$$u_0 = \begin{cases} 1 \text{ in } B(x_0, R_1) \\ 0 \text{ elsewhere} \end{cases} \tag{VI-2.1}$$

with $x_0 = (0.5, 0.5)$ and $R_1 = 0.3$.

Fluid domain	$\Omega = (0,1) \times (0,1)$ [m×m]
Fluid density	ρ=1 [Kg m^{-3}]
Plasticity yield	g=2 [Pa]
Fluid viscosity	$\mu = 0.25, 0.0025$ [Pa s]
Pressure drop	$C = 0$ [Pa m^{-1}]

Table IV.1: Values of the parameters used in the numerical simulations.

Case II - Superposition of two characteristic functions. The initial velocity u_0 is given by:

$$u_0 = \begin{cases} 2 \text{ in } B(x_0, R_2) \\ 1 \text{ in } B(x_0, R_1) \setminus B(x_0, R_2) \\ 0 \text{ elsewhere} \end{cases} \tag{VI-2.2}$$

with $x_0 = (0.5, 0.5)$, $R_1 = 0.3$, and $R_2 = 0.2$.

Case III - Characteristic function of two (distant) disjoint disks. The initial velocity u_0 is given by:

$$u_0 = \begin{cases} 1 \text{ in } B(x_1, R_1) \cup B(x_2, R_2) \\ 0 \text{ elsewhere} \end{cases} \tag{VI-2.3}$$

with $x_1 = (0.2750, 0.2750)$, $x_2 = (0.7250, 0.7250)$, and $R_1 = R_2 = 0.1$.

Case IV - Characteristic function of two (close) disjoint disks. The initial velocity u_0 is given by:

$$u_0 = \begin{cases} 1 \text{ in } B(x_1, R_1) \cup B(x_2, R_2) \\ 0 \text{ elsewhere} \end{cases} \tag{VI-2.4}$$

with $x_1 = (0.4242, 0.4242)$, $x_2 = (0.5758, 0.5758)$, and $R_1 = R_2 = 0.1$.

Case V - Characteristic function of a square. The initial velocity u_0 is given

by:

$$u_0 = \begin{cases} 1 \text{ in } S = (a,b) \times (a,b) \\ 0 \text{ elsewhere} \end{cases} \tag{VI-2.5}$$

with $a = 0.25$ and $b = 0.75$.

3 Numerical Results

Problem (III-1.6) was solved using the iterative method *á la Uzawa* (VI-1.9)-(VI-1.11). We validated our results by repeating the simulations using different time steps, different mesh sizes and different tolerances for the convergence of the Uzawa algorithm. More precisely, we used $\Delta t = 10^{-4}, 5 \times 10^{-4}$, and 10^{-5} as time steps; we used $1/70, 1/100, 1/120$, and $1/150$ as mesh sizes; we used $tol = 10^{-6}, 5 \times 10^{-6}$, and 10^{-7} as tolerances for the convergence of the Uzawa algorithm. Excellent agreement was found between results obtained with different combinations of these parameters.

Finite extinction time. Our results show a finite extinction time of the solution, as predicted by the theory. Figures IV.1, IV.6, IV.11, IV.16, IV.21 show the time evolution of the L^2-norm of the solution, namely $\|u\|_{L^2(\Omega)}(t)$, for each of the five different initial conditions. The pictures show that the extinction time increases as the fluid viscosity decreases, see Table IV.2. This is due to the fact that a less viscous system has a less efficient dissipative mechanism and therefore it takes longer for the solution to decay to zero.

In particular, Case I admits the following exact solution

$$u(t,x) = \text{sign}(k)\frac{N}{r}\left(\frac{|k|r}{gN} - t\right)^+ \chi_{B(0,r)}(x), \tag{VI-3.1}$$

as shown in Lemma III-2.4. It is easy to see that $u(t,x)$ vanishes for $t = \frac{|k|r}{gN}$, and this represents the extinction time in the case of $\mu = 0$. For the values in Table IV.1, we find that $\frac{|k|r}{gN} = 0.075$ [s]. The agreement with the extinction time obtained with our simulations is very good: we get $t = 0.0705$ for $\mu = 0.0025$ [Pa s], see Table

	Case I	Case II	Case III	Case IV	Case V
$\mu = 0.25$ [Pa s]	0.0505	0.071	0.012	0.019	0.0465
$\mu = 0.0025$ [Pa s]	0.0705	0.1025	0.0215	0.028	0.064

Table IV.2: Numerically computed values of extinction times corresponding to different initial conditions (Cases I to V) and to different fluid viscosities ($\mu = 0.25$ and $\mu = 0.0025$ [Pa s].)

IV.2. We emphasize that the theoretical value of the extinction time is obtained for the total variation flow problem, which corresponds to a Bingham fluid with no viscosity. On the other hand, our simulations include a non-zero fluid viscosity and, as a consequence, the solution extinction time is smaller than the theoretical value. As expected though, as the fluid viscosity decreases, the extinction time increases.

Solution and normalized solution. We have visualized the time evolution of the solution $u(t,x)$ and of the normalized solution $u(t,x)/\|u\|_{L^2(\Omega)}(t)$. The solution $u(t,x)$ progressively decreases to zero, while the normalized solution reaches a non-zero and non-smooth limit in a finite time. In order to better visualize the comparison between the solution and the normalized solution, we show their time-evolution restricted to the domain diagonal, see Figures IV.4 and IV.5 for Case I, Figures IV.9 and IV.10 for Case II, Figures IV.14 and IV.15 for Case III, Figures IV.19 and IV.20 for Case IV, Figures IV.24 and IV.25 for Case V. The fact that the normalized solution reaches a non-zero and non-smooth limit at the extinction time should not be a surprise. Solutions to total variation flow problems do not gain any spatial differentiability, in contrast with what happens for the linear heat equation and many other quasilinear parabolic problems, see [4].

No propagation of the support. The theory for total variation flow predicts no propagation of support of the initial datum, if the support is regular enough. We recall that the total variation flow corresponds to the case of fluid viscosity equal to

zero, therefore it is reasonable to expect that the propagation of the support depends on the value of the fluid viscosity, see Figures IV.3, IV.8, IV.13, IV.18, and IV.23. Our simulations indeed reflect these mathematical properties. In Cases I, II, and III, the support of the initial datum is very regular (either a ball or two disjoint balls). The results obtained in these cases for the smaller viscosity value, namely $\mu = 0.0025$, show almost no propagation of support of the initial datum, as shown in Figures IV.2 and IV.5 for Case I; Figures IV.7 and IV.10 for Case II; Figures IV.12 and IV.15 for Case III. In Cases IV and V we see a change in topology of the support. More precisely, the support of the initial datum in Case IV is made of two disjoint disks whose boundaries are quite close to each other. The time evolution of the normalized solution $u(t,x)/\|u\|_{L^2(\Omega)}(t)$ shows that the two disks progressively merge, see Figures IV.17 and IV.20 and, finally, the support of the normalized solution at the extinction time has the shape of an hour-glass. In Case V, the support of the initial datum is a square while, at the extinction time, the support of the normalized solution is a disk, see Figures IV.22 and IV.23.

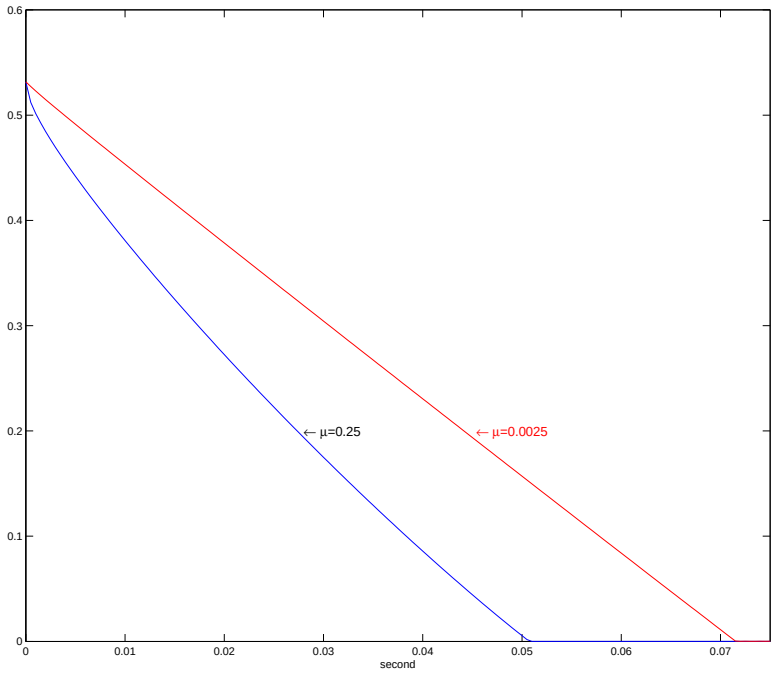

Figure IV.1: Case I - Time evolution of $\|u\|_{L^2(\Omega)}(t)$ for $\mu = 0.25$ and $\mu = 0.0025$ [Pa s].

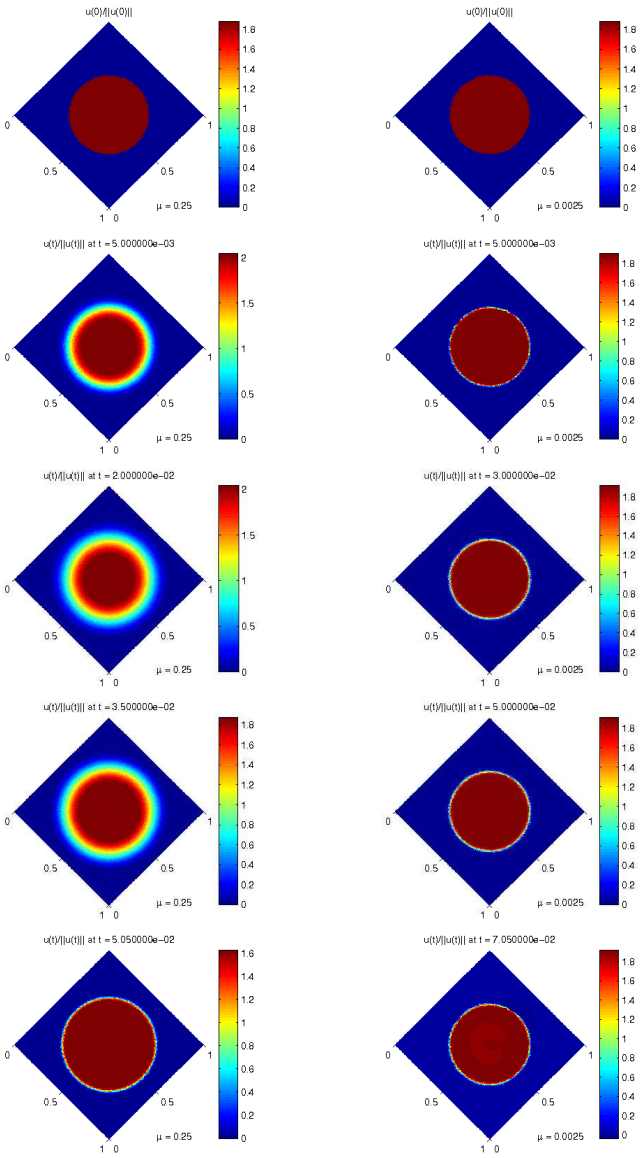

Figure IV.2: Case I - *On the left:* Snapshots of the normalized solution $u(t,x)/||u||_{L^2(\Omega)}(t)$ obtained with $\mu = 0.25$ at $t = 0, 0.005, 0.02, 0.035, 0.0505$ seconds; *On the right:* Snapshots of the normalized solution $u(t,x)/||u||_{L^2(\Omega)}(t)$ obtained with $\mu = 0.0025$ at $t = 0, 0.005, 0.03, 0.05, 0.0705$ seconds.

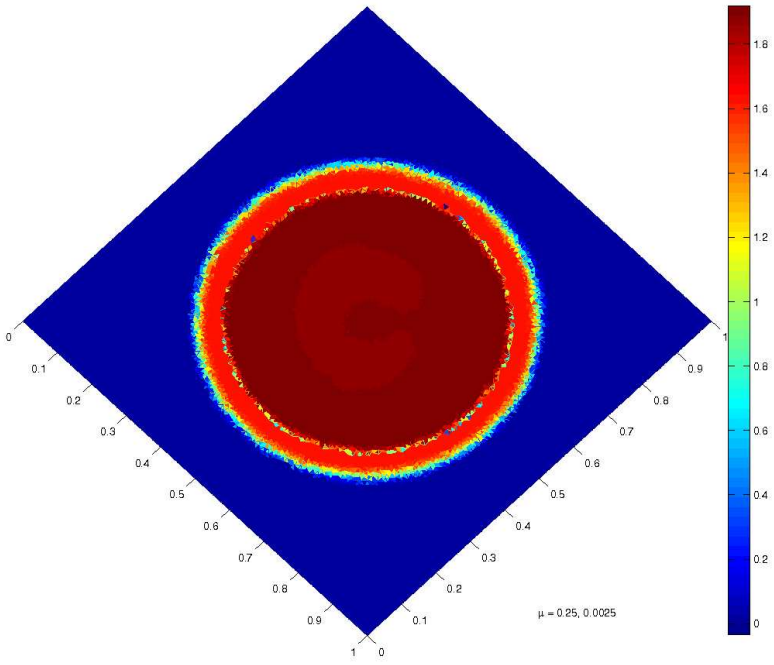

Figure IV.3: Case I - Comparison between the supports of the normalized solutions at extinction time obtained with $\mu = 0.25$ (outer circle) and with $\mu = 0.0025$ (inner circle).

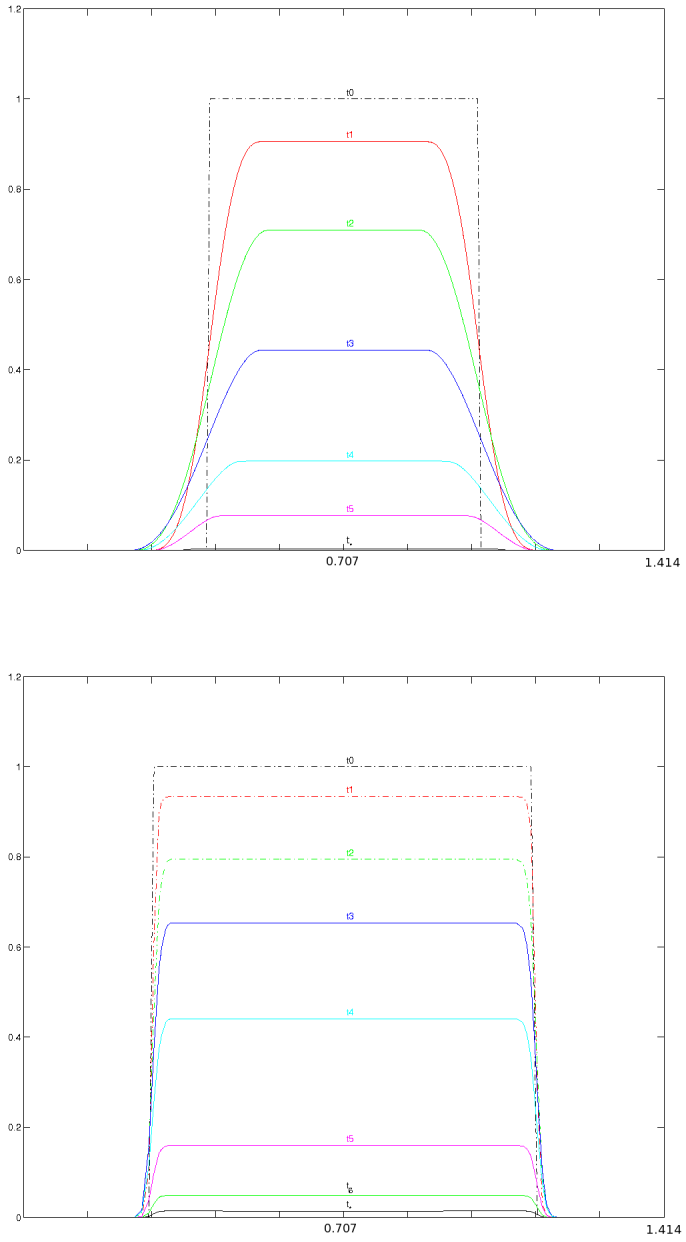

Figure IV.4: Case I - *On the top:* Snapshots of the solution $u(t,x)$ restricted to the domain diagonal obtained with $\mu = 0.25$ at $t_0 = 0,\ t_1 = 0.005,\ t_2 = 0.0135,\ t_3 = 0.025,\ t_4 = 0.0375,\ t_5 = 0.045,\ t^* = 0.0505$ seconds; *On the bottom:* Snapshots of the solution $u(t,x)$ restricted to the domain diagonal obtained with $\mu = 0.0025$ at $t_0 = 0,\ t_1 = 0.005,\ t_2 = 0.015,\ t_3 = 0.025,\ t_4 = 0.04,\ t_5 = 0.06,\ t6 = 0.068,\ t^* = 0.0705$ seconds.

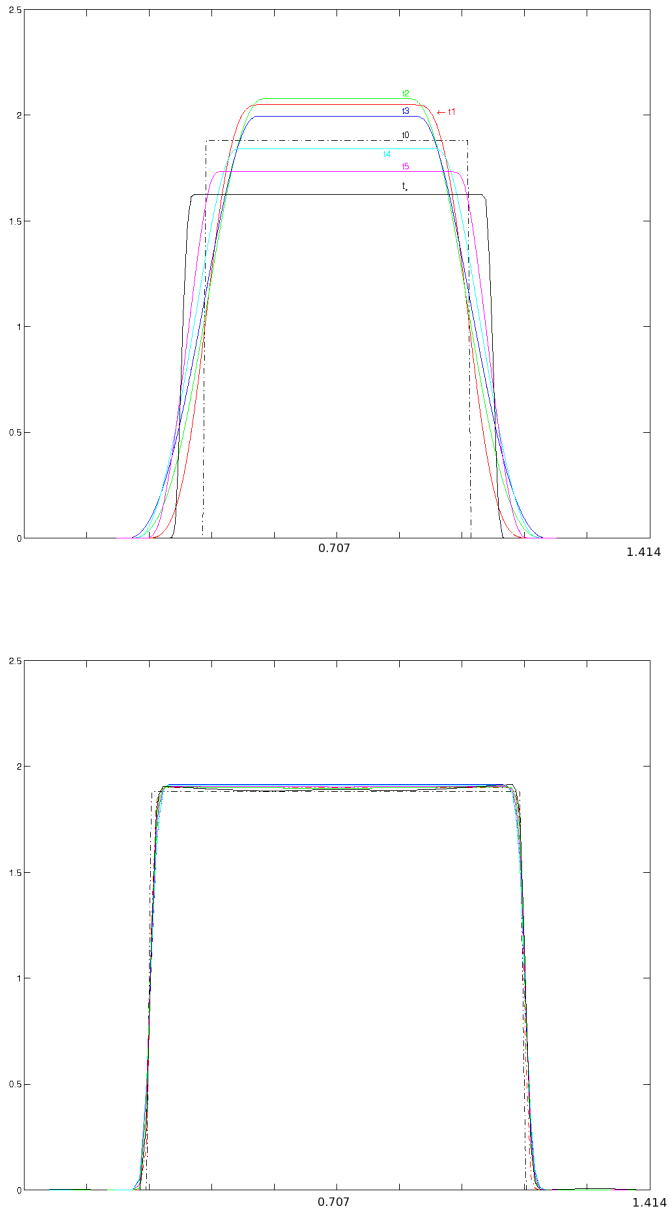

Figure IV.5: Case I - *On the top:* Snapshots of the normalized solution $u(t,x)/||u||_{L^2(\Omega)}(t)$ restricted to the domain diagonal obtained with $\mu = 0.25$ at $t_0 = 0,\ t_1 = 0.005,\ t_2 = 0.0135,\ t_3 = 0.025,\ t_4 = 0.0375,\ t_5 = 0.045,\ t^* = 0.0505$ seconds; *On the bottom:* Snapshots of the normalized solution $u(t,x)/||u||_{L^2(\Omega)}(t)$ restricted to the domain diagonal obtained with $\mu = 0.0025$ at $t_0 = 0,\ t_1 = 0.005,\ t_2 = 0.015,\ t_3 = 0.025,\ t_4 = 0.04,\ t_5 = 0.06,\ t_6 = 0.068,\ t^* = 0.0705$ seconds.

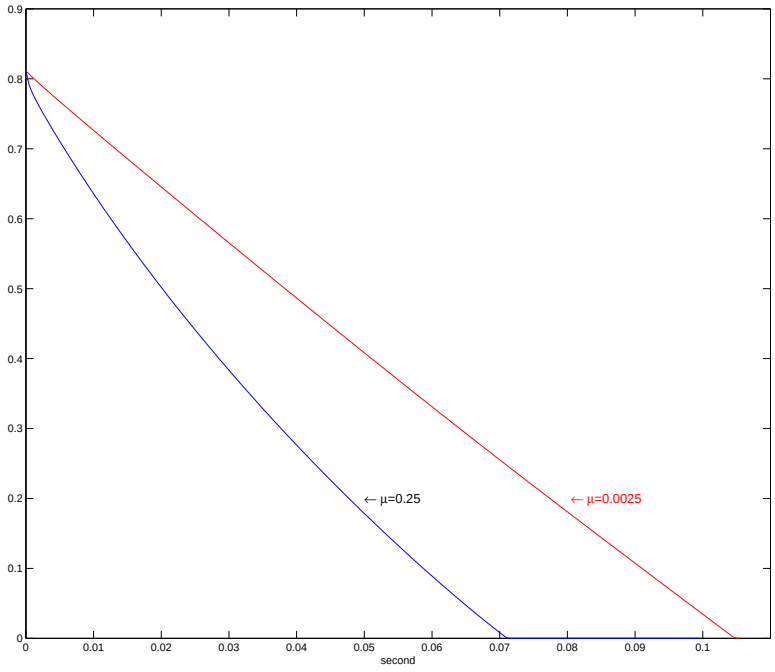

Figure IV.6: Case II - Time evolution of $\|u\|_{L^2(\Omega)}(t)$ for $\mu = 0.25$ and $\mu = 0.0025$ [Pa s].

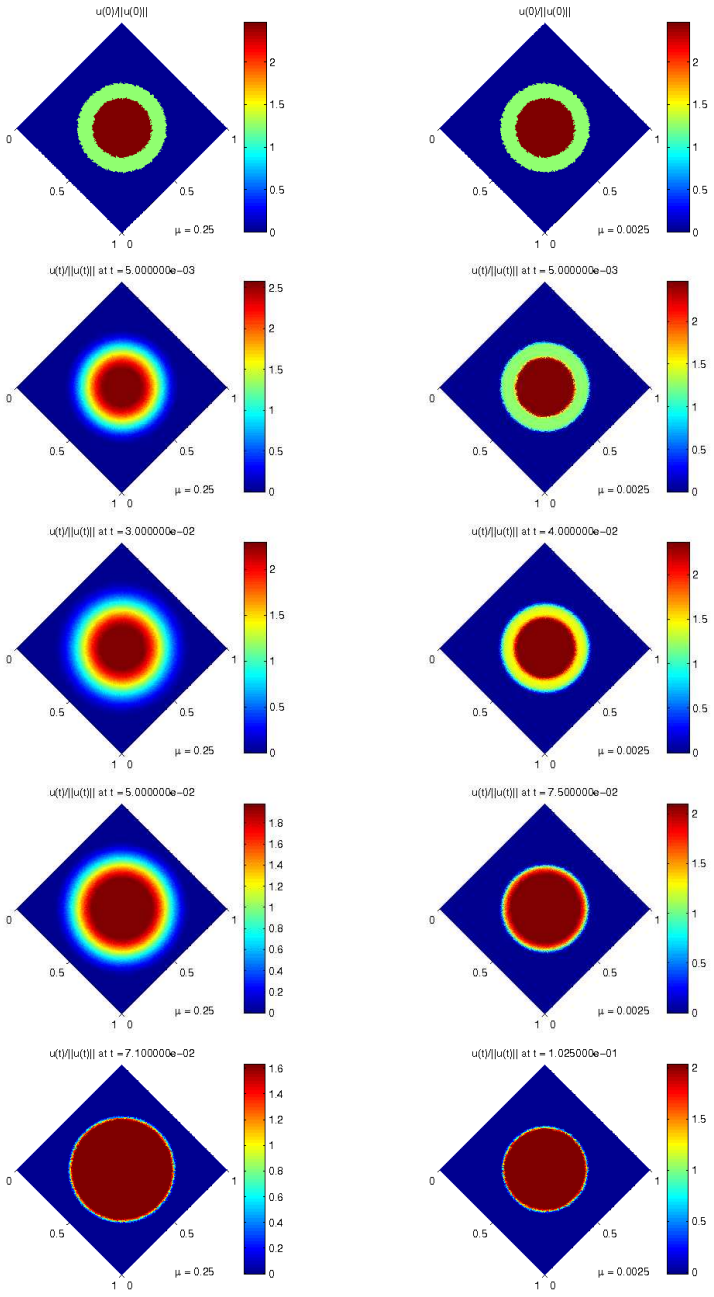

Figure IV.7: Case II - *On the left:* Snapshots of the normalized solution $u(t,x)/||u||_{L^2(\Omega)}(t)$ obtained with $\mu = 0.25$ at $t = 0, 0.005, 0.03, 0.05, 0.071$ seconds; *On the right:* Snapshots of the normalized solution $u(t,x)/||u||_{L^2(\Omega)}(t)$ obtained with $\mu = 0.0025$ at $t = 0, 0.005, 0.004, 0.075, 0.1025$ seconds.

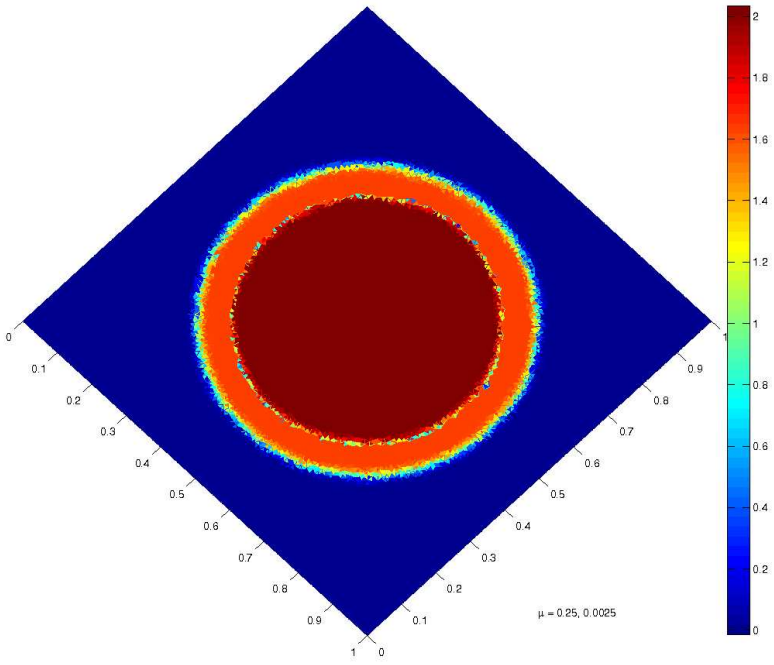

Figure IV.8: Case II - Comparison between the supports of the normalized solutions at extinction time obtained with $\mu = 0.25$ (outer circle) and with $\mu = 0.0025$ (inner circle).

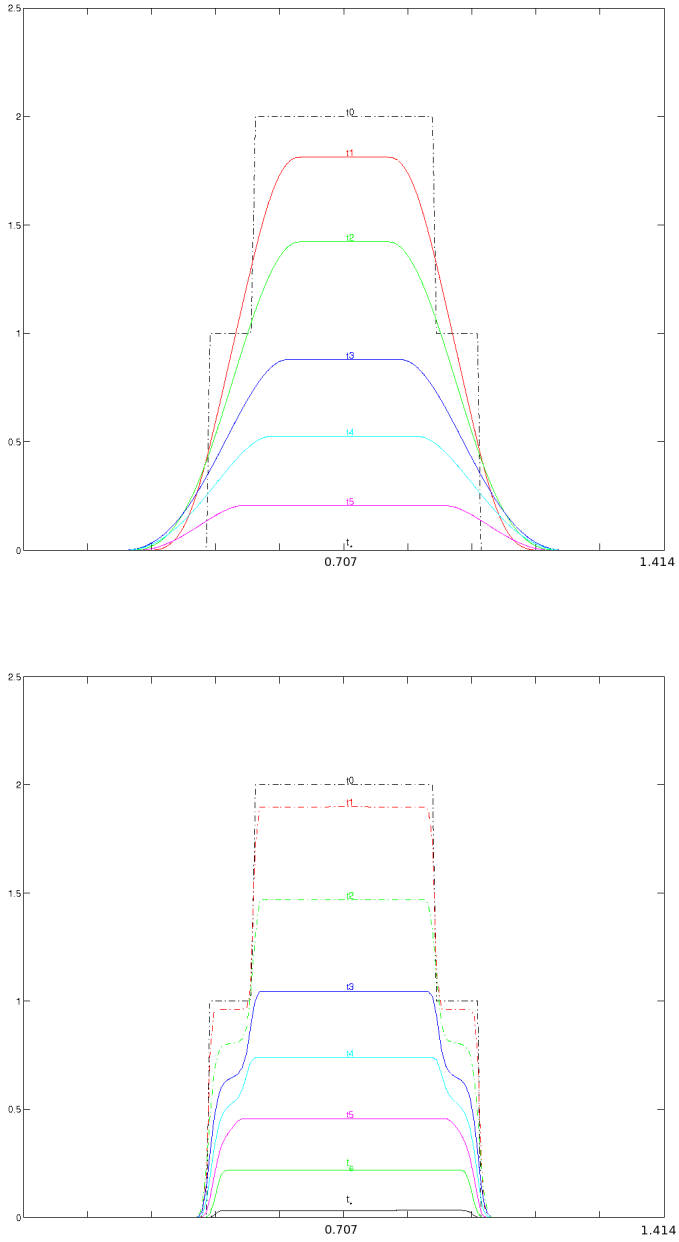

Figure IV.9: Case II - *On the top:* Snapshots of the solution $u(t,x)$ restricted to the domain diagonal obtained with $\mu = 0.25$ at $t_0 = 0,\ t_1 = 0.0055,\ t_2 = 0.015,\ t_3 = 0.003,\ t_4 = 0.0425,\ t_5 = 0.0575, t^* = 0.071$ seconds; *On the bottom:* Snapshots of the solution $u(t,x)$ restricted to the domain diagonal obtained with $\mu = 0.0025$ at $t_0 = 0,\ t_1 = 0.0045,\ t_2 = 0.0245,\ t_3 = 0.0445,\ t_4 = 0.0595,\ t_5 = 0.0745,\ t_6 = 0.095,\ t^* = 0.1025$ seconds.

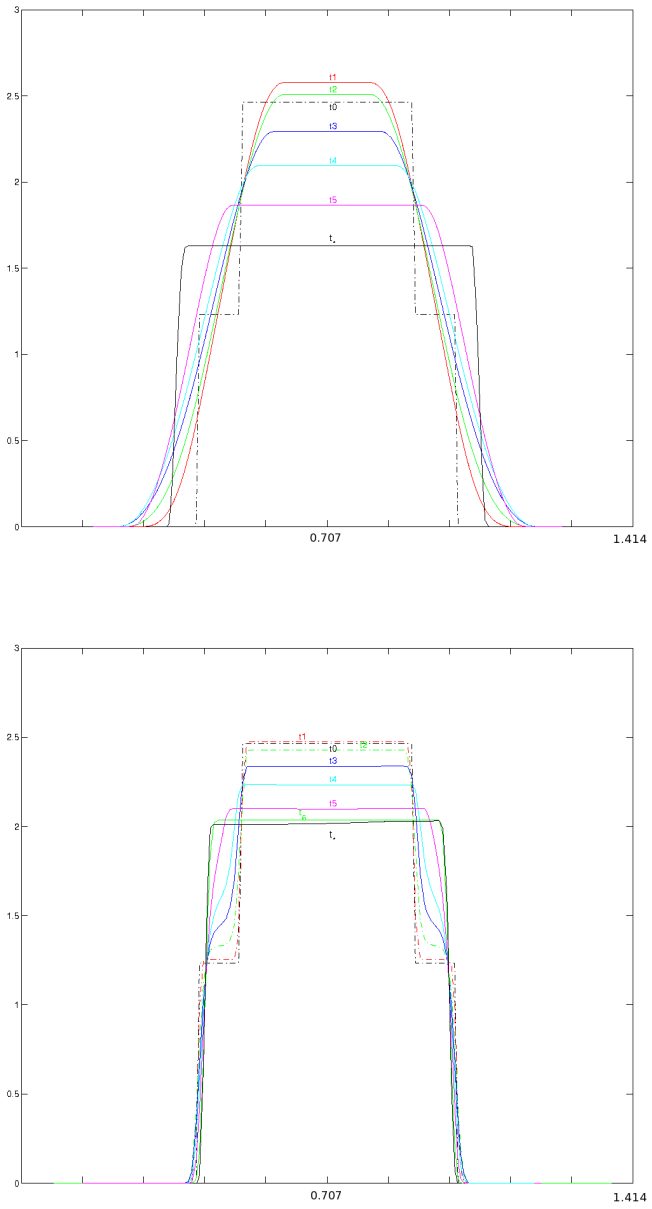

Figure IV.10: Case II - *On the top:* Snapshots of the normalized solution $u(t,x)/||u||_{L^2(\Omega)}(t)$ restricted to the domain diagonal obtained with $\mu = 0.25$ at $t_0 = 0,\ t_1 = 0.0055,\ t_2 = 0.015,\ t_3 = 0.003,\ t_4 = 0.0425,\ t_5 = 0.0575, t_* = 0.071$ seconds; *On the bottom:* Snapshots of the normalized solution $u(t,x)/||u||_{L^2(\Omega)}(t)$ restricted to the domain diagonal obtained with $\mu = 0.0025$ at $t_0 = 0,\ t_1 = 0.0045,\ t_2 = 0.0245,\ t_3 = 0.0445,\ t_4 = 0.0595,\ t_5 = 0.0745,\ t_6 = 0.095,\ t_* = 0.1025$ seconds.

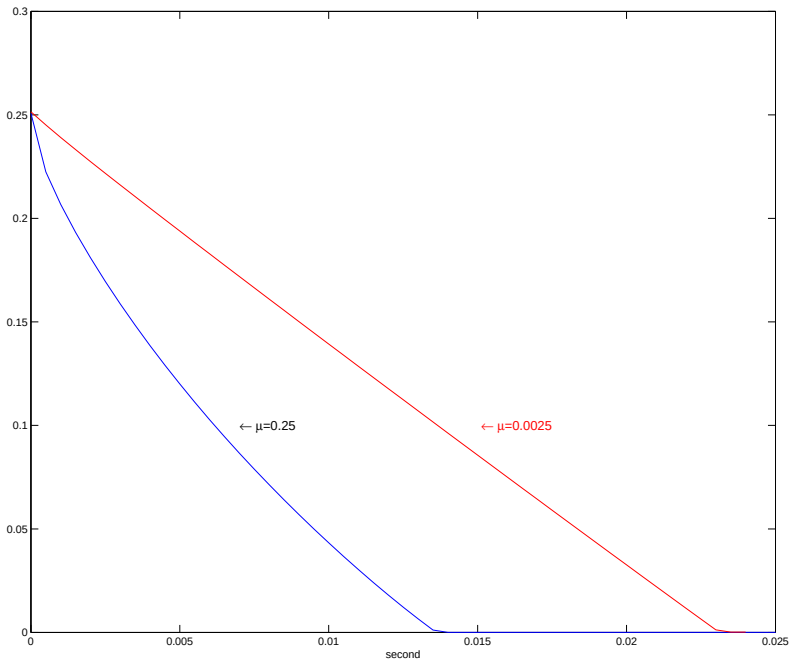

Figure IV.11: Case III - Time evolution of $\|u\|_{L^2(\Omega)}(t)$ for $\mu = 0.25$ and $\mu = 0.0025$ [Pa s].

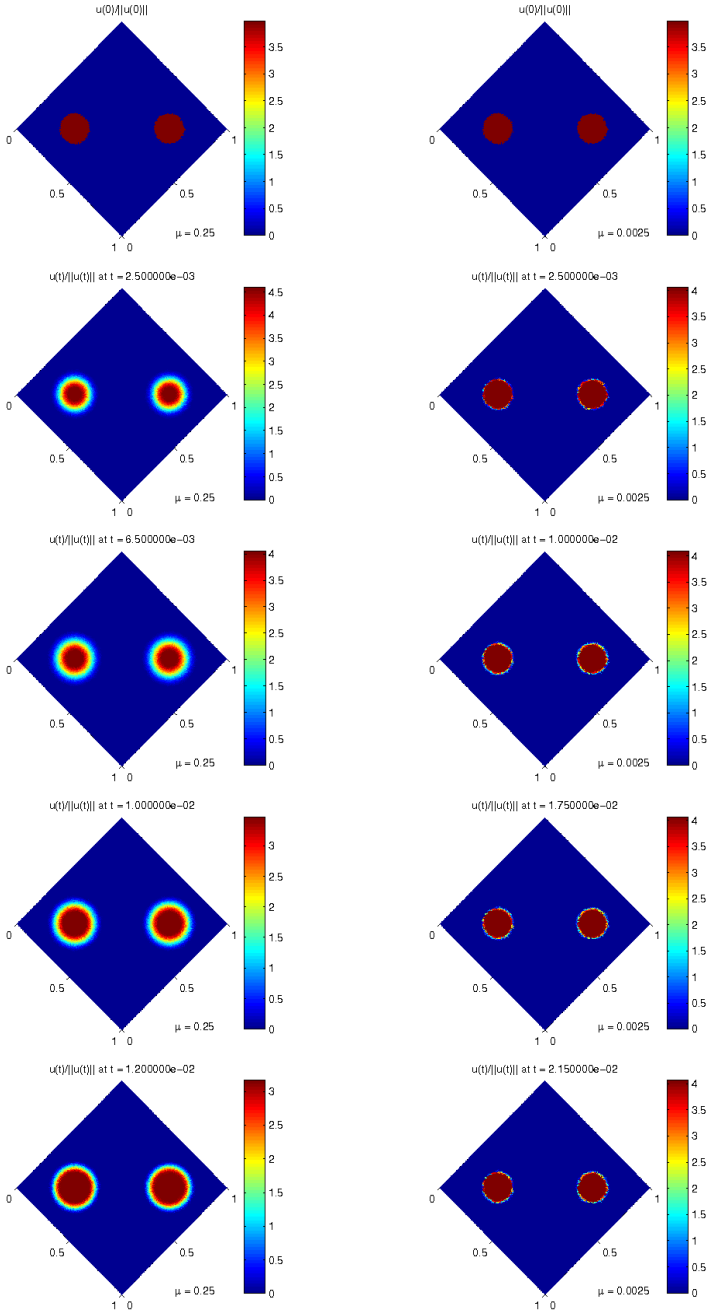

Figure IV.12: Case III - *On the left:* Snapshots of the normalized solution $u(t,x)/||u||_{L^2(\Omega)}(t)$ obtained with $\mu = 0.25$ at $t = 0, 0.0025, 0.0065, 0.01, 0.012$ seconds; *On the right:* Snapshots of the normalized solution $u(t,x)/||u||_{L^2(\Omega)}(t)$ obtained with $\mu = 0.0025$ at $t = 0, 0.0025, 0.01, 0.0175, 0.0215$ seconds.

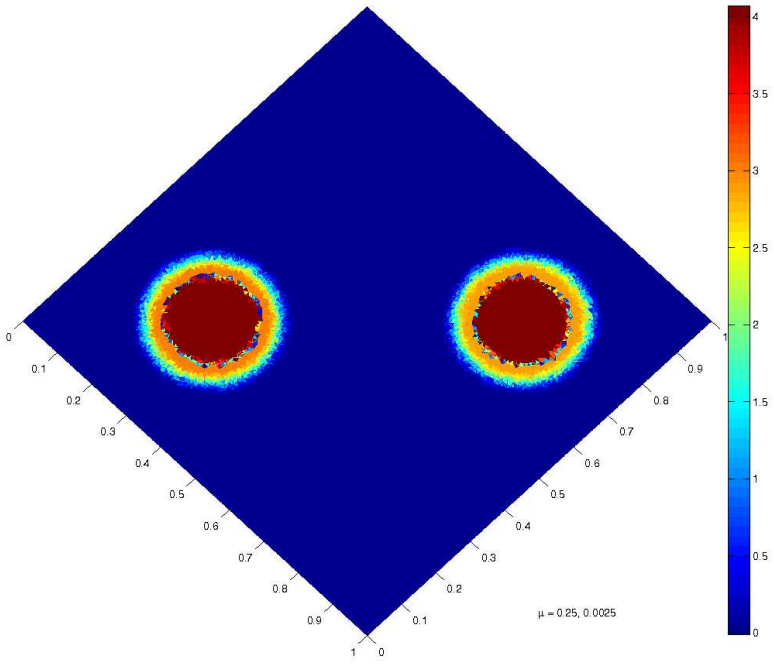

Figure IV.13: Case III - Comparison between the supports of the normalized solutions at extinction time obtained with $\mu = 0.25$ (outer circles) and with $\mu = 0.0025$ (inner circles).

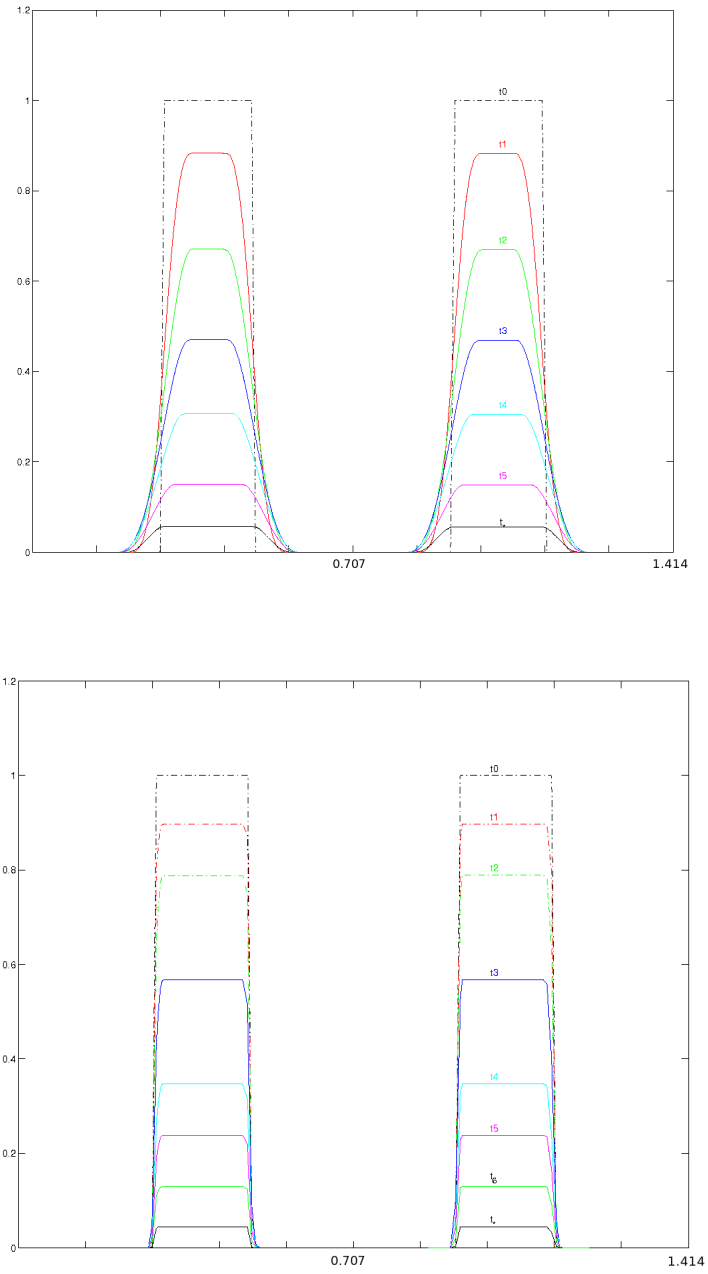

Figure IV.14: Case III - *On the top:* Snapshots of the solution $u(t,x)$ restricted to the domain diagonal obtained with $\mu = 0.25$ at$t_0 = 0,\ t_1 = 0.002,\ t_2 = 0.004,\ t_3 = 0.0065,\ t_4 = 0.009,\ t_5 = 0.0115, t_* = 0.012$ seconds; *On the bottom:* Snapshots of the solution $u(t,x)$ restricted to the domain diagonal obtained with $\mu = 0.0025$ at $t_0 = 0,\ t_1 = 0.0025,\ t_2 = 0.005,\ t_3 = 0.01,\ t_4 = 0.015,\ t_5 = 0.0175,\ t_6 = 0.02,\ t_* = 0.0215$ seconds.

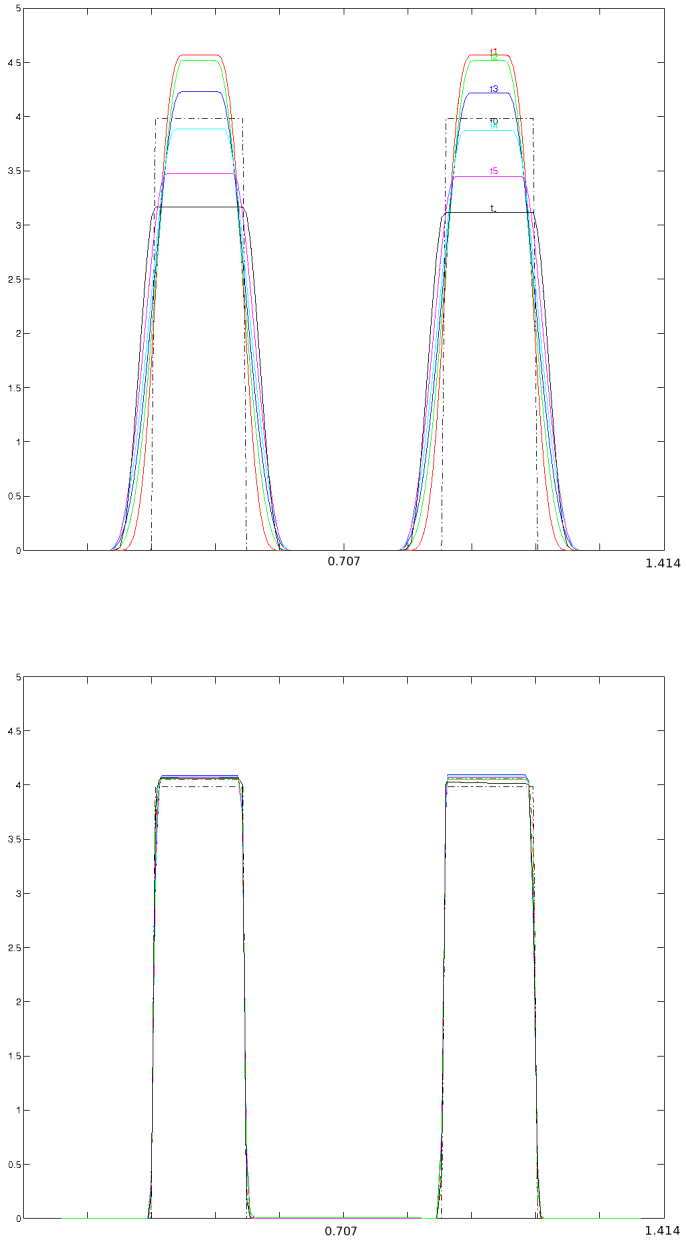

Figure IV.15: Case III - *On the top:* Snapshots of the normalized solution $u(t,x)/||u||_{L^2(\Omega)}(t)$ restricted to the domain diagonal obtained with $\mu = 0.25$ at $t_0 = 0,\ t_1 = 0.002,\ t_2 = 0.004,\ t_3 = 0.0065,\ t_4 = 0.009,\ t_5 = 0.0115, t_* = 0.012$ seconds; *On the bottom:* Snapshots of the normalized solution $u(t,x)/||u||_{L^2(\Omega)}(t)$ restricted to the domain diagonal obtained with $\mu = 0.0025$ at $t_0 = 0,\ t_1 = 0.0025,\ t_2 = 0.005,\ t_3 = 0.01,\ t_4 = 0.015,\ t_5 = 0.0175,\ t_6 = 0.02,\ t_* = 0.0215$ seconds.

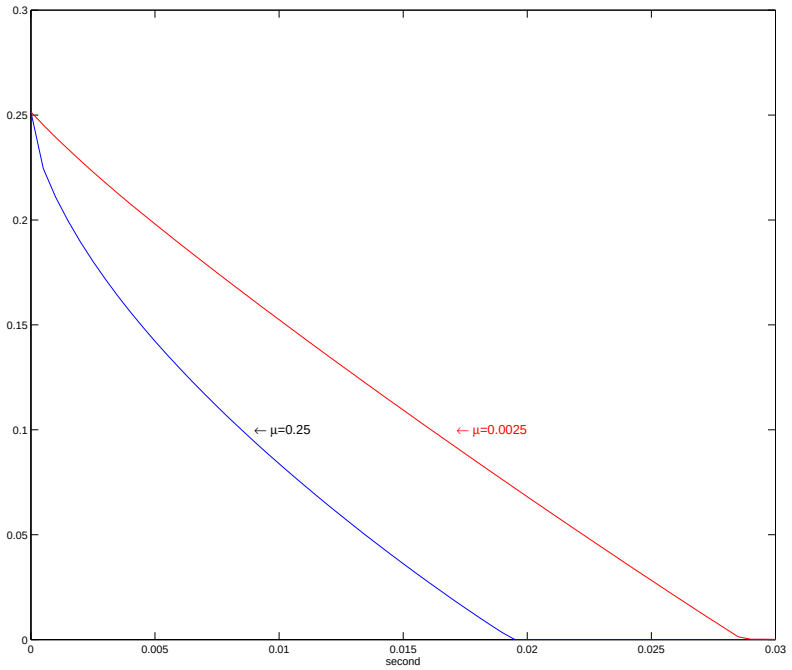

Figure IV.16: Case IV - Time evolution of $\|u\|_{L^2(\Omega)}(t)$ for $\mu = 0.25$ and $\mu = 0.0025$ [Pa s].

4 Conclusions

In this section we have presented some numerical results related to Bingham flow in a cylinder. In the limiting case of fluid viscosity equal to zero, the problem reduces to a total variation flow problem, in which solutions go to zero in a finite (extinction) time and there is no propagation of the support of the initial datum (if the support is regular enough).

Our simulations show that similar qualitative properties hold also in the case of non-zero viscosity. We have considered two different viscosity values, $\mu = 0.25$ [Pa s] and $\mu = 0.0025$ [Pa s], and five different initial conditions, see Section 2, and we have solved the corresponding Bingham flow problem using a backward Euler scheme in combination with an algorithm á la Uzawa.

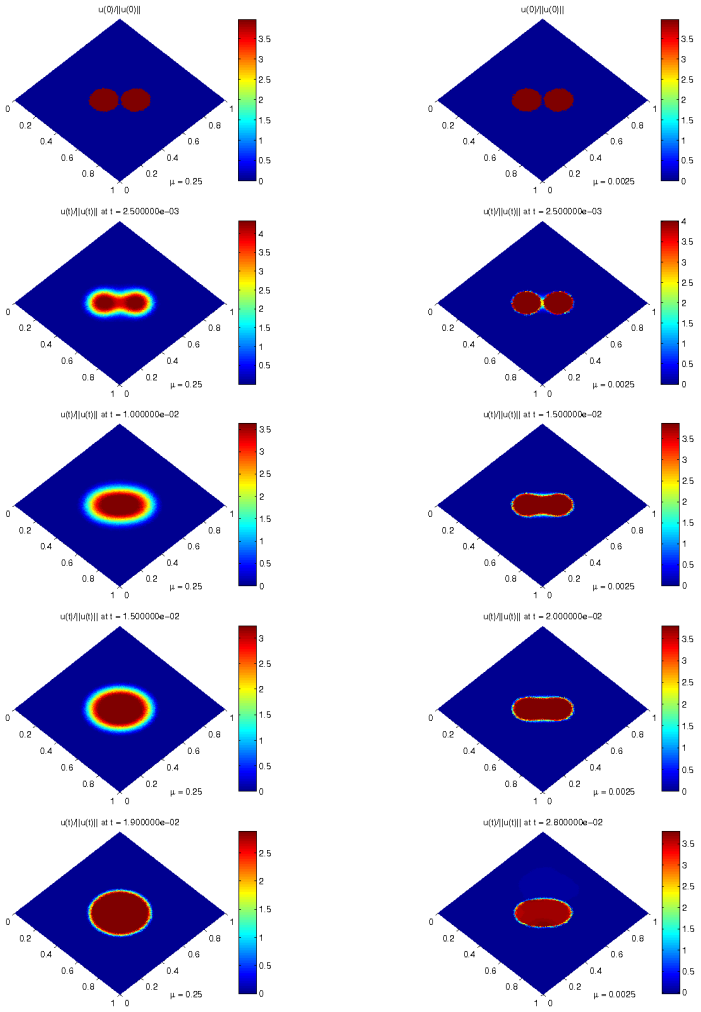

Figure IV.17: Case IV - *On the left:* Snapshots of the normalized solution $u(t,x)/||u||_{L^2(\Omega)}(t)$ obtained with $\mu = 0.25$ at $t = 0, 0.0025, 0.01, 0.015, 0.019$ seconds; *On the right:* Snapshots of the normalized solution $u(t,x)/||u||_{L^2(\Omega)}(t)$ obtained with $\mu = 0.0025$ at $t = 0, 0.0025, 0.015, 0.02, 0.028$ seconds.

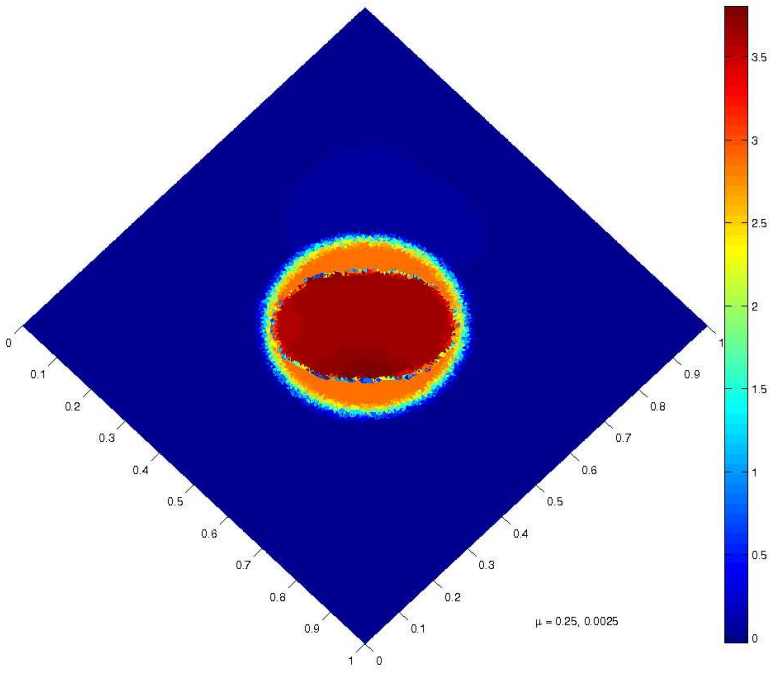

Figure IV.18: Case IV - Comparison between the supports of the normalized solutions at extinction time obtained with $\mu = 0.25$ (outer shape) and with $\mu = 0.0025$ (inner shape).

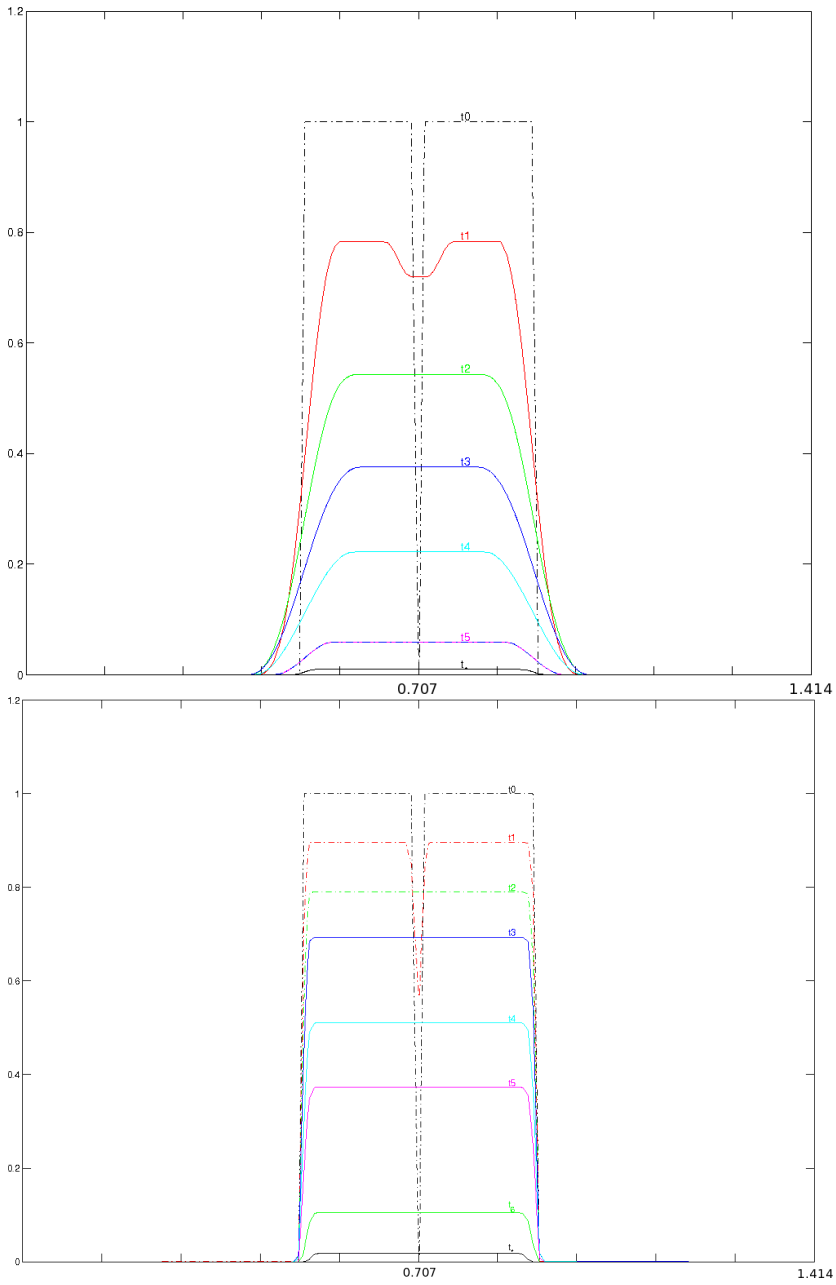

Figure IV.19: Case IV - *On the top:* Snapshots of the solution $u(t,x)$ restricted to the domain diagonal obtained with $\mu = 0.25$ at $t_0 = 0,\ t_1 = 0.0025,\ t_2 = 0.0055,\ t_3 = 0.0085,\ t_4 = 0.012,\ t_5 = 0.017, t_* = 0.019$ seconds; *On the bottom:* Snapshots of the solution $u(t,x)$ restricted to the domain diagonal obtained with $\mu = 0.0025$ at $t_0 = 0,\ t_1 = 0.0025,\ t_2 = 0.005,\ t_3 = 0.0075,\ t_4 = 0.0125,\ t_5 = 0.0165,\ t_6 = 0.025,\ t_* = 0.028$ seconds.

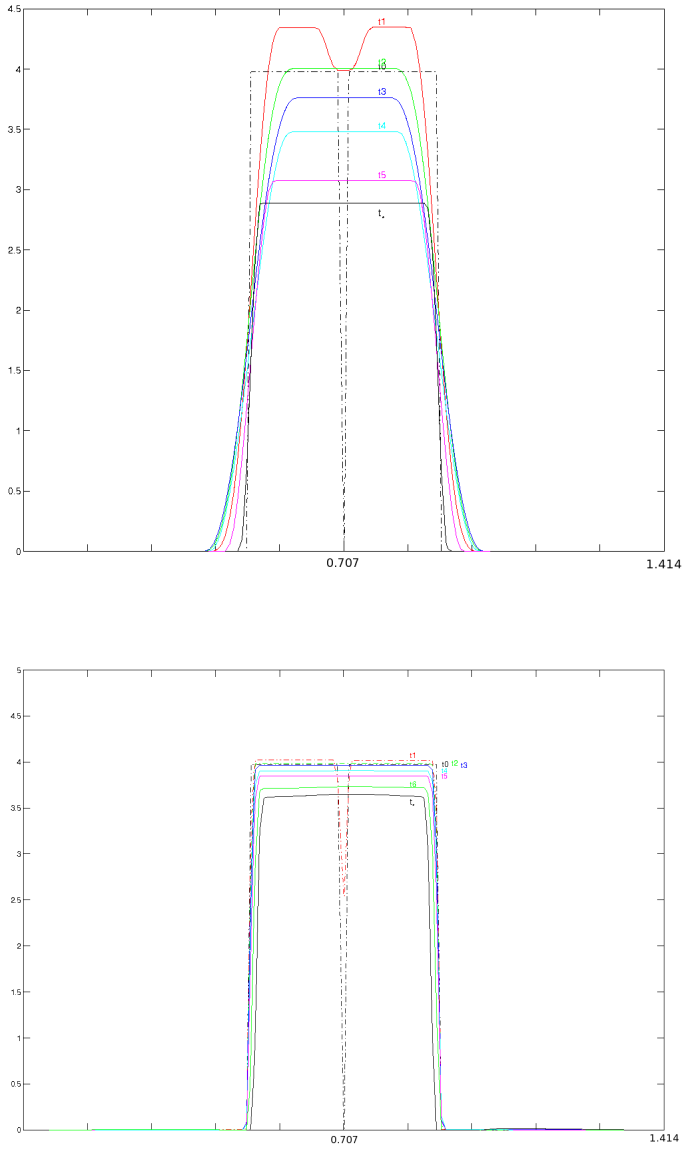

Figure IV.20: Case IV - *On the top:* Snapshots of the normalized solution $u(t,x)/||u||_{L^2(\Omega)}(t)$ restricted to the domain diagonal obtained with $\mu = 0.25$ at $t_0 = 0,\ t_1 = 0.0025,\ t_2 = 0.0055,\ t_3 = 0.0085,\ t_4 = 0.012,\ t_5 = 0.017, t_* = 0.019$ seconds; *On the bottom:* Snapshots of the normalized solution $u(t,x)/||u||_{L^2(\Omega)}(t)$ restricted to the domain diagonal obtained with $\mu = 0.0025$ at $t_0 = 0,\ t_1 = 0.0025,\ t_2 = 0.005,\ t_3 = 0.0075,\ t_4 = 0.0125,\ t_5 = 0.0165,\ t_6 = 0.025,\ t_* = 0.028$ seconds.

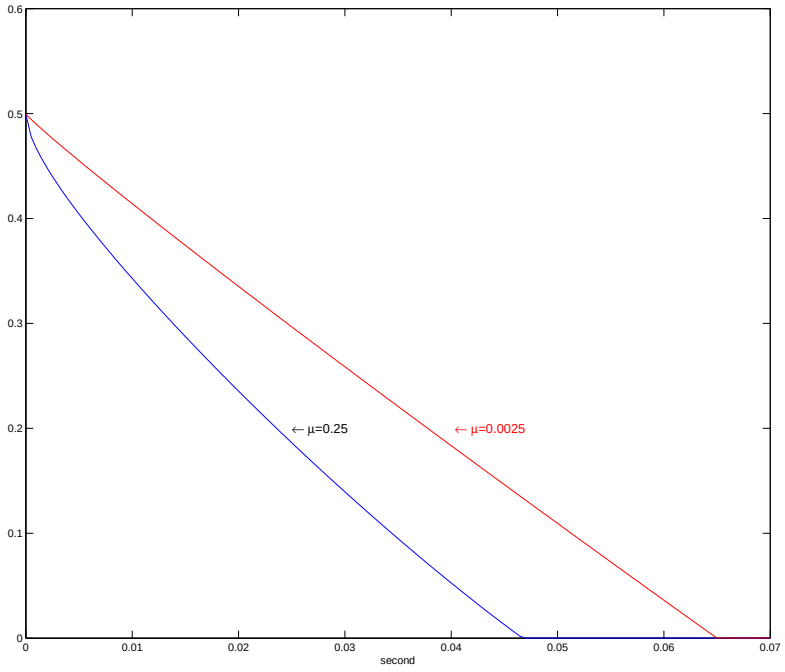

Figure IV.21: Case V - Time evolution of $\|u\|_{L^2(\Omega)}(t)$ for $\mu = 0.25$ and $\mu = 0.0025$ [Pa s].

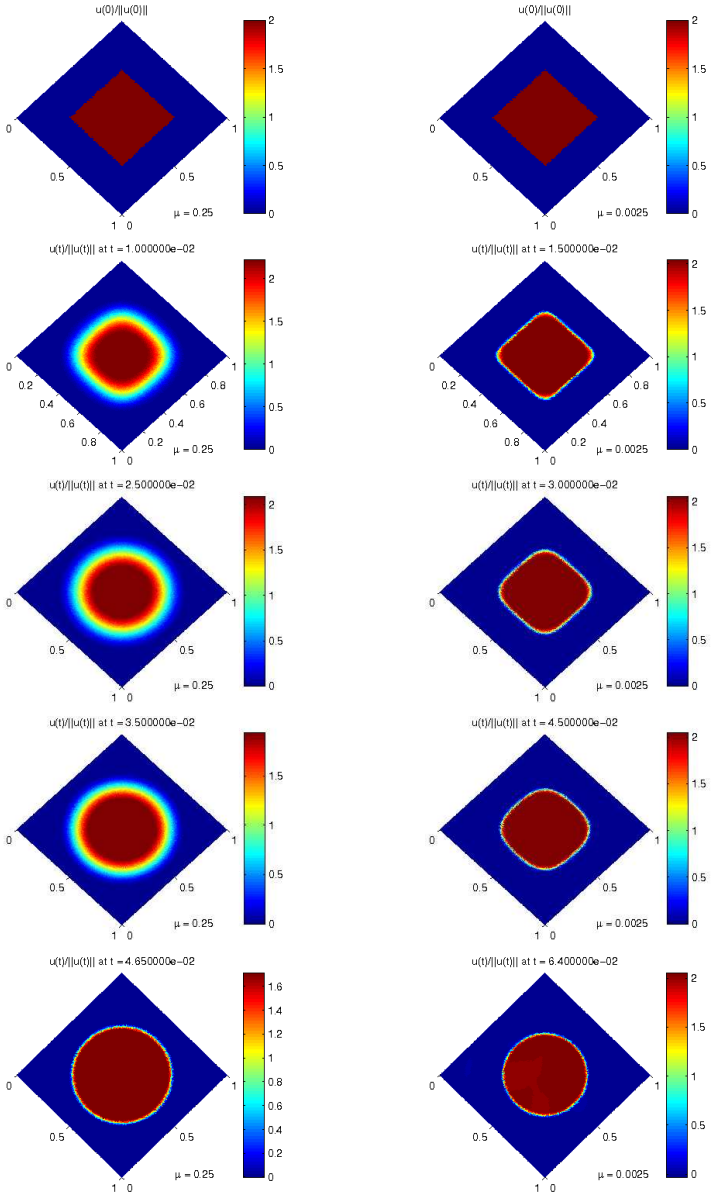

Figure IV.22: Case V - *On the left:* Snapshots of the normalized solution $u(t,x)/||u||_{L^2(\Omega)}(t)$ obtained with $\mu = 0.25$ at $t = 0, 0.01, 0.025, 0.035, 0.045$ seconds; *On the right:* Snapshots of the normalized solution $u(t,x)/||u||_{L^2(\Omega)}(t)$ obtained with $\mu = 0.0025$ at $t = 0, 0.015, 0.03, 0.045, 0.064$ seconds.

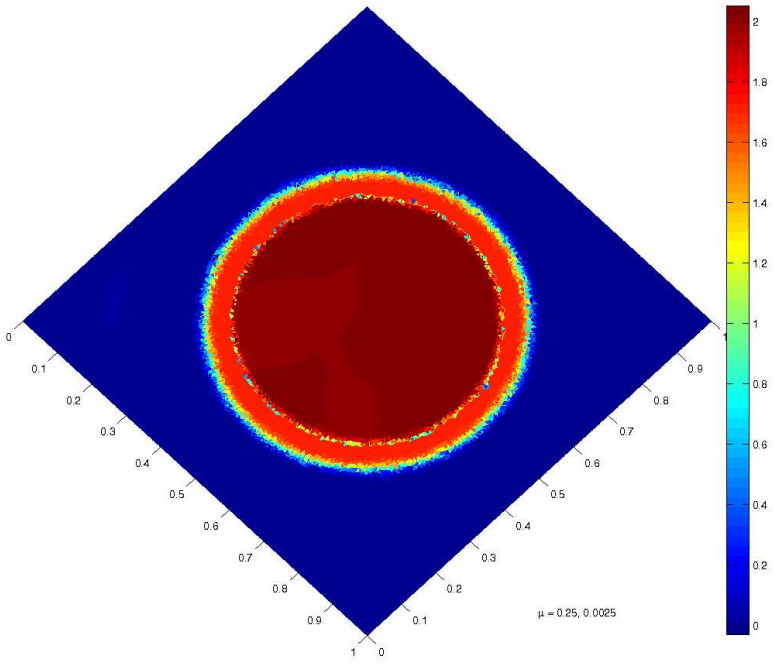

Figure IV.23: Case V - Comparison between the supports of the normalized solutions at extinction time obtained with $\mu = 0.25$ (outer circle) and with $\mu = 0.0025$ (inner circle).

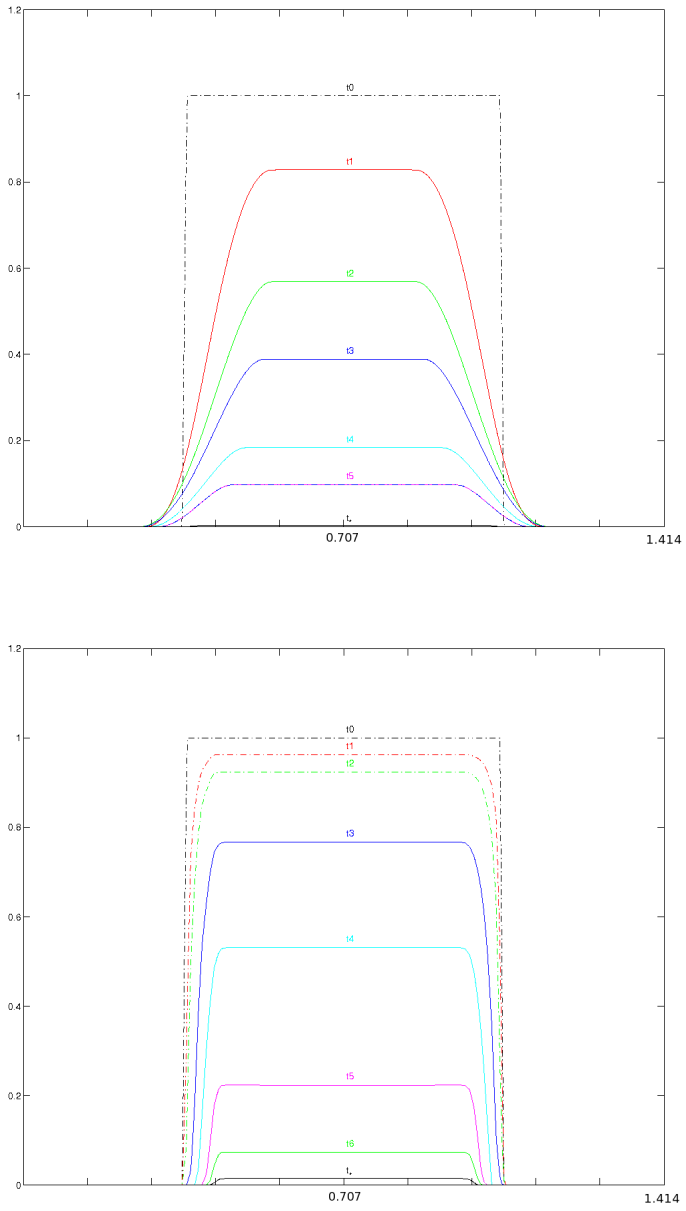

Figure IV.24: Case V - *On the top:* Snapshots of the solution $u(t,x)$ restricted to the domain diagonal obtained with $\mu = 0.25$ at $t_0 = 0,\ t_1 = 0.0075,\ t_2 = 0.0175,\ t_3 = 0.025,\ t_4 = 0.035,\ t_5 = 0.04, t_* = 0.0465$ seconds; *On the bottom:* Snapshots of the solution $u(t,x)$ restricted to the domain diagonal obtained with $\mu = 0.0025$ at $\mu = 0.0025$, $t_0 = 0,\ t_1 = 0.0025,\ t_2 = 0.005,\ t_3 = 0.015,\ t_4 = 0.03,\ t_5 = 0.05,\ t_6 = 0.06,\ t_* = 0.064$ seconds.

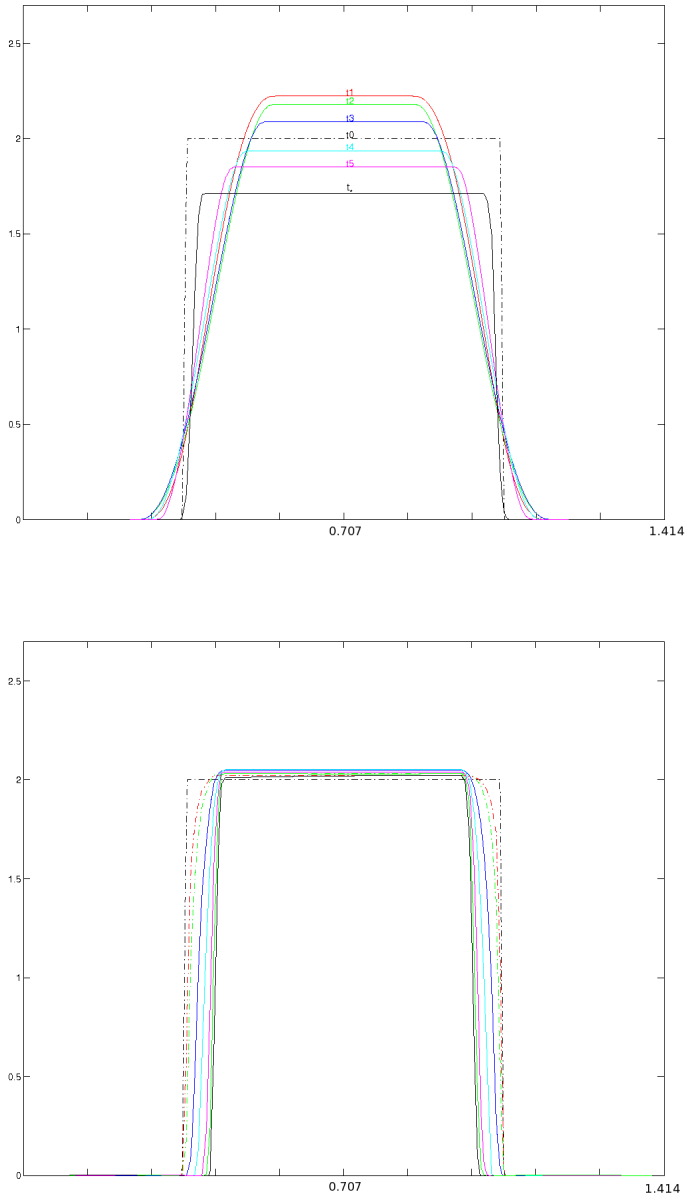

Figure IV.25: Case V - *On the top:* Snapshots of the normalized solution $u(t,x)/||u||_{L^2(\Omega)}(t)$ restricted to the domain diagonal obtained with $\mu = 0.25$ at $t_0 = 0,\ t_1 = 0.0075,\ t_2 = 0.0175,\ t_3 = 0.025,\ t_4 = 0.035,\ t_5 = 0.04, t_* = 0.0465$ seconds; *On the bottom:* Snapshots of the normalized solution $u(t,x)/||u||_{L^2(\Omega)}(t)$ restricted to the domain diagonal obtained with $\mu = 0.0025$ at $t_0 = 0,\ t_1 = 0.0025,\ t_2 = 0.005,\ t_3 = 0.015,\ t_4 = 0.03,\ t_5 = 0.05,\ t_6 = 0.06,\ t_* = 0.064$ seconds.

Our results showed existence of a finite extinction time, as predicted by the theory. We also found that the extinction time increases as the fluid viscosity decreases, as expected. This is due to the fact that a less viscous system has a less efficient dissipative mechanism and therefore it takes longer for the solution to decay to zero.

The theory for total variation flow also predicts no propagation of support of the initial datum, if the support is regular enough. In order to study this property, we visualized the time evolution of the normalized velocity $u(t,x)/\|u\|_{L^2(\Omega)}(t)$, for the different initial conditions and viscosity values. When the support of the initial datum is very regular (either a ball or two distant disjoint balls), the results corresponding to the smaller viscosity value, namely $\mu = 0.0025$, show almost no propagation of support of the initial datum, as predicted by the theory. When the support of the initial datum is not very regular (two close disjoint balls or a square), our results show a change in topology of the support.

Bibliography

[1] R. Adams, *Sobolev Spaces,* Academic Press, New York (1975).

[2] F.Andreu, C. Ballester, V. Caselles, J. M. Mazón *Minimizing total variation flow,* Differential Integral Equations 14, pp. 321-360 (2001).

[3] F.Andreu, C. Ballester, V. Caselles, and J. M. Mazón *The Dirichlet problem for the total variation flow,* J. of Functional Analysis, 180, pp. 347-403 (2001).

[4] F.Andreu, V. Caselles, J.I. Díaz, J. M. Mazón *Some qualitative properties for the total variation flow,* J. of Functional Analysis, 188, pp. 516-547 (2002).

[5] G. Anzellotti, *Paring between measures and bounded functions and compensated compactness,* Ann. Mat. Pura Appl. 135 (1), pp. 293-318 (1983).

[6] R. L. Armentano, J.G. Barra, J. Levenson, A. Simon, R.H. weak Pichel. *Arterial wall mechanics in conscious dogs: assessment of viscous, inertial, and elastic moduli to characterize aortic wall behavior.* Circ. Res. 76, pp. 468-478 (1995).

[7] R. L. Armentano, J.L. Megnien, A. Simon, F. Bellenfant, J.G. Barra, J. Levenson. *Effects of hypertension on viscoelasticity of carotid and femoral arteries in humans.* Hypertension 26, pp. 48-54 (1995).

[8] R. D. Bauer, R. Busse, A. Shabert, Y. Summa, E. Wetterer. *Separate determination of the pulsatile elastic and viscous forces developed in the arterial wall in vivo.* Pflugers Arch. 380, pp. 221-226 (1979).

[9] Ph. Benilan, M. G. Crandall, *Completely accretive operators,* in "Semigroups Theory and Evolution Equations" Ph. Clement et al., Eds., pp 41-76, Marcel Dekker, New York, (1991).

[10] E.C. Bingham, *An Investigation of the Laws of Plastic Flow* U.S. Bureau of Standards Bulletin, 13, pp. 309-353 (1916)

[11] S. Canic, Eun-Heui Kim. *Mathematical analysis of the quasilinear effects in a hyperbolic model of blood flow through compliant axi–symmetric vessels*, Mathematical Methods in the Applied Sciences, 26(14), pp. 1161-1186 (2003).

[12] S. Canic, J. Tambaca, G. Guidoboni, A. Mikelic, C.J. Hartley, and D. Rosenstrauch. *Modeling viscoelastic behavior of arterial walls and their interaction with pulsatile blood flow* SIAM J. App. Math., 67 (1), pp. 164-193 (2006).

[13] S. Canic, A. Mikelic, D. Lamponi, and J. Tambaca. *Self-consistent effective equations modeling blood flow in medium-to-large compliant arteries.* SIAM J. Multiscale Analysis and Simulation 3(3), pp. 559-596 (2005).

[14] S. Canic, C.J. Hartley, D. Rosenstrauch, J. Tambaca, G. Guidoboni, A. Mikelic. *Blood flow in compliant arteries: An effective viscoelastic reduced model, numerics and experimental validation.* Annals of Biomedical Engineering. 34, pp. 575-592 (2006).

[15] J. Cea, R. Glowinski, *Méthodes numériques pour l'écoulement lamminare d'un fluide rigide visco-plastique incompressible,* Int. J. comput. Math.m Section B 3, pp. 225-255 (1972).

[16] A. Chambolle, B. Desjardins, M. Esteban and C. Grandmont. *Existence of weak solutions for an unsteady fluid-plate interaction problem.* J Math. Fluid Mech. 7, pp.368-404 (2005).

[17] D. Coutand and S. Shkoller. *On the motion of an elastic solid inside of an incompressible viscous fluid.* Archive for rational mechanics and analysis, 176, pp. 25-102 (2005)

[18] D. Coutand and S. Shkoller. *On the interaction between quasilinear elastodynamics and the Navier-Stokes equations* Archive for Rational Mechanics and Analysis, 179, pp. 303-352 (2006).

[19] M.G. Crandall, T. M. Liggett, *Generation of semigroups of nonlinear transformations on general Banach spaces,* Amer. J. Math. 93, pp. 265-298 (1971).

[20] E.J. Dean, R. Glowinski, G. Guidoboni, *On the numerical simulation of Bingham visco-plastic flow: Old and new results,* J. non-Newtonian Fluid Mech. 142, pp. 36-62 (2007).

[21] B. Desjardin, M.J. Esteban, C. Grandmont, P. Le Tallec *Weak solutions for a fluid-elastic structure interaction model.* Revista Mathem'atica complutense, 14 (2), pp. 523-538 (2001).

[22] G. Duvaut, J.L. Lion, *Inequalities in Mechanics an Physics,* Springer, Berlin, (1976).

[23] G. Duvaut, J.L. Lion, *Les Inéquations en Mécanique et Physique,* Dunod, Paris, (1972).

[24] L. C. Evans, *Partial Differential Equations* Graduate Studies in Mathematics, (19), American Mathematical Society, RI (2002).

[25] R. Glowinski, *Finite element methods for incompressible viscous flow. In Handbook of Numerical Analysis, Vol. IX, P.G. Ciarlet and J.L. Lions eds.,* North-Holland, Amsterdam, pp. 3-1176 (2003).

[26] R. Glowinski, *Numerical Methods for Nonlinear Variational Problems,* Springer, New-York, NY (1984).

[27] R. Glowinski, J.L. Lions, R. Trémoliéres, *Numerical Analysis of Variational Inequalities,* North-Holland, Amsterdam (1981).

[28] M. Guidorzi, M. Padula and P. Plotnikov. *Galerkin Method for Fluids in Domains with Elastic Walls.* University of Ferrara, Preprint.

[29] M. Hardit, X Zhou, *An evolution problem for linear growth functionals*, Interdisciplinary Applied Mathematics. Vol. 8, Springer, New York, (1998).

[30] R. Kobayashi, Y. Giga, *Equations with singular diffusivity,* J. Statist. Phys. 95 pp. 1187-1220, (1999).

[31] A. Mikelic, G. Guidoboni and S. Canic. *Fluid-structure interaction in a pre-stressed tube with thick elastic walls I: The stationary Stokes problem.* Networks and Heterogeneous Media. 2 (3) pp. 397-423 (2007).

[32] F. Nobile, *Numerical Approximation of Fluid-Structure Interaction Problems with Application to Haemodynamics*, Ph.D. Thesis, EPFL, Lausanne (2001).

[33] G. Pontrelli. *A mathematical model of flow through a viscoelastic tube.* Med. Biol. Eng. Comput, (2002).

[34] A. Quarteroni, M. Tuveri and A. Veneziani, *Computational vascular fluid dynamics*: *problems, models and methods. Survey article*, Comput. Visual. Sci. 2, pp. 163-197, (2000).

[35] L. Rudin, S. Osher, E. Fatemi, *Nonlinear total variation based noise removal algorithms.* Physica D 60, pp. 171-200 (1992).

[36] R. Temam *Navier Stokes Equations: Theory and Numerical Analysis* North-Holland Publishing Company Amsterdam, New York, Oxford, (1977)

[37] B. da Vega. *On the existence of strong solutions to a coupled fluid-structure evolution problem.* Journal of Mathematical Fluid Mechanics, 6 (1), pp. 21-52, (2004).

[38] Lee Waite, Jerry Michael Fine, *Applied Biofluid Mechanics,* McGraw-Hill Professional Publishing, (2007).

[39] K. Yosida, *Functional Analysis,* Springer-Verlag, (1966).

[40] E. Zeidler. *Nonlinear Functional Analysis and its Applications I. (Fixed Point Theorems)* Springer-Verlag New York, Inc. (1986).